HUMAN EFFECTS ON WATER QUALITY IN THE NORTHERN ROCKY MOUNTAINS:

RELATIONSHIPS AMONG SOLUTE SOURCES, TRANSFORMATIONS, AND FLOW

by

Meryl Biesiot Storb

A dissertation submitted in partial fulfillment
of the requirements for the degree

of

Doctor of Philosophy

in

Ecology and Environmental Science

MONTANA STATE UNIVERSITY
Bozeman, Montana

May 2024

DEDICATION

This is dedicated to my family, especially my two children Gus, and Magnus, who shaped this process more than I could have ever imagined. They have taught me patience, persistence, and the true nature of curiosity. And they have shown me the value and necessity in improving scientific understanding of mechanisms that shape the remaining wild places on this earth, for the sake of their future.

ACKNOWLEDGEMENTS

This dissertation would not have been possible without the unwavering support and love my family and my parents, the guidance and mentorship provided by my committee members, and support from people at the USGS. I had an unconventional path through this experience, and I want to extend enormous gratitude to my advisor Rob Payn. Rob supported me while I pursued a family and started a career during my time as a student. I recognize that through Rob giving me grace with my choices, I likely made his tenure more challenging, but I am forever grateful for his patience, understanding, and support. Rob pushed my intellectual development, but what I most admire about him is his unwavering dedication to mentoring and challenging students to think critically, I aspire to carry this trait with me moving forward. Thank you to my committee members, Wyatt Cross, Kristin Gardner, and Geoff Poole, for providing intellectual support, advice, feedback, and for challenging me. With special thanks to Stephanie Ewing for mentorship in navigating this process and leading by example, showing me how to be a successful scientist and a mother. Thank you to all the members of the Payn Lab and past field and lab assistants. Many hours standing in the West Fork and scrubbing rocks with toothbrushes made Chapter 2 possible. With a special thank you to Juliana D'Andrilli, for your enthusiasm for science, continued guidance, and friendship. Caitlin Mitchell and Katie Fogg helped me navigate the end of this experience, I'm not sure I would have made it without their help. Thank you to USGS colleagues, especially Bob Hirsch and Travis Schmidt. Finally, this whole thing never would have happened without my biggest supporter, my husband Forrest. Forrest's love, encouragement, and support allowed me to push myself to a place that I wasn't sure was possible.

TABLE OF CONTENTS

TABLE OF CONTENTS CONTINUED

TABLE OF CONTENTS CONTINUED

LIST OF TABLES

Table Page

LIST OF FIGURES

LIST OF FIGURES CONTINUED

Figure Page

GLOSSARY

NRM, Northern Rocky Mountains

KOC, Koocanusa Reservoir

ERM, Elk River Mines

RWQM, Teck Resources Regional Water Quality Model

WRTDS, Weighted Regression on Time Discharge and Season

MT, Montana

ID, Idaho

USGS, United States Geologic Survey

B.C., British Columbia

CA, Canada

U.S. United States

ECCC, Environment and Climate Change Canada

SiZer, Significant Zero Crossings of the Derivative

ABSTRACT

Humans have profoundly altered water quality within streams and rivers. Degradation of water quality has manifested through direct effects on stream water chemistry via changes to physical and chemical mechanisms of solute delivery across the landscape. Indirect effects on water quality have also resulted from the influence of human-induced climate change on the hydrologic regimes that determine solute transport. This dissertation contributes research on the controls of water quality in streams and rivers of the northern Rocky Mountains (NRM), which drain a snowmelt dominated region consisting of parts of Montana and Idaho in the United States (US) and southern British Columbia, Canada. This area includes the largest contiguous wilderness area in the continental US and contains watersheds that have undergone land use change from large-scale mining and urban development. The NRM consists of headwater systems draining high elevation regions subject to disproportionate effects of climate change. We consider pathways of human influence on water quality in the NRM via examination of spatiotemporal relationships among solute concentrations, solute loads, and the flow of water. First, an investigation of the influence of large-scale coal mining operations on solute delivery provides evidence of mechanisms underlying increases in selenium and nitrate contributions to a river. These results suggest hydrologic processes responsible for delivering solutes to the river have shifted over time with changing mining operations. Next, we describe how chronic nitrate loading from distributed releases of treated wastewater have fueled autotrophic growth that influences both seasonal and diel concentration dynamics. These results highlight the importance of understanding biologic feedbacks on nutrient concentration dynamics for biogeochemically reactive solutes. Finally, application of a novel hydrograph differentiation technique reveals evidence that climate change is shifting ecologically relevant transitions in snowmelt hydrologic regimes to earlier in the year for over half the NRM watersheds assessed. These results reveal an objective approach to identifying inflections of hydrographs that are related to key transitions in catchment storage behaviors underlying snowmelt hydrologic regimes. Results across these studies suggest that effective decisions surrounding mitigating water quality problems sit at the nexus of understanding sources of contaminants, their potential to be transformed by watershed systems, and the hydrologic regimes that control their transport.

CHAPTER ONE

INTRODUCTION: INTERACTIONS BETWEEN HUMANS, SOLUTES, AND FLOW

Freshwater has been described as ‘the bloodstream of the biosphere’, meaning freshwater systems are essential for Earth system processes, interactions, and feedbacks. However, freshwater systems are being altered by humans at an alarming rate and at a global scale (Gleeson *et al.* 2020). Humans have chemically altered nearly every body of water on the planet, from microplastics in the deepest waters of the ocean (Zhao *et al.* 2022) to synthetic chemicals found in snow in the most remote regions of the world (Xie *et al.* 2022). In addition to changes in water chemistry, humans are now affecting the hydrologic cycle as a result of climate change, thereby changing the timing, distribution, and forms of water across the planet (Gleeson *et al.* 2020). Freshwater systems comprise only 2.5% of water on the planet, with only 0.01% of the world's water found in freshwater lakes, wetlands, swamps, and rivers (Van Meter *et al.* 2016), but these resources supply roughly three quarters of the water withdrawn for human use and provide a wealth of ecosystem services (Carpenter *et al.* 2011). The “bloodstream” of freshwater is fundamentally essential for life (Westall and Brack 2018), but the consequences of human activity have caused clean and reliable freshwater to be among the greatest existential concerns for humanity moving into the future (UNESCO 2009, 2020).

Humans are influencing water quality in streams and rivers via two major pathways: the effects of introduced nutrients and contaminants on water chemistry (Van Meter *et al.* 2016) and the effects on local to global hydrologic regimes that influence contaminant transport (Poff *et al.* 1997). The nature of the influence from human activity on stream and river water quality varies widely across the globe, but more than 99% of streams and rivers are considered to be somehow impaired by human activity with respect to regulatory definitions of “beneficial use” (Hynes 2001; Dudgeon *et al.* 2006; Van Meter *et al.* 2016). Over 75% of the Earth’s land surface is affected by human development and land use change (Kaushal *et al.* 2014). Physical transformation of soils, land surfaces, and geological structure can alter runoff generation mechanisms and change solute sources and delivery pathways within watersheds (Runkel and Bencala 1995; Godsey *et al.* 2009; Giri and Qiu 2016). The organization of a stream or river system is first controlled by its hydrologic regime, where annual patterns in flow are dictated by the catchment’s structure and climate. The flow regime has been described as an ecological “maestro”, meaning a master controller that shapes the physical, chemical, and biotic structures within stream ecosystems (Power *et al.* 1995; Poff *et al.* 1997; Poff and Zimmerman 2010). The multiple scales of human influence on the landscape and climate interact to influence the processes and pathways within watersheds that control the quantity and quality of stream and river waters (Kaushal *et al.* 2017).

Increased understanding of the drivers of water quality has become critical in the northern Rocky Mountains (NRM) of the US and Canada, in part due to transboundary and culturally significant waterways that include important freshwater resources for two countries and six tribal nations (Storb *et al.* 2023). The NRM represents an area draining relatively high elevation watersheds (Luce 2018) and land cover under a variety of land uses. This region encompasses the largest contiguous wilderness area in the continental United States (US) and also includes watersheds that have undergone rapid land use change due to urban development and resource extraction projects. Research in this dissertation provides critical insight into the controls on water quality in an area of the NRM that includes portions of Montana and Idaho in the US and southern British Columbia in Canada (BC).

Water quality in the NRM is particularly sensitive to the influence of solute transport by snowmelt-driven hydrologic regimes. Seasonal snowmelt-driven streamflow is one of the fastest changing aspects of the global hydrologic cycle in response to climate change (Musselman *et al.* 2017), making snowmelt dominated watersheds an important focus for the study of both direct and indirect human effects on water quality. Regular seasonal patterns in snowmelt dominated hydrologic regimes make them particularly useful for identifying the effects of climate change (Patterson *et al.* 2020b). Likewise, snowmelt dominated flow regimes determine the phenological cycles of aquatic ecosystems dictated by biotic and abiotic conditions linked to variation in stream flow (Poff *et al.* 1997; Yarnell *et al.* 2010a). These interactions create a more predictable system, compared to other hydrologic regimes, when exploring process-based understanding of mechanisms influencing water quality.

Early recognition of the links between the controls on stream water chemistry and the watershed hydrologic regime were identified in investigations in the US from the 1920s to the 1950s, primarily involving patterns in chemistry during snowmelt runoff in western rivers (Clarke 1924; Hem 1948; Durum 1953). These investigations described dilution of solutes as river discharge increased from runoff. Subsequent studies focused on the form of relationships between solute concentrations and discharge, which resulted in the concentration-discharge relationship (C–Q) paradigm (Hall 1970, 1971). The C-Q framework enabled inferences related to process-based controls on water quality via hypothesized solute generation and dilution mechanisms that affect observed C–Q patterns in runoff (Hall 1970; Hem 1985; Godsey *et al.*

2009; Burns *et al.* 2019). Additional work explored differences between how point versus nonpoint sources of nitrate influenced C-Q relationships (Edwards 1973; Walling and Foster 1975), which further advanced mechanistic understanding of hydrological and biogeochemical processes that generally occur outside of the immediate stream environment (Burns *et al.* 2019). C-Q relationships provide an approach that can reflect an aggregation of solute sources, proximity of sources, storage mechanisms, biogeochemical reactivity, and transport within watersheds, where different hydrologic pathways, connectivity, and instream biogeochemistry influence observed C-Q patterns at the outlet (Rose *et al.* 2018).

Broadly, this dissertation contributes to understanding the controls on water quality due to dramatic changes to the landscape and widespread changes to hydrologic regimes ultimately stemming from human activity. Controls on water chemistry are hopelessly intertwined with changes in the hydrologic cycle, so my work considers both direct and indirect pathways of influence. The chapters in this dissertation represent exploration of the relationships between solute concentrations, discharge, and load, considering time scales of variation from daily (Chapter 3) to seasonal (Chapters 2, 3, and 4) to decadal (Chapters 2 and 4). Most of this research generally fits within the C-Q approach. I use relationships between solute concentrations, solute loads, and stream flows to build understanding of how water quality is determined from human activates influencing solute sources and biogeochemical transformations within the stream.

The research chapters of this dissertation begin with two studies that explore human influence on water quality related to dramatic changes in the landscape or land use. These human influences include mining activities that have resulted in the introduction of toxins (selenium) and amenity community urbanization that is introducing agents of stream eutrophication (nitrate).

Chapter 2 explores how large-scale landscape alteration from coal mining in the Elk River Valley, BC has induced increasing changes in water quality in the downstream Koocanusa Reservoir for over four decades. We used flow-normalized trend analysis and C-Q relationships at different timescales and flow conditions to illustrate changes in solute delivery mechanisms over time. The profound influence of the coal mining operations on the timing and magnitude of selenium and nitrate concentrations are being observed at the outlet of the watershed over 100 km downstream of mining operations. Findings suggest the mines affect water quality via nonpoint source pollution originating from altered groundwater aquifers, as indicated by a consistent decadal time scale shift from a chemostatic C-Q relationship before mining operations began to a dilution pattern suggesting groundwater sources of contaminants.

Chapter 3 explores the ecological consequences of a known increase in nitrate concentration along a 3-km stretch of the West Fork of the Gallatin River, where increases in nitrate are likely attributable to rapid urbanization and amenity development. This chapter is focused on links between wastewater derived nitrate sources and ecosystem response to additional nitrate loads. Results highlight the importance of considering feedbacks on daily and seasonal variations in nutrient concentrations created by fertilization of the stream ecosystem. Findings show that chronic nitrogen loading fueled additional autotrophic growth and primary production, which in turn tended to decrease observed nitrate concentrations during the daytime hours of the algal growing season. These results suggest that nutrient impairment evident in excess algal growth can be underestimated from water chemistry measurements alone when stream waters are sampled just once during the day and predominantly during the summer and fall seasons.

Chapters 2 and 3 both demonstrate that the snowmelt hydrologic regime interacts with contaminant delivery and biogeochemical processes to strongly control water quality. Therefore, Chapter 4 explores changes in the timing of snowmelt driven hydrologic regimes associated with climate change over decadal time scales. This research required development of a new method for analyzing hydrographs using differentiation of smoothed annual signals from USGS data. We refined a statistical smoothing method that objectively quantifies timing of key hydrograph inflections using numerical differentiation. A simple algorithm objectively identifies inflection-based timing of smoothed hydrographs instead of evaluating timing based on conventional flow metrics that are typically related to absolute volumes and magnitudes. This approach allows us to take advantage of more information contained within the shape of the hydrograph and explore the timing of events related to storage and drivers of snowmelt. Findings suggest that climate change is influencing snowmelt drivers in some watersheds, and we generally had more confidence that data from watersheds at higher elevations and more southern latitudes reflected trends toward earlier transitions in snowmelt.

Chapter 5 provides a synthesis and discussion related to themes that emerged across the individual research chapters and provides a framework for future considerations of human effects on water quality. Based on findings in this dissertation, effective decisions regarding mitigating water quality problems sit at the nexus of understanding the sources of contaminants, the potential of contaminants to be transformed by watershed systems, and the hydrologic regimes that control contaminant transport.

CHAPTER TWO

GROWTH OF COAL MINING OPERATIONS IN THE ELK RIVER VALLEY (CANADA) LINKED TO INCREASING SOLUTE TRANSPORT OF Se, NO_3^-, AND SO_4^{2-} INTO THE TRANSBOUNDARY KOOCANUSA RESERVOIR (USA-CANADA)

Contribution of Authors and Co-Authors

Manuscript in Chapter 3

Author: Meryl B. Storb

Contributions: Study design and implementation of all analysys except for the mass removal analysis with which I assisted. Generated all text, figures, and tables except for the study map. Wrote the manuscript, facilitated all revisions, and submission.

Co-Author: Ashley M. Bussell

Contributions: GIS mapping and copy editing.

Co-Author: Sara L. Caldwell Eldridge

Contributions: Copy editing and reference management.

Co-Author: Robert M. Hirsch

Contributions: Assisted with ensuring accuracy of methods. Facilitated mass removal analysis and provided edits to the manuscript.

Co-Author: Travis S. Schmidt

Contributions: Provided the most editorial assistance and reference management.

Manuscript Information

Meryl B. Storb, Ashley M. Bussell, Sara L. Caldwell Eldridge, Robert M. Hirsch, and Travis S.

Schmidt

Environmental Science & Technology

Status of Manuscript:
☐ Prepared for submission to a peer-reviewed journal
☐ Officially submitted to a peer-reviewed journal
☐ Accepted by a peer-reviewed journal
X Published in a peer-reviewed journal

American Chemical Society (ACS)
July 5, 2023
November 3, 2023
2023 57 (45), 17465-17480
DOI:10.1021/acs.est.3c05090.

Abstract

Koocanusa Reservoir (KOC) is a waterbody that spans the United States (U.S.) and Canadian border. Increasing concentrations of total selenium (Se), nitrate + nitrite (NO_3^-, nitrite is insignificant or not present), and sulfate (SO_4^{2-}) in KOC and downstream in the Kootenai River (Kootenay River in Canada) are tied to expanding coal mining operations in the Elk River Watershed, Canada. Using a paired watershed approach, trends in flow-normalized concentrations and loads were evaluated for Se, NO_3^-, and SO_4^{2-} for the two largest tributaries, the Kootenay and Elk Rivers, Canada. Increases in concentration (SO_4^{2-} 120%, Se 581%, NO_3^- 784%) and load (SO_4^{2-} 129%, Se 443% , NO_3^- 697%) in the Elk River (1979-2022 for NO_3^-, 1984-2022 for Se and SO_4^{2-}) are among the largest documented increases in the primary literature, while only a small magnitude increase in SO_4^{2-} (7.7% concentration) and decreases in Se (-10%) and NO_3^- (-8.5%) were observed in the Kootenay River. Between 2009-2019, the Elk River contributed, on average, 29% of the combined flow, 95% of the total Se, 76% of the NO_3^-, and 38% of the SO_4^{2-} entering the reservoir from these two major tributaries. The largest increase in solute concentrations occurred during baseflows, indicating a change in solute transport and delivery dynamics in the Elk River Watershed, which may be attributable to altered landscapes from coal mining operations including altered groundwater flow paths, and increased chemical weathering in waste rock dumps. More recently there is evidence of surface water treatment operations providing some reduction in concentrations during low flow times of year, however these appear to have a limited effect on annual loads entering KOC. These findings imply that current mine water treatment, which is focused on surface waters, may not sufficiently

reduce the influence of mine waste derived solutes in the Elk River to allow constituent concentrations in KOC to meet U.S. water quality standards.

SYNOPSIS: Increasing solute concentrations in the transboundary Koocanusa Reservoir are linked to coal mining in Elk Valley British Columbia, Canada. Historic solute loads and concentrations from paired watersheds were evaluated to identify effects to water quality and solute transport from coal mining operations.

1. Introduction

Worldwide, over 260 river basins are divided and shared by multiple nations. Managing and preserving transboundary watersheds, their water resources, and cultural heritage is exceptionally difficult because political borders rarely coincide with watershed boundaries, and governments may have conflicting regulatory approaches.[1-3] Without cooperative resource management between governments, transboundary waterways are uniquely vulnerable to the influences of human land use on water quality and ecosystem integrity. One example is large scale mining and the alteration of land surfaces and aquifers due to placement of waste rock, which are known to profoundly influence groundwater and surface water quality.[4-6] Mining supports regional and national economies, but has been shown to alter water, solute, and sediment dynamics, and harm aquatic ecosystems.[7] Understanding environmental and water quality impacts from mines located near borders provides information that may be used to protect, restore, and manage natural resources in the complex regulatory setting of transboundary watersheds.[8]

Koocanusa Reservoir (KOC, also called “Lake Koocanusa”) is a transboundary reservoir that is split between northwestern Montana (MT), United States (U.S.) and southeastern British

Columbia (B.C.), Canada (CA). The reservoir was impounded in 1972 by Libby Dam, near Libby, MT (Figure 1). KOC encompasses the headwaters of the Kootenai (Kootenay in CA) River Basin. Including KOC, the Kootenai River crosses the U.S./CA border twice, and drains into the Columbia River just north of where the river crosses the international border a third time (Figure 1). The Kootenai and Columbia Rivers have significant cultural importance - the watershed itself is the basis for the Ktunaxa Creation Story.[9] Ecologically and culturally important fish resources in the Kootenai Watershed (U.S.) include the federally endangered Kootenai River White Sturgeon (*Acipenser transmontanus*), the threatened Bull Trout (*Salvelinus confluentus*), and two species of concern, Burbot (*Lota lota*) and Westslope Cutthroat Trout (*Oncorhynchus clarkii lewisi*).[10] The headwater drainages for KOC are present on both sides of the border. However, the three largest tributaries are in B.C., and the second largest is the Elk River, which drains a watershed that contains several open-pit, coal mining operations (Figure 1).[11, 12]

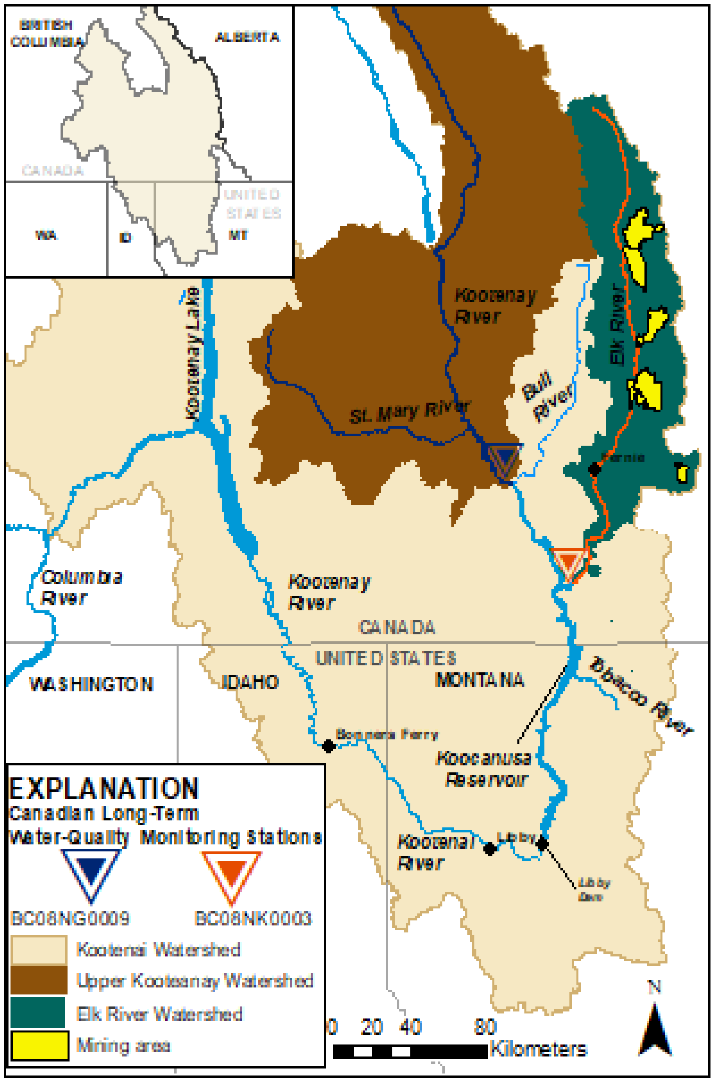

C2 Figure 1. Study area map showing Kootenai Basin (and partial Columbia River Basin) including the Elk River and Kootenay River Watersheds and other major tributary watersheds, the Bull River, and the Tobacco River. Mine areas in the Elk River Watershed are shown in yellow.[11, 12]

Coal mines have operated in the Elk River Watershed since 1897 and are known sources of contaminants to the transboundary waters in the Kootenai River Basin (Figure 2).[5, 13-15] Current coal mines in the Elk River Watershed (Elk River Mines, ERM) are classified in Canada as open-pit mines, but they are analogous to mountain top removal coal mines in the United

States[7] where mining operations create abundant volumes of waste rock that are deposited in valley areas more than 100-m thick.[4, 13]

Open-pit coal mining in the Elk River Watershed results in the removal of coal and waste rock and subsequent waste rock dump generation (valley fill) – these mining operations alter the slopes, physical landscape, hydrologic, hydrogeologic, and geochemical functions of the mountain headwater systems where the mines are present (Figure 2).[5, 14] As a result, these mountain headwaters have less relief and more low gradient surfaces, which alters infiltration and runoff processes.[5, 14] Geochemical processes are also altered when solid bedrock is removed and replaced by porous crushed waste rock. Waste rock dumps change the porosity and transmissivity of the system and increase the surface area and exposure of waste rock to air [16] and water, enabling more rapid chemical weathering.[4, 5, 17] Changing mining practices, including the development of new technologies, treatments, and best managements also further complicate the landscape and runoff and infiltration mechanisms, including lag times that affect solute movement through waste rock.[18-21]

Past literature has correlated Se and NO_3^- concentrations in the Elk River with the volume of waste rock produced in the ERMs (Figure 2), however complete understanding of the mechanisms driving the changing concentrations (e.g. the increase in concentrations around 2005) are not well understood.[5, 13] Likewise, Se, NO_3^-, and SO_4^{2-} concentrations measured in the Elk River where it enters KOC have been increasing since concentrations were first measured in 1984, concentrations are also increasing in KOC (station # 12300110) (Figure 3).[22-24] Water-quality sampling on the Elk River was initiated roughly 80 years after coal mining began, but it is likely that mining affected water quality before monitoring started.[15]

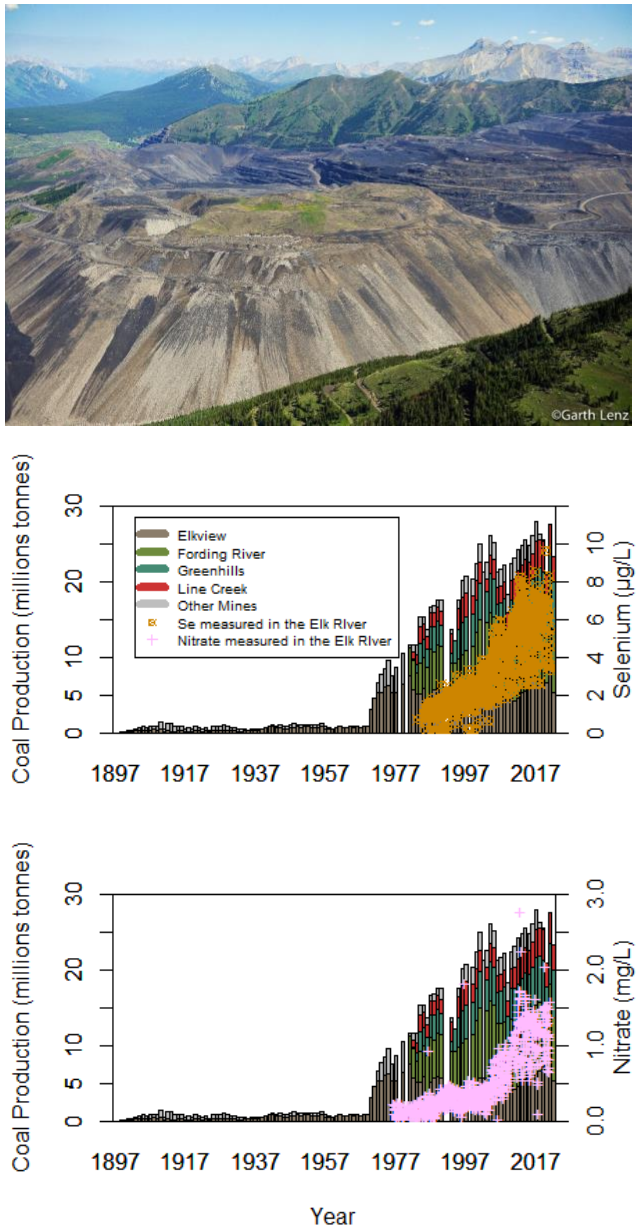

C2 Figure 2. Coal production in the Elk River Watershed. Aerial image of one area of mine operations within the watershed. Copyrighted, used with permission via licensing agreement with Garth Lenz. Plots illustrate yearly coal production by mine, represented by different colors[16] and measured concentrations of total Se and NO_3^- in the Elk River and Highway 93.[22]

Coal-associated waste rock contains sulfide minerals (pyrite, most commonly) and organosulfide compounds which are associated with Se and other trace elements.[25-27] Se is of particular importance because its crustal concentrations can be enriched up to 82 times in coal-bearing geologic formations.[27] Chemical weathering through the oxidation of sulfide minerals releases SO_4^{2-} and associated trace elements to both surface water and groundwater.[28] Increasing NO_3^- concentrations in the Elk River have been tied to blasting practices from coal mining operations,[13] and excess ammonium may originate directly from coal.[29] Release of these mine-waste-derived solutes has negative implications for beneficial uses, including potential to harm ecosystems in downstream water bodies.

KOC is oligotrophic, due to low background phosphorous concentrations and limited sediment delivery to the downstream section of the reservoir because of the Libby Dam. Increasing NO_3^- loads from the Elk River coupled with limited phosphorous has the potential to alter food webs through an imbalance of nutrients.[30-33] Food web effects from the nutrient imbalance have known ecological consequences downstream of the reservoir in the Kootenai River in MT and Idaho (ID), where phosphorous is now being added to improve food webs for fisheries.[30, 34] Se is an essential trace element for life, but excess Se can be toxic to vertebrates and invertebrates.[35] In egg-laying organisms, Se substitutes for sulfur in proteins causing teratogenesis (deformities) in early-life stages, among other effects.[31, 36-39] Thus, elevated Se entering from the Elk River poses a risk to organisms and ecological function of KOC and the entire Kootenai Watershed.

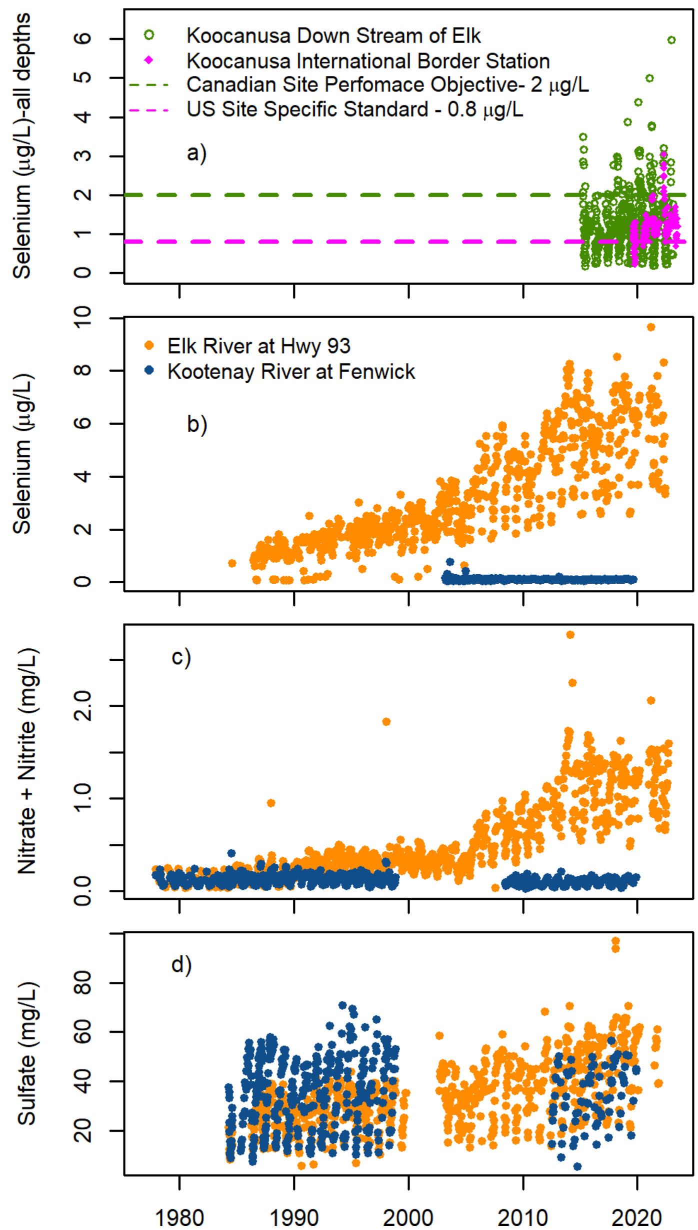

C2 Figure 3. Solute concentration measurements in Koocanusa Reservoir and the Elk River at Highway 93.22 (a) Koocanusa Reservoir Se concentrations measurements at a Canadian compliance point (green)[46] and the United States side of the international boarder (U.S. Geological Survey Site ID 12300110, magenta)[24] with their respective regulatory criteria.[45, 46] Concentration measurements of total Se (b) NO_3^- (c), and SO_4^{2-} (d) at the Elk River at Highway 93 (Orange) and the Kootenay River at Fenwick (Blue).[22]

In 2012, KOC and the Kootenai River were listed as impaired for Se on Montana's Clean Water Act section 303(d) list.[40] Idaho's listing for Se occurred in 2020 with a second section of the Kootenai listed in 2022.[41, 42] From 2015-2020, the State of MT and province of B.C. worked to develop site-specific Se standards to protect water resources in KOC. The water column Se criterion of 0.8 ug/L was set for the U.S. portion of KOC (along with fish tissue criteria) (Figure 3) and 3.1 µg/L for the Kootenai River in MT and ID.[43-45] However, as of September, 2023, B.C. has yet to officially establish a site-specific water quality guideline for the CA portion of the reservoir. B.C. is the primary regulatory entity and they have specified water quality performance objectives (i.e., CA regulatory criteria for water column concentrations) at order stations (i.e. CA regulatory compliance points) associated with mining permits, which are site specific objectives that differ from CA water quality guidelines.[46] The water quality performance objectives for Se, at the order station within the CA portion of KOC, match the provincial recommended guideline value of 2 µg/L (Figure 3a).[47] Water quality criteria for Se are now being regularly exceeded on both sides of the border. At the time of publication, water Se concentrations collected at the international boundary (USGS Site ID 12300110) have not been less than the U.S. site specific regulatory standard since July, 2020 (Figure 3a).[24]

Here, we aimed to gain a better understanding of how the history of Elk Valley mining operations has influenced the quality of waters flowing into the United States via a retrospective analysis of Canadian water quality and discharge records. Our analysis included three constituents (Se, NO_3^-, and SO_4^{2-}) in the two largest tributaries of KOC (The Kootenay River and Elk River), near their entries to the reservoir. For all three constituents in each river, we built empirical models of concentrations, using weighted regression as a function of time trend, discharge, and season (WRTDS).[48] Based on these models we estimated daily and annual concentrations and loads and evaluated trends in flow-normalized concentrations and loads. Through a paired watershed study with three objectives, our goal was to address the following research question: How does the export of potential contaminants such as Se, NO_3^-, and SO_4^{2-} reflect the history of coal mining land use and waste rock management in watersheds? Our first objective was to model and estimate the masses of Se, NO_3^-, and SO_4^{2-} that enter KOC annually from the two major tributaries and assess how annual delivery of solutes has changed through time via flow-normalized trends in concentration and load. Our second objective was to determine the relative contributions of Se, NO_3^-, and SO_4^{2-} over time, from the two tributaries into KOC. Lastly, we looked for evidence of changing solute dynamics in the two tributaries in relation to the coal mining operational history, including the recent implementation of water treatment at the ERM.

While public concern and scientific study related to mining contaminants in the Elk River watershed have been previously documented in government reports, Canadian and US national news sources, and primary literature[5, 14, 27, 49-52], this study provides the first comprehensive and comparative analysis in the primary literature of historical water quality effects to U.S. waters from solutes derived from coal mine operations in the Elk River Valley. Our efforts demonstrate how flexible analysis techniques (WRTDS) can be used to improve understanding of changing solute dynamics and the fate and transport of mine waste derived solutes (Se, NO_3^-, and SO_4^{-2}).

2. Methods

2.1 Site Information

KOC is 145 km long and is bisected by the international border in southeastern B.C., Canada, and northwestern MT, United States (Figure 1).[53] There are four gauged tributaries that contribute water to KOC; the three largest are Canadian tributaries, the Kootenay, Elk, and Bull Rivers – which together supply approximately 87% of the inflow to the reservoir, with roughly 50% coming from the Kootenay River and 25% from the Elk River (Figure 1).[23, 54, 55]

Large growth of mining operations in the Elk River Watershed occurred in the 1970's, with the transition from underground mining to large scale surface mining with valley-fill waste rock dumps (Figure 2).[16, 56] In 2020, ERM were responsible for producing 80% of Canada's annual steelmaking coal exports and 43% of B.C.'s mining revenues. In 2021, ERM produced 24.6 million tons of coal, with the majority exported to the Asia Pacific region.[57, 58] In 2022, the ERM encompassed over 145 km^2 (3%) of the Elk River Watershed (SI Figure 1, SI Table 1a,b). At present (2023), there are also three additional proposed mines and one proposed mine expansion.[56] As of 2020 the ERM had generated over 6.74 billion bank (*in situ*) cubic meters (B.B.C.M) of waste rock,[29] a 43% increase from the 4.7 B.B.C.M of waste rock that was present in 2010.[59] Current permitted mine operations allow 11.03 B.B.C.M of waste rock, so volumes could nearly double from their present sizes under existing mine permits (SI Table 2).[29] The areal extent of waste rock dumps is specified by permitting,[5, 60] so future waste rock generation from existing operations is likely to alter the geometry of the dump areas, by increasing their depth.

In 2013, based on rising concentrations of five constituents (Se, NO_3^-, SO_4^{2-}, Cadmium and Calcite) in the Elk River, B.C. began requiring ERM to address mining contamination.[61]

Remedial measures implemented by ERM included piloting of water treatment technologies to remove Se and NO_3^- beginning in late 2014, leading to 4 operating treatment facilities by the end of 2022 (SI Table 4).[29]

2.2 Data Compilation

Water quality and discharge data were obtained from the online B.C. Water Tool (downloaded on 7/7/2022)[55] and the Environment and Climate Change Canada (ECCC) data portal (downloaded on 11/12/2022).[62] Water quality data for the Kootenay River were obtained from the Kootenay River near the Fenwick site (B.C.08NG0009), the site has a drainage area of 11,754 km^2. Discharge and water quality sampling locations were not coincident, so discharge data from the Kootenay River at Fort Steele (station ID 08NG065)[55] were adjusted based on the drainage area ratio between the discharge monitoring and the water quality sampling locations (SI Figure 2).[22] The Elk River is 220 km long and has a drainage area of 4,450 km^2 to the water quality monitoring site located at Highway 93 Near Elko (B.C.08NK0003).[23] Because the discharge and water sampling locations were not coincident, the Maintenance of Variance Extension, Type 2 (MOVE.2)[63] for record extension was used to extend the daily discharge record at the Elk River at Phillips Bridge site (08NK005)[55] - the closest gauge - but discharge measurements were discontinued after 1996. Record extension for Phillips Bridge was based on the discharge relationship with the Elk River at Fernie site (08NK002) (correlation coefficient 0.9805) (SI Figure 2).[63, 64] A drainage area ratio correction was then applied to adjust for the differences in contributing area between the Phillips Bridge discharge records and the Highway 93 water quality monitoring locations.[22] Additional information is in the SI Methods: Additional

Site information and Geology. Concentration and discharge input files, in addition to the models, associated metadata, and additional details are available in Lange and Storb.[22]

Both the Elk and Kootenay Rivers have snowmelt-dominated flow regimes, generally characterized by peak discharges in late May through early June, transitioning to baseflow recession in the late summer and early fall, and steady low discharge dominated by baseflow contributions throughout the winter months (SI Figure 3).[5] Water quality samples at each location were generally collected two times each month over the period of record for each solute and generally spanned the range of flow conditions (SI Figure 4). Additional information regarding data quality screening, and corrections, are available in Lange and Storb.[22]

2.3 Analysis Methods

Weighted Regression on Time, Discharge and Season (WRTDS) was implemented using R Studio (version 1.4.1106), and the EGRET (version 3.0.7), and EGRETci (Version 2.0.4) packages.[48, 65, 66] Six individual models were generated, one model for each constituent of interest at each site. Additional details, including the governing equation are included in the Supporting Information (SI Analysis Methods).

2.3.1 Evaluation of Flow Stationarity.

To determine the appropriate implementations of WRTDS (stationary flow-normalization or generalized flow-normalization), eight metrics of variation in annual stream discharge (SI Figure 5 and 6) were examined for monotonic trends at each river location.[67] The statistics were evaluated using the non-parametric Mann-Kendall trend test with Theil-Sen slope (SI Figure 5 and 6). In addition, Quantile-Kendall plots were examined for changes in discharge quantiles for the periods of record with discrete water-quality data (Elk 1979-2021; Kootenay 1979-2019) (SI Figure 7).[68] These statistical tests suggested that trends in discharge were small and not statistically significant, so we implemented WRTDS using stationary flow-normalization.

2.3.2 Flow-Normalized Trends. Trends in flow-normalized concentration and load were examined visually and quantitatively for each model using the WRTDS framework. WRTDS was developed to evaluate the combined effects of discharge, season, and interannual trends in water quality. It does this by creating a statistical model of concentrations for each day in the record as a function of discharge, trends in time (expressed in decimal years) and season (SI Analysis methods; Kalman). The model results were integrated over the frequency distribution of discharge to compute flow-normalized estimates. These estimates are designed to allow comparison of year-to-year variations in concentration and load that are independent of the effects of variations in discharge. Removing this source of variation facilitates the identification and estimation of long-term, non-monotonic, trends.[48,69]

The EGRETci package was used to estimate the uncertainty associated with these trends through block bootstrapping.[70] This method, constructs confidence intervals around a trend by randomly subsampling the dataset and recreating the WRTDS model over many iterations to capture variability in the trend estimate. Uncertainty was described using likelihood terminology following Hirsch, Archfield and De Cicco[70], where a trend likelihood is described based on the percentage of increasing or decreasing trends from hundreds of bootstrapped iterations, with higher likelihoods corresponding to higher percentages.[70]

Trend estimates for load are generally presented in the results sections as yield (i.e. area normalized load). Loads are presented as yields to make results more directly comparable, because the Kootenay Watershed has more than twice the contributing area of the Elk Watershed (Figure 1).

Additionally, we chose to explore general effects that the recent implementation of ERM water treatment (post 2015) may have had on the contaminant loading trends at the Elk River at the Highway 93 Bridge sampling location (80-120 km downstream of mining operations). Daily mass removal data from ERM water treatment for Se and NO_3^- through September 2022 are available in Lange and Storb.[22] We carried out a mass balance calculation for Se using the combined daily Se mass removals from all treatment locations. The calculations make two simplifying assumptions. The first is that the Se removed by the treatment plants would have otherwise been transported conservatively (i.e., in its entirety) 80-120 km downstream to the Highway 93 sampling location. The second assumption is that the load reduction at the monitoring location on any given day is equal to the running mean of the Se removal for the prior 30 days. This averaging was selected to account for different treatment locations upstream and to account for surface water advection and dispersion, as well as exchange of the solute between the surface water and groundwater systems. This second assumption results in a smoothing of the overall treatment effect assessment but doesn't have a significant effect on the concentration reduction estimates at longer time scales (e.g. seasonal to annual). The smoothed data were used to construct a concentration surface using the same indexing (for time and logQ) as the original Se concentrations computed from the monitoring data within the Elk Se WRTDS model.[22]

2.3.3 Load Estimates. The EGRET package[65] was used to provide daily estimates of concentration and load, which were then summarized into a time series of annual mean concentration and annual load using a state space modeling approach with the WRTDS_Kalman method.[71, 72] The WRTDS_Kalman method uses the WRTDS model and the measured sample values to compute optimal estimates for each day, in a manner that accounts for serial correlation in the model residuals. It is a method that has been shown to generate some of the most accurate estimates of load based on comparisons with measurements.[71, 72] Comparisons between observed and modeled daily loads and WRTDS and WRTDS_Kalman annual estimates are in SI Figure 8 and 9.

2.3.4 Concentration – Discharge Relationships. Concentration-discharge relationships (C-Q) were plotted and assessed for variation with respect to seasons and over time, providing a summary of solute dynamics and insights into changing watershed flushing and dilution processes. WRTDS captures changes in C-Q relationships over time and generates a modeled 3D surface that shows expected concentrations across a range of possible discharge values for each day in the period of record (SI Figure 10). Information contained within this 3D surface allows for inferences about the effects of changing hydrologic conditions, evidenced through changing behavior in the C-Q relationship over time.[48, 73, 74]

Two different visualizations were explored; The first set of visualizations are like traditional C-Q plots, but on an arithmetic scale and relationships at three different days over time are shown on the same graph. Multiple iterations of these graphs were examined looking at historical changes during high and low discharge times of year. The second set of plots looked at changes in concentration over time for each constituent at specific discharges based off a flow duration curve generated for 60 days surrounding a specific date (high – 95th quantile, intermediate- 50th quantile, and low discharges – 5th quantile), during peak discharge (June 13) and low discharge (January 1) times of the year. These two graphical tools provide visual assessment of patterns that can illustrate potential changes in solute delivery dynamics over time, because patterns in the relationship of C-Q provide perspective on the mechanisms related to the mixture of precipitation water and stored water in stream-flow generation.

There are three common patterns that are frequently described for C-Q relationships: dilution, mobilization and chemostasis. Often these patterns vary between individual solutes and watersheds, so they are useful for characterizing the average behavior of a watershed.[75-80] As such, a change in C–Q behavior over time may indicate hydrologic shifts, such as changes in land use that effect basin characteristics, changes or transformations in constituents and sources, or altered flow paths (i.e. solute delivery dynamics). [76, 81, 82]

3. Results and Discussion

3.1 Concentration

Within the two watersheds both land use and bedrock geologies are generally different, suggesting the possibility that the background concentrations of solutes might vary (SI Methods Geology). Background Se concentrations have the potential to be higher in the Elk River than the Kootenay River, based on bedrock geologic sources independent of mining.[83] The mean Se concentration on the Kootenay River (2003-2019) is near 0.1 μg/L and is likely to have decreased 10% over this time (Table 1). The annual mean concentration for Se on the Elk River at Highway 93 in 2022 was 5.77 μg/L, but in 1985 it was 0.89μg/L (Table 1).[22] The 1985 value is 295% greater than concentrations on the Elk River upstream of the mines and in the neighboring Flathead River watershed, based on values that were measured by Hauer and Sexton [15] (0.3 μg/L). There is limited literature surrounding background concentrations in the Elk River, but values upstream of the mines and the concentration increases early in the record (SI Table 3) suggest that concentrations of mine related contaminants may have been increasing since before concentrations were initially measured.

C2 Table 1. Trends in loads and concentrations (flow-normalized) for select time periods for the Elk River at Highway 93 Bridge and the Kootenay River at Fenwick.[22] Uncertainty is described in terms of likelihood from bootstrapped replicates.

	Elk River at Highway 93							
	Constituent	First year	Last year	Percent change over period: Entire period	Start to 2002	2002 to end	first year mean	Last year mean
Se	Annual load (t/yr)	1985	2022	+443%	+146%	+121%	1.97	10.72
	Concentration (µg/l)			+551%	+178%	+134%	0.89	5.77
NO_3^-	Annual load (t/yr)	1979	2022	+697%	+155%	+213%	279	2226
	Concentration (mg/l)			+784%	+165%	+234%	0.13	1.18
SO_4^{2-}	Annual load (t/yr)	1985	2022	+129%	+57%	+46%	35872	82165
	Concentration (mg/l)			+120%	+51%	+45%	22.40	49.30

	Kootenay River at Fenwick							
	Constituent	First year	Last year	Percent change over period: Entire period	Start to 1998	1998 to end	first year mean	Last year mean
Se	Annual load (t/yr)	2003	2019	-15%	NA	NA	0.50	0.43
	Concentration (µg/l)			-10%	NA	NA	0.10	0.09
NO_3^-	Annual load (t/yr)	1979	2019	-4.60%	-2.50%	-2%	607.79	580.55
	Concentration (mg/l)			-8.50%	+2.1%	-11%	0.12	0.11
SO_4^{2-}	Annual load (t/yr)	1985	2019	+19%	+18%	+0.58%	113974	135136
	Concentration (mg/l)			+7.7%	+13%	-5%	35.50	38.20

Likelihood category name	**Likelihood results from bootstrap confidence interval analysis**
Highly likely downward trend	>95% likelihood trend is downward
Likely downward trend	70% to 95% likelihood trend is downward
Highly uncertain	30% to 70% likelihood trend is downward
Likely upward trend	70% to 90% likelihood trend is upward
Highly likely upward trend	>95% likelihood trend is upward

Like Se, NO_3^- and SO_4^{2-} concentrations in the Elk River have followed a trajectory where average, maximum, and minimum concentrations are all increasing, in addition to increases in amplitude in annual patterns among high and low concentrations (Figure 3b,c,d). While NO_3^- concentrations have remained stable or decreased marginally in the Kootenay River (Figure 3b,c,d).[84] NO_3^- and SO_4^{2-} concentrations entering KOC do not exceed current CA regulatory guidance for water quality.[85, 86] However, NO_3^- concentrations in the Elk River have increased 784% between 1979-2022, more than any other solute (Table 1). NO_3^- concentrations in the Elk River were like those in the Kootenay River when concentrations were first measured in the 1980's, but recently measured high values each year are nearing half the 3 mg/L CA guidance level (Table 1).[85]

Since the year 2000, measured Se concentrations in the Elk River have constantly exceeded recommended ambient water quality guidelines to protect aquatic life set by both the Canadian Council for Ministers of the Environment (1 µg/L) and the British Columbia Ministry of Environment and Climate Change Strategy (alert concentration: 1 µg/L; guideline: 2 µg/ L).[47, 87] In KOC, Se concentrations have exceeded U.S. regulatory criteria since July, 2020 (Figure 3a).[45] In contrast Se concentrations in the Kootenay remain one to two orders of magnitude lower and stable (Figure 3b).

The Elk River location at Highway 93 is not a CA regulatory compliance point, therefore concentrations here are being compared to the CA recommended federal and provincial Se guidelines.[47, 87] In 2021, the average annual measured Se concentration in the Elk River where it enters KOC was 5.87 µg/L, the maximum was 9.65 µg/L, and the minimum was 3.51 µg/L. We used the WRTDS model output, to calculate the expected number of days that modeled concentrations exceeded the guideline criteria (SI Methods, Exceedance Probability). For the Federal guideline of 1 µg/L; exceedances increased from 70 days a year in 1984, to 252 in 1990, to 350 in 2000, and by 2006 exceedances were greater than the alert guideline for more than 360 days per year, for each year until the present. Similarly, for the 2 µg/L provincial guideline; the expected number of exceedances per year rose from 7 days in 1984, to 31 days in 1990, to 217 days in 2000, and by 2010 it is greater than the CA recommended guidance concentration for more than 360 days per year for every year since 2010.

3.2 Loads

Loads discussed in this section are based on estimates optimized for accuracy (WTRDS_Kalman) and not flow-normalized.[71, 72] Within the Elk and the Kootenay Watersheds, snowmelt runoff is the time of year when most of the discharge moves through each system and with it most of the mass of solutes delivered to KOC over the water year. The mean annual discharge for the Kootenay River is roughly twice that of the Elk River (SI Figure 3, SI Table 3) and generally, the proportion of water from the two tributaries discharged into KOC did not change over the last 40 years (SI Table 3). On average, the Elk River contributed 29% of the combined discharges, but in the last decade contributed 95.3% of the Se, 76% of the NO_3^- and 38% of the SO_4^{2-} to KOC from the two tributaries combined (SI Table 3). Annual variations in loads for both rivers were driven by year-to-year variations in discharge and within the Elk River variation in loads were also coupled with the large increase in solute concentrations from mining operations.

The masses of SO_4^{2-} delivered to KOC from these rivers were the most similar relative to the other solutes (SI Table 3). Mining in the Elk River Watershed has added additional mass to background weathering and other SO_4^{2-} sources, which was evident by the increase in annual load estimates over time, from 25% of the combined load in the late 1980's to 38% in the 2010's (SI Table 3).

NO_3^- load increased more than the other two constituents within the Elk River over its respective period of record. This increase is likely driven by ammonium nitrate used in mine blasting[13] and to some extent geogenic ammonium ions in the coal-bearing strata.[29] In 1979, when NO_3^- was first measured, roughly 30% of the NO_3^- entering KOC was coming from the Elk River, a proportion like the discharge volume, (concentrations were similar in both rivers), but by 2014, it had increased up to 83% of the combined NO_3^- contributed to KOC (SI Table 3).

Annual loads of Se have grown by over an order of magnitude over the past 35 years (SI Table 3). When water quality monitoring was initiated in the Elk River in 1984, estimated loads were already 3-4 times greater than loads entering KOC from the Kootenay River (SI Table 3).

The mass of NO_3^- and Se being delivered to KOC is now dominated by contributions from the Elk River, despite its much lower discharge volume (SI Table 3). Discharge in the vicinity of waste rock dumps in the Elk River Watershed have been shown to be attenuating, with decreasing peak and stormflows and increasing baseflows.[58] Thus, the timing of solute mass delivery may shift towards a greater proportion during baseflow periods, due to increased transient storage and solute sources from growing volumes of waste rock.[4] Likewise, several studies have shown that transport is the limitation for solute delivery out of waste rock within the Elk River Watershed.[5, 13, 14] This limitation is present despite increased infiltration capacities that can be three times greater than the infiltration capacity of the natural catchment.[60] This suggests that if more flow through waste rock occurred, more solute mass would be mobilized – an important consideration given changing precipitation patterns and form (rain vs snow) as a result of climate change.

A portion of the most contaminated surface waters are now being treated, and the volume of water to be treated is planned to increase through 2027.[88] Wellen, Shatilla and Carey[14] and Wellen, Shatilla and Carey[5] found that mining practices, including surface reclamation, the shape of waste rock piles, and the age of waste rock dumps, also have potential to reduce Se delivery to water bodies, suggesting operational practices, which change in time, are likely to influence loads (increase or decrease). Water treatments may reduce loads to KOC going forward, but the magnitude and timing of that reduction is not well understood. Likewise, there has been little published study of surface water-groundwater interaction in mine-effected areas and areas downstream. A recent update to the Regional Water Quality Model (RWQM) added a surface water-groundwater partitioning component, suggesting solute movement in groundwater is an important mechanism that needs to be understood in the context of downstream water quality.[29, 89, 90] Loads from both shallow and deep groundwater are a source of uncertainty in this system, and very little is known about the effects on deep groundwater from waste rock dumps on top of bedrock limestone with high karst potential.[89, 91] Presently only surface water is treated and current plans are to treat only surface waters into the future.[29] With limited knowledge surrounding surface water-groundwater interaction and potential groundwater contamination, it is unclear if treatment of surface water alone will sufficiently reduce the mass of solutes moving downgradient in the watershed and into KOC to meet U.S. water quality regulations (Figure 3a).

<u>3.3 C-Q Relationships</u>

For each of the three solutes in the Kootenay River, the C-Q relationships for individual solutes were consistent over time, suggesting consistency in the solute delivery mechanisms for the watershed (SI Figure 11a-c). Se and SO_4^{2-} both showed a dilution signal. Se shows a slight decrease across all concentrations from 2003 to 2019 while SO_4^{2-} shows an increase across all discharges between 1986 and 2019, but more so at lower discharges (SI Figure 11a,c). NO_3^- exhibited a mobilization pattern, suggesting that the mechanisms behind the Kootenay's delivery of NO_3^- to KOC is driven by runoff solute delivery mechanisms, coupled with an overall decrease across all concentrations between 1986 and 2019 (SI Figure 11b).

In contrast to the Kootenay River, the Elk River C-Q relationships for Se and NO_3^- changed in time (Figure 4), while SO_4^{2-} maintained a consistent dilution signal, but the magnitude of concentrations increased across all discharges (SI Figure 11f). In 1986 Se and NO_3^- in the Elk River exhibit C-Q relationships that were indicative of mobilization or chemostasis solute delivery mechanisms (Figure 4). However, by 2008 and into 2021, the solute delivery for both Se and NO_3^- changed to dilution (Figure 4a, b). Like SO_4^{2-}, as time progressed both Se and NO_3^- exhibit an overall increase in concentrations across all discharges, with the largest magnitude of increase occurring at the lowest flows.

In addition to more traditional perspectives on C-Q relationships we used information within the WRTDS models to evaluate how concentrations have changed at different discharges (i.e. seasonal high, average or low discharge), during different seasons (Figure 4c, d and SI Figure 12).[65] In the Elk River for all three constituents, we observed that solute concentrations at lower discharges increased faster than those at higher discharges (SI Figure 12). This was the case during both high discharge (June 13) and low discharge (January 1) times of the year (Figure

4c,d). However, the magnitude of concentration increase was greatest during the lowest discharges, during the baseflow time of year (Figure 4c,d). Patterns shown in Figure 4 display a notable change in relative rates of increase (slope) that occurred in the mid-2000’s, where the concentrations begin to increase more rapidly across the different discharges – this is particularly evident in Se during the low flow time of year (Figure 4d). In contrast, patterns across discharges in the Kootenay River for all three solutes during high and low discharge periods are relatively flat over time (not shown). The shift in Se and NO_3^- C-Q signals, (Figure 4a, b) and the largest concentration increase during low flows (Figure 4), suggests that processes controlling solute delivery to surface water have changed over the last 40 years in the Elk River Watershed, with a notable increase in the lowest flows relative to higher flows taking place in the early to mid-2000's (Figure 4d).

Concentrations of solutes at baseflow conditions are generally a good indicator of the chemistry of shallow groundwater. Existing reports suggests that most streams in the Elk Valley gain shallow groundwater.[58] Therefore, shifts in C-Q behavior (increased concentrations during baseflow) may reflect increased solute loading to streams from shallow groundwater. However, increasing concentrations at low discharges are also consistent with observations made by Nippgen et al.[4] who suggest waste rock dumps may be altering the hydrologic storage and release of solutes within Appalachian coal mine affected watersheds, causing increased solute mobilization during the baseflow period via surface water drainage from dumps. The switch in Se and NO_3^- C-Q behavior to dilution and the largest increase in concentrations at the lowest baseflows in (Figures 3, 4) suggest that the ERM may now behave like a point source, with a near continuous release of higher concentration solutes that are being diluted by water from unmined portions of the Elk River Watershed. The changing solute behavior in the Elk River could be the result of contaminated groundwater downgradient of waste rock dumps and or increases in surface water sources (concentration and/or discharge) emerging from waste rock dumps, or both – suggesting that additional investigation to understand the mechanisms driving the change in solute delivery in the Elk River Watershed may support understanding the source(s). In contrast, solute dynamics in the Kootenay River have remained relatively consistent over time.

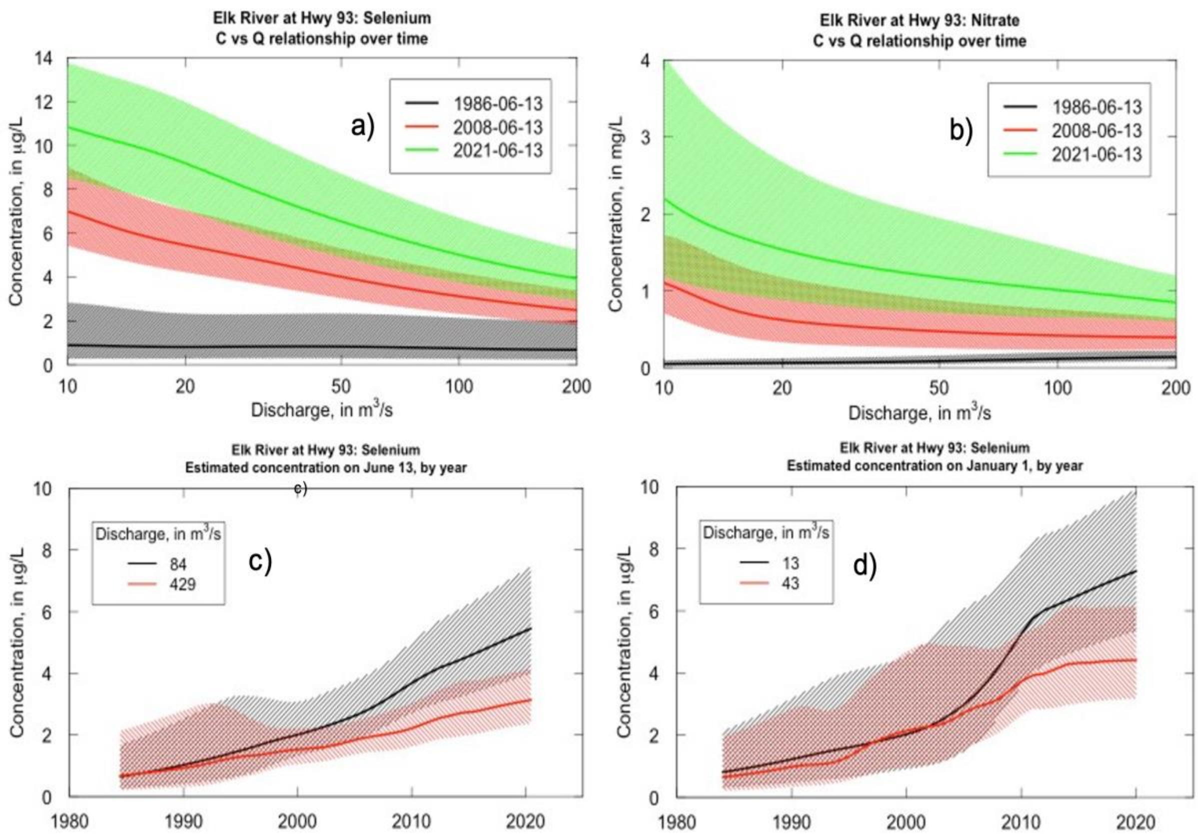

C2 Figure 4. Concentration vs discharge relationships for Se (a) and NO3- (b) in the Elk River at Highway 93.[22, 65] Colored lines show modeled C-Q relationships for three different dates, illustrating changes in solute behavior over time. Shading (a,b) shows the 90% prediction interval for each date. Changes in concentration over time at two different discharges and two times of the year (c, d) illustrates patterns at the high discharge time of year (June 13, c) and shows a low discharge time of year (Jan 1, d). Lines (c, d) represent the 5th, and 95th percentiles for flow duration curves for 60 days around (30 days before and after) each date. Shading (c, d) shows the 90% prediction interval for each flow. Additional solutes and Kootenay River data are shown in SI Figure 11 and 12.

3.4 Trends

3.4.1 Differing Trends from the Paired Watersheds. Trends in load are presented in this section as yields, to facilitate direct comparisons between the two watersheds which are different in size. In the Kootenay River there are gaps in the SO_4^{2-} and NO_3^- record and a shorter Se record due to discrepancies in concentration measurements after methods changes, thus the time periods for comparison vary slightly (Figure 5). However, the flow-normalized trends (concentration and yield) for these constituents in the Kootenay River either decreased (Se and NO_3^-) or increased marginally (SO_4^{2-}) (Figure 5, Table 1).[22]

The flow-normalized trends of Se, NO_3^-, and SO_4^{2-}, for both concentrations and yields in the Elk River document significant water quality changes (Figure 5, Table 1); Se concentrations in the mine-affected tributaries to the Elk River are among the largest in published literature and the increases in Se and NO_3^- in the Elk River at Highway 93 are the largest percent increases documented in the primary literature that are known to the authors.[35, 92] Flow-normalized concentrations of Se, NO_3^-, and SO_4^{2-} in the Elk River increased over their respective periods of record by 551% (Se), 784% (NO_3^-) and 120% (SO_4^{2-}). Trends in yield mirrored those in concentration but were slightly smaller in magnitude for Se (443%), and NO_3^- (697%) and slightly larger for SO_4^{2-} (129%) (Table 1). This occurred while marginal decreasing trends in Se and NO_3^- and a slight increase in SO_4^{2-} were observed in the Kootenay River.

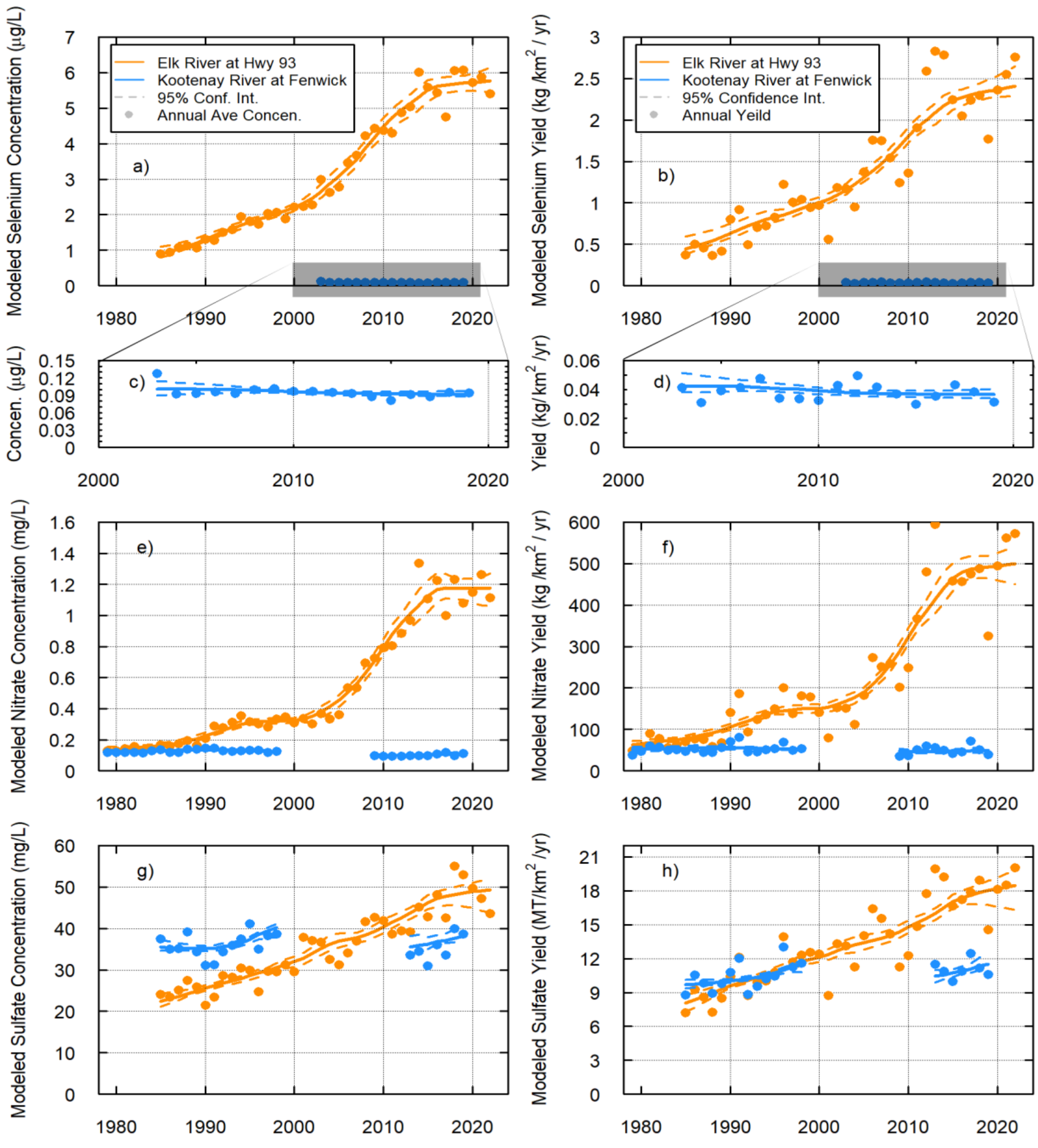

C2 Figure 5. Flow-normalized trends for the Elk River (orange) and the Kootenay River (blue).[22,48,65] Concentration trends for each constituent are on the left (a,c,e,g), trends in yield (i.e., area normalized load) are on the right (b,d,f,g).22 Each row is a constituent; (a,b) are total Se, (c,d) illustrates lower total Se for the Kootenay River only, (e,f) illustrates lower total Se for the Kootenay River only, (e,f) illustrates NO3-, and (g,h) are SO42-. Solid dots are mean annual concentration or annual yield. Dashed lines are 90% confidence intervals.[65]

Modeled annual average NO_3^- concentrations in the Kootenay River and the Elk River were nearly the same when monitoring began in 1984 (Figure 5c). Since 1984, concentrations of NO_3^- have been declining in the Kootenay. There were likely significant declines after the closure of a fertilizer manufacturing plant (ammonia phosphate) on the Saint Mary River in 1987 (a major tributary to the Kootenay, Figure 1).[93] Conversely, NO_3^- concentrations have been on an upward trajectory in the Elk River from mining operations.

SO_4^{2-} concentrations in the Elk River in 1984 were lower than concentrations in the Kootenay River, concentrations were comparable between the two rivers in the mid 2000's, but have been higher in the Elk River ever since (Figure 5e). Generally, SO_4^{2-} and Se weather from the same parent material, however the difference in concentration trends over time (Figure 5a, g) suggest that different geochemical or biogeochemical mechanisms affect these solutes in different ways within the Elk River Watershed.

In the Kootenay River percent change for SO_4^{2-} and Se yield are greater than the respective changes in concentrations. However, NO_3^- is the opposite, again suggesting mechanisms delivering NO_3^- are different from the other two solutes (Table 1, Figure 5), which aligns with the mobilization signal that was observed in the C-Q relationship for NO_3^- on the Kootenay River (SI Figure 11). Overall concentration and yields entering KOC from the Kootenay River have been consistent historically, especially in comparison to the large magnitude increase in all three solutes from the Elk River.

For NO_3^- and Se in the Elk River, the increase in concentration has been larger in percentage terms than the corresponding increase in yield, but this pattern was the opposite for SO_4^{2-} (Table 1, Figure 5a-d). This is driven by the larger relative increases in concentration during baseflow, but due to low discharge volumes during those times, trends in load have not increased at the same rate. The relative magnitude of increase in SO_4^{2-} (concentration and yield) was less than the other two constituents, and the trend was more consistent in terms of the magnitude of the slope through time (Figure 5e, f). The difference in the SO_4^{2-} trends in the Elk River (compared to NO_3^- and Se) was likely driven by chemical weathering of other geologic sources of sulfate delivering higher baseline concentrations.

3.4.2 Mining operations drive trends in the Elk River. Three distinct time periods of increasing trends in NO_3^- and Se were observed in the Elk River (Figure 5a-d). The first period was from the start of the record through the early 2000's and was characterized by a moderate (relative) slope. The second period showed an increase in the slope around 2002, suggesting the concentrations and corresponding solute delivery were increasing at a faster rate. The third period coincided with a taper in the slope around 2015. The 2015 inflection is noteworthy for NO_3^- and Se – as the first reduction in the slope of the trend that has been underway for 3 to 4 decades. What caused the taper in both the concentration and yield trends around 2016 is uncertain, but we pose three hypotheses that could explain changes in hydrologic processes that could cause a slowing in the rate of increase late in the record:

1) The RWQM [58] incorporates lag times, to account for the time it takes for weathering or release of solutes after waste rock deposition, to begin appearing in surface waters. Those times in the RWQM average to 7 years, across all watersheds. Similar work in primary literature has also shown that 8-year lag times were necessary to model solute delivery within the West Line Creek mine site. Past work has tied concentration with waste rock volume and areal extent [5, 13, 14]. Other work has also shown the possibility of some depletion to occur in this time scale for

NO_3^-; however, it is unlikely that depletion of Se is occurring on the same time scale, the similarity in trends between Se and NO_3^- suggest that the pattern in trends is not driven by depletion alone.[27, 94, 95] Thus, we hypothesize that the lag times coupled with decreases in waste rock production from economic conditions [16] could explain the inflection in trend near 2015, as they begin to present themselves roughly 7 years after the economic recession of 2008 when there was a decrease in coal production (Figure 2). This hypothesis could be tested by evaluating annual waste rock production over time; however, those data are not publicly available since 2010.[96]

2) Alternatively, other mine engineering processes could have affected the trend. A transition to deeper waste rock dumps with fixed aerial extent, could increase flow path lengths and limit or delay solute transport temporarily.[5, 13, 25] Past work has shown that solute loss in waste rock dumps is driven by vertical percolation and not lateral inputs of water [5] Similarly, Villeneuve et al. [60] describe three stages in the evolution of the dump footprint for the West Line Creek operation, which is part of the Line Creek Mine in the ERM; first a linear increase in dump area from 1981 to 1998; followed by decreasing rates of areal expansion between 1998 and 2003; and a relatively constant dump area from 2003 to 2014, suggesting an increase in thickness (longer vertical flow paths) during this time.[5] Here we hypothesize that the inflection point could occur because of the lagged effect of these longer flow paths through waste rock, resulting in longer time periods before solutes will enter downstream surface waters. However, longer flow paths are also associated with more oxidation of sulfide minerals and may cause a subsequent increase in concentrations and loads later in time.[5, 13, 25]

3) The third hypothesis is that the reduction in the trend slope is a result of water treatment. ERM have invested in active and passive water treatment technologies to mitigate NO_3^- and Se concentrations into the Elk River Watershed. Pilot efforts began as early as 2014 but the first treatment system was not fully operational until 2018 (SI Table 4).[29] To explore the effect that the treatment may have had on the contaminant loading at the Elk River at the Highway 93 Bridge sampling location (80-120 km downstream of mining operations), we carried out a mass balance calculation, (described here in terms of Se) using daily mass removals from ERM water treatment facilities between October 2015 and September 2022.[22]

Figure 6a shows the sum of the 30-day running mean of the daily Se removal from all treatment locations. Figure 6b shows modeled daily concentrations at Elk River and the estimated concentrations that could have occurred if there were no treatment removals upstream and assuming our assumptions are reasonable. There were notable reductions in simulated concentration during times of low discharge (late summer through early spring). But, at times of high discharge (June) the decreases due to treatment were limited. Figure 6d shows a load perspective; the simulated effect of the treatment plants approaches a 40% reduction for portions of the months of lowest discharge in 2022 but limited in the months of the highest discharge. During high discharge months, the amounts removed are minor (less than 5%) compared to the total amount of Se being transported by the Elk River (SI Figure 13a). Additional perspective on the effect of treatment can be seen in SI Figure 13b & c which illustrates (like the patterns in Figure 4) that concentrations are generally higher in the months of lower discharges. Concentration increases between 2006-2015 and 2016-2022 were substantial for high and low discharge segments of the year, and the effect of the treatment was greater for the months of low discharge than it was for the months of high discharge.

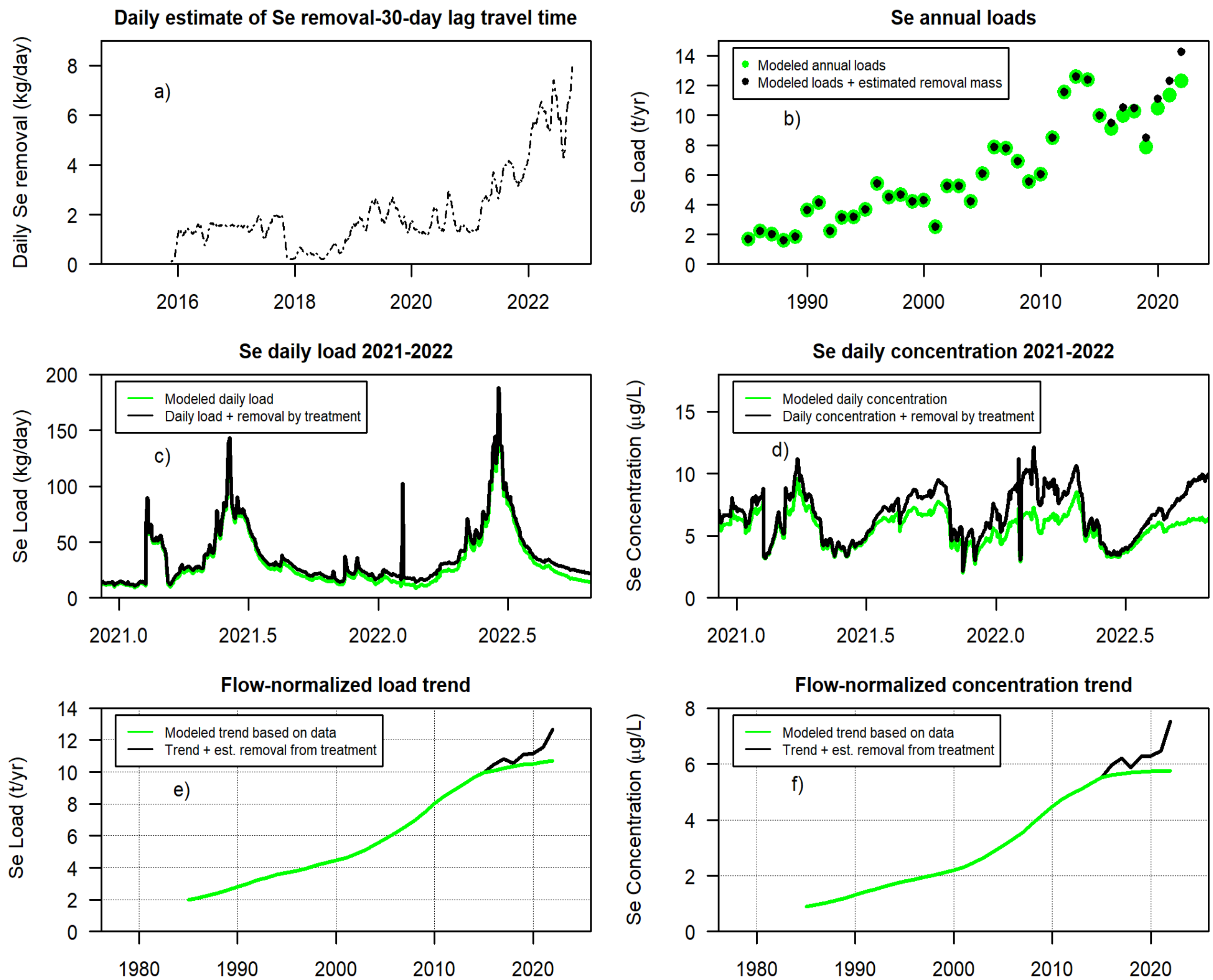

C2 Figure 6. Modeled influence of Se mass removal from three water treatment facilities in the Elk River Watershed.[22] Estimated Se removal by water treatment in the Elk River at Highway 93, using a 30-day lagged running mean (a). Estimated daily concentration (b) and load (c) of Se, Elk River at Highway 93. The green line (c,d,e,f) is an estimate based on the model optimized for accuracy (WRTDS_Kalman)[71,72]. The black line (c,d,e,f) is based on this same model with the addition of the estimated amount of Se that was removed by treatment (only 2021 and 2022 shown for temporal resolution). Green dots (d) are the estimated annual load of Se for the Elk River WRTDS_Kalman model. Black dots (d) are the annual loads if there were no treatment. Flow normalized trend for load (e) and concentration (f) in green, black is an estimate of the trend in the absence of treatment.

In general, with our assumptions in mind, our analysis suggests the water treatment has been successful in reducing concentrations during the months of lower discharge (when concentrations tend to be highest). But, for the high discharge months, the effect of treatment has been modest. This translates directly to treatment effects on loads, suggesting treatment will have less effect on annual loads and more on some seasonal and annual average concentrations. Accurate understanding of treatment effects on concentrations downstream may be supported by a more complete understanding of the hydrologic and hydrogeologic system between the ERM and the outlet to KOC than is currently available. How mass removals by treatment have actually affected concentrations and loads at the Highway 93 Bridge site (without our two simplifying assumptions) is not yet clear.

Incorporating masses removed from treatment back into the WRTDS model of Se in the Elk River, provides support for a combination of hypotheses. The plateau in the Se trends is still present even with mass removals incorporated (i.e., without treatment) and we see an increase in the delivery rate after 2021(Figure 6e, f). This suggests the reduction in rate around 2016 may not only be the result of treatment but may be more likely attributed to; hypothesis 1, showing a possible lagged rebound in production post-recession, or hypothesis 2, dump construction practices that are focused on increasing height of dumps have resulted in longer flow paths and further lagged times for solutes to enter downstream surface waters. The absence of the rise in solute concentration and load around 2021 (Figure 5a, b and Figure 6e, f) suggests that in recent years concentrations could have resumed a more rapid rate of increase without treatment, which aligns with increases in solutes from longer flow paths in hypothesis 2. The modeled trends (Figure 5a-d) and trends incorporating removal (Figure 6e, f) suggest that the overall patterns in trends may be more likely attributed to hypotheses 2 and 3, with the plateau driven by operational practices that increased flow path lengths and coincident timing that would have resulted in another rapid increase in the trend around 2021 if treatment had not been present in its current capacity. Fundamentally the combination of changes in waste rock production, waste rock management and water treatment are likely to drive the magnitude of downstream solute delivery.

4. Implications and Future Outlook

Through retrospective analyses of water quality and discharge data, this study indicates increasing mine waste solute loads have been exported from ERM operations to the transboundary KOC, while solute delivery from the Kootenay River has remained largely unchanged. The large differences in load contributions from these two watersheds point to the potential further increase in solutes into the Elk River with coal mine expansions or new coal mines and for solutes to continue to be released after the end of mining.[20, 95] The physiographic setting of the ERM and their operational practices have resulted in tons of Se and thousands of tons of other mine wastes (NO_3^-, SO_4^{2-}) entering U.S. waters (SI Table 3) that are now resulting in exceedances of United States and Canadian water quality regulations in KOC (Figure 3a).[22, 24, 45, 46, 97]

Within the mining affected watershed of the Elk River, beginning in the early 1980's, there have been large, documented increases in both load and concentration for Se, and NO_3^-.[5, 14, 22, 23] There have been large relative increases in SO_4^{2-} as well. In the case of Se, the Elk River is now delivering on average 95% of the combined annual Se mass to KOC. Large increases and recent plateaus in the concentration and load trends suggest that changes may be driven by waste rock production, waste rock dump geometry (vertical vs. lateral expansion), and mine surface water treatment in the last 1-2 years; these processes seemingly dictate the magnitude of downstream delivery of solutes.

The changes in the C-Q relationships and increasing baseflow concentrations in the Elk River indicate increased chemical weathering of solutes due to increased waste rock volume and year-round mobilization of solutes into surface water. Solutes may be transported to the Elk River via waste rock dump discharge to surface water and/or through groundwater discharge to surface water. Changes in the solute delivery dynamics in the Elk River suggest the hydrologic processes responsible for delivering solutes have changed over the past four decades. In the 1980's C-Q relationships for Se and NO_3^- showed patterns indicative of surface runoff mechanisms exhibited through mobilization and chemostatic behavior but are now dominated by dilution. This is further evidenced by the largest increase in concentrations of all three solutes in the Elk River during the lowest discharges during the late fall and winter baseflow months. However, a better understanding of surface water-groundwater interaction may support observations in the study by filling a knowledge gap, as the increase in solute concentrations at low discharges could be partially attributed to a contaminated groundwater source.

Past studies have shown that lower topographic relief and higher infiltration rates, coupled with increased transmissivity of material from waste rock dumps (i.e., valley fill), can alter the flow paths and residence time of water within mined watersheds.[4] What is surprising is that we can observe this through changing solute dynamics 80-120 km downriver from the ERM, at the outflow of the larger Elk River Watershed, indicating the profundity of the change that large-scale mining is having on solute transport.

The spring freshet is still the period when the largest mass of solutes is delivered to KOC. However, baseflow is the time when the highest concentration waters flow into the reservoir. Based on the patterns we have observed in the changes in solute dynamics, increasing transient storage and solute generation from the growing volume of waste rock has raised baseflow solute concentrations more than those occurring at other times in the year, which may increase further with additional mining. High baseflow concentrations are likely to persist unless water treatment can increase and outpace growing solute delivery from additional mining and address all major sources. Our analyses suggest that current ERM water treatment has potential to decrease concentrations in the Elk River during low discharge portions of the year; however, treatment will have much less effect on the annual loads being delivered to KOC – meaning, how solute concentrations are distributed in time and space within the reservoir may have significant implications for downstream ecosystems, fisheries, and water quality targets. This is an important finding that could assist in management of beneficial uses in KOC because the mass of contaminants being delivered to KOC post ERM water treatment may not have the same proportional reduction that annual average concentrations may have. Likewise, there is limited primary literature on the effects to the aquatic ecosystem in KOC thus far. But this work is a first step in quantifying masses of solutes entering the reservoir over time, which is context for ecological studies going forward.

Mining operations have changed the solute delivery dynamics within the Elk River Watershed between 1984 and 2022, while the Kootenay River has remained largely unchanged. With the introduction of water treatment and planned treatment expansions, understanding how treatment further changes the hydrologic and geochemical system in conjunction with planned and proposed mining operations may support management decision making. There are still many areas that could benefit from further research, including: surface water-groundwater interaction in the Elk Valley and its mine-affected tributaries, an understanding of the magnitude and extent of groundwater contamination, the long-range transport potential of Se, and better understanding of how treatment will affect downstream concentrations and loads. In addition, an assessment of the Se and NO_3^- mass balance in KOC including developing understanding of spatial and temporal distribution of contaminants within KOC both current and historic, may improve understanding of the downstream effects on solute concentrations and loads from mining operations and associated water treatment – an important consideration given the potential for effects to aquatic ecosystems and fisheries. Given current and planned mine operations and water treatment, it is unclear whether current and planned surface water treatment will be sufficient to meet downstream water-quality regulations. This transboundary system presents a unique challenge for managers and decision makers on both sides of the border and has implications for water quality throughout the Kootenai Basin and the broader Columbia River system.

Associated Content

Supporting Information.

Additional tables, figures, and method details. The Supporting Information is available free of charge at https://pubs.acs.org/doi/10.1021/acs.est.3c05090.

Funding Sources

This work was funded by United States Geologic Survey (USGS) appropriations to the USGS Wyoming-Montana Water Science Center and funding from USGS Water Mission Area.

Acknowledgments

Thank you to; Lauren Zinsser, Jennifer Murphy, and Dr. Chris Parsons (Environment and Climate Change Canada) for providing technical review of this work. David Lange assisted in the preparation of Figure 2. Roy Sando provided help with Figure 1 and Table 1 in the supporting information. Ayisha Yeow (Environment and Climate Change Canada) provided information surrounding Canadian data sources and quality, the study area, and history and to Chelsey Cameron (Environment and Climate Change Canada) for reviewing some of the language surrounding Canadian water quality regulations. British Columbia Ministry of Environment and Climate Change Strategy for providing information about the study area. The Ktunaxa Nation Council for information about the study area and history. Teck Resources Limited for providing us with daily mass removal data for water treatment operations. Any use of trade, firm, or product names is for descriptive purposes only and does not imply endorsement by the U.S. Government.

Abbreviations

KOC, Koocanusa Reservoir

ERM, Elk River Mines

RWQM, Teck Resources Regional Water Quality Model

WRTDS, Weighted Regression on Time Discharge and Season

MT, Montana

ID, Idaho

USGS, United States Geologic Survey

B.C., British Columbia

CA, Canada

U.S. United States

ECCC, Environment and Climate Change Canada

References

(1) Cooley, H.; Gleick, P. H. Climate-proofing transboundary water agreements. Hydrological Sciences Journal 2011, 56 (4), 711-718. DOI: 10.1080/02626667.2011.576651.

(2) Wolf, A. T. Criteria for equitable allocations: The heart of international water conflict. Natural Resources Forum 1999, 23 (1), 3-30. DOI: 10.1111/j.1477-8947.1999.tb00235.x.

(3) Puri, S.; Aureli, A. Atlas of transboundary aquifers: Global maps, regional cooperation and local inventories; ISARM Program, 2009.

(4) Nippgen, F.; Ross, M. R. V.; Bernhardt, E. S.; McGlynn, B. L. Creating a more perennial problem? Mountaintop removal coal mining enhances and sustains saline baseflows of Appalachian watersheds. Environmental Science & Technology 2017, 51 (15), 8324-8334. DOI: 10.1021/acs.est.7b02288.

(5) Wellen, C.; Shatilla, N. J.; Carey, S. K. The influence of mining on hydrology and solute transport in the Elk Valley, British Columbia, Canada. Environmental Research Letters 2018, 13 (7), 074012. DOI: 10.1088/1748-9326/aaca9d.

(6) Meredith, E.; Wheaton, J.; Kuzara, S. Hydrogeologic responses to 50 years of surface coal mining and 20 years of coalbed-methane production in southeastern Montana with an emphasis on reclamation at Big Sky Mine; Special Publication 122: Geology of Montana; Montana Bureau of Mines and Geology, 2021. https://www.mbmg.mtech.edu/pubs/GeologyofMontana/#gsc.tab=0 (accessed March 22, 2023).

(7) Palmer, M. A.; Bernhardt, E. S.; Schlesinger, W. H.; Eshleman, K. N.; Foufoula-Georgiou, E.; Hendryx, M. S.; Lemly, A. D.; Likens, G. E.; Loucks, O. L.; Power, M. E.; et al. Mountaintop mining consequences. Science 2010, 327 (5962), 148-149. DOI: 10.1126/science.1180543.

(8) Sergeant, C. J.; Sexton, E. K.; Moore, J. W.; Westwood, A. R.; Nagorski, S. A.; Ebersole, J. L.; Chambers, D. M.; O'Neal, S. L.; Malison, R. L.; Hauer, F. R.; et al. Risks of mining to salmonid-bearing watersheds. Science Advances 2022, 8 (26). DOI: 10.1126/sciadv.abn0929.

(9) Ktunaxa Nation Home Page. Who We Are. 2023. https://www.ktunaxa.org/who-we-are/ (accessed December 2022).

(10) Presser, T. S.; Naftz, D. L. Understanding and documenting the scientific basis of selenium ecological protection in support of site-specific guidelines development for Lake Koocanusa, Montana, U.S.A., and British Columbia, Canada: U.S. Geological Survey Open-File Regport 2020-1098, 40p.; Reston, VA, 2020. DOI: 10.3133/ofr20201098.

(11) Government of Canada. Provinces/territories, cartographic boundary file-2016 census. 2023. https://open.canada.ca/data/en/dataset/a883eb14-0c0e-45c4-b8c4-b54c4a819edb (accessed 2023 June 22).

(12) U.S. Census Bureau. Cartographic boundary files-Shapefile. 2023. https://www.census.gov/geographies/mapping-files/time-series/geo/carto-boundary-file.2015.html#list-tab-1556094155 (accessed 2023 June 22).

(13) Mahmood, F. N.; Barbour, S. L.; Kennedy, C.; Hendry, M. J. Nitrate release from waste rock dumps in the Elk Valley, British Columbia, Canada. Science of The Total Environment 2017, 605-606, 915-928. DOI: 10.1016/j.scitotenv.2017.05.253.

(14) Wellen, C. C.; Shatilla, N. J.; Carey, S. K. Regional scale selenium loading associated with surface coal mining, Elk Valley, British Columbia, Canada. Science of The Total Environment 2015, 532, 791-802. DOI: 10.1016/j.scitotenv.2015.06.040.

(15) Hauer, F. R.; Sexton, E. K. Transboundary Flathead River: Water quality and aquatic life use final report; Flathead Lake Biological Station, The University of Montana, Polson, Montana, 2013. https://files.cfc.umt.edu/cesu/NPS/UMT/2008/08Hauer_GLAC_water_quality_fnlrpt.pdf (accessed December 2022).

(16) Cooke, C. A.; Drevnick, P. E. Transboundary atmospheric pollution from mountaintop coal mining. Environmental Science & Technology Letters 2022, 9 (11), 943-948. DOI: 10.1021/acs.estlett.2c00677.

(17) Essilfie-Dughan, J.; Hendry, M. J.; Dynes, J. J.; Hu, Y.; Biswas, A.; Lee Barbour, S.; Day, S. Geochemical and mineralogical characterization of sulfur and iron in coal waste rock, Elk Valley, British Columbia, Canada. Science of the Total Environment 2017, 586, 753-769. DOI: 10.1016/j.scitotenv.2017.02.053.

(18) Ross, M. R.; McGlynn, B. L.; Bernhardt, E. S. Deep Impact: Effects of Mountaintop Mining on Surface Topography, Bedrock Structure, and Downstream Waters. Environ Sci Technol 2016, 50 (4), 2064-2074. DOI: 10.1021/acs.est.5b04532.

(19) Lindberg, T. T.; Bernhardt, E. S.; Bier, R.; Helton, A. M.; Merola, R. B.; Vengosh, A.; Di Giulio, R. T. Cumulative impacts of mountaintop mining on an Appalachian watershed.

Proceedings of the National Academy of Sciences 2011, 108 (52), 20929-20934. DOI: doi:10.1073/pnas.1112381108.

(20) Brooks, Alexander C.; Ross, M. R. V.; Nippgen, F.; McGlynn, Brian L.; Bernhardt, Emily S. Excess Nitrate Export in Mountaintop Removal Coal Mining Watersheds. Journal of Geophysical Research: Biogeosciences 2019, 124 (12), 3867-3880. DOI: 10.1029/2019jg005174.

(21) Welch, C.; Barbour, S. L.; Hendry, M. J. The geochemistry and hydrology of coal waste rock dumps: A systematic global review. Science of The Total Environment 2021, 795, 148798. DOI: https://doi.org/10.1016/j.scitotenv.2021.148798.

(22) Lange, D. A.; Storb, M. B. Input files and WRTDS model output for the two major tributaries of Lake Koocanusa: U.S. Geological Survey Data Release; 2023. (accessed June 2023). DOI: 10.5066/P9JP8VGL.

(23) British Columbia Ministry of Forests Lands Natural Resource Operations and Rural Development. BC Water Tool - Watershed. 2023. https://kwt.bcwatertool.ca/watershed (accessed February 9, 2023).

(24) U.S. Geological Survey. USGS water data for the Nation: U.S. Geological Survey National Water Information System database; 2023. (accessed May 25, 2023). DOI: 10.5066/F7P55KJN.

(25) Jamieson, H. E. Geochemistry and mineralogy of solid mine waste: Essential knowledge for predicting environmental impact. Elements 2011, 7 (6), 381-386. DOI: 10.2113/gselements.7.6.381 (accessed December 5, 2022).

(26) Huggins, F. E.; Seidu, L. B. A.; Shah, N.; Huffman, G. P.; Honaker, R. Q.; Kyger, J. R.; Higgins, B. L.; Robertson, J. D.; Pal, S.; Seehra, M. S. Elemental modes of occurrence in an Illinois #6 coal and fractions prepared by physical separation techniques at a coal preparation plant. International Journal of Coal Geology 2009, 78 (1), 65-76. DOI: 10.1016/j.coal.2008.10.002.

(27) Lussier, C.; Veiga, V.; Baldwin, S. The geochemistry of selenium associated with coal waste in the Elk River Valley, Canada. Environmental Geology 2003, 44 (8), 905-913. DOI: 10.1007/s00254-003-0833-y.

(28) Ross, M. R. V.; Nippgen, F.; Hassett, B. A.; McGlynn, B. L.; Bernhardt, E. S. Pyrite Oxidation Drives Exceptionally High Weathering Rates and Geologic CO2 Release in Mountaintop-Mined Landscapes. Global Biogeochem Cy 2018, 32 (8), 1182-1194. DOI: https://doi.org/10.1029/2017GB005798.

(29) Teck Resources Limited. Elk Valley water quality plan: 2022 implementation plan adjustment; 2022.

https://www.teck.com/media/EVWQP_2022_ImplementationPlanAdjustment_Main_Report.pdf (accessed January 9, 2023).

(30) Chowanski, K.; Kunza, L.; Hoffman, G.; Genzoli, L.; Stickney, E. River management alters ecosystem metabolism in a large oligotrophic river. Freshwater Science 2020, 39 (3), 534-548. DOI: 10.1086/710082.

(31) Cianciolo, T. R.; McLaughlin, D. L.; Zipper, C. E.; Timpano, A. J.; Soucek, D. J.; Whitmore, K. M.; Schoenholtz, S. H. Selenium bioaccumulation across trophic levels and along a longitudinal gradient in headwater streams. Environmental Toxicology and Chemistry 2020, 39 (3), 692-704. DOI: 10.1002/etc.4660.

(32) Elser, J. J.; Dobberfuhl, D. R.; MacKay, N. A.; Schampel, J. H. Organism size, life history, and N:P stoichiometry: Toward a unified view of cellular and ecosystem processes. BioScience 1996, 46 (9), 674-684. DOI: 10.2307/1312897.

(33) Elser, J. J.; Andersen, T.; Baron, J. S.; Bergström, A. K.; Jansson, M.; Kyle, M.; Nydick, K. R.; Steger, L.; Hessen, D. O. Shifts in lake N:P stoichiometry and nutrient limitation driven by atmospheric nitrogen deposition. Science 2009, 326 (5954), 835-837. DOI: 10.1126/science.1176199.

(34) Stickney, E.; Kunza, L.; Hoffman, G.; Chowanski, K. Small land cover changes in the transboundary Kootenai River basin greatly alter water quality. River Research and Applications 2021, 37 (4), 605-614. DOI: 10.1002/rra.3783.

(35) Tan, L. C.; Nancharaiah, Y. V.; van Hullebusch, E. D.; Lens, P. N. L. Selenium: environmental significance, pollution, and biological treatment technologies. Biotechnology Advances 2016, 34 (5), 886-907. DOI: 10.1016/j.biotechadv.2016.05.005.

(36) Etteieb, S.; Magdouli, S.; Zolfaghari, M.; Brar, S. Monitoring and analysis of selenium as an emerging contaminant in mining industry: A critical review. Science of The Total Environment 2020, 698, 134339. DOI: 10.1016/j.scitotenv.2019.134339.

(37) Hamilton, S. J. Review of selenium toxicity in the aquatic food chain. Science of The Total Environment 2004, 326 (1), 1-31. DOI: 10.1016/j.scitotenv.2004.01.019.

(38) English, S. G.; Hess, H.; Bishop, C. A.; Porter, E.; Cheng, K. M.; Elliott, J. E. Bioaccumulation and effects of selenium from surface coal mining in an aquatic songbird. Environmental Research 2022, 208, 112702. DOI: 10.1016/j.envres.2022.112702.

(39) Lemly, A. D. Selenium impacts on fish: an insidious time bomb. Human and Ecological Risk Assessment 1999, 5 (6), 1139-1151.

(40) Montana Department of Environmental Quality. Final 2018 Water Quality Integrated Report, 2018. http://kootenaiisrpreview.org/resources/Ecosystem-Restoration-Docs/Monday-Feb-10/LoticEnvironmental2018.pdf (accessed April 4, 2022).

(41) Idaho Department of Environmental Quality. Idaho's 2018/2020 integrated report; State of Idaho Department of Environmental Quality, 2020. https://www2.deq.idaho.gov/admin/LEIA/api/document/download/14888 (accessed March 22, 2023).

(42) Idaho Department of Environmental Quality. Idaho's 2022 integrated report; State of Idaho Department of Environmental Quality, 2022. https://www2.deq.idaho.gov/admin/LEIA/api/document/download/16619 (accessed June 21, 2023).

(43) Administrative Rules of Montana. Selenium standards for Lake Koocanusa and the Kootenai River; Montana Department of Environmental Quality, 2020. http://www.mtrules.org/gateway/RuleNo.asp?RN=17%2E30%2E632 (accessed February 9, 2023).

(44) Idaho Department of Environmental Quality. IDAPA 58.01.02 - Water quality standards; Idaho Department of Environmental Quality, Surface Water Division, 2023. https://adminrules.idaho.gov/rules/current/58/580102.pdf (accessed June 21, 2023).

(45) Montana Department of Environmental Quality. Derivation of a site-specific water column selenium standard for Lake Koocanusa, Montana. Helena, MT: Montana Dept. of Enviornmental Quality; Helena, MT, 2020. https://deq.mt.gov/files/Water/WQPB/Standards/Koocanusa/TSD_Lake%20Koocanusa_Sep2020_Final.pdf (accessed October 3, 2023).

(46) Waste discharge authorization: Authorization management system, authorization #107517. https://www2.gov.bc.ca/gov/content/environment/waste-management/waste-discharge-authorization/find-authorization#searchdocuments (accessed June 1, 2023).

(47) British Columbia Ministry of Environment. Ambient water quality guidelines for selenium technical report update; Water Protection and Sustainability Branch, 2014. https://www2.gov.bc.ca/assets/gov/environment/air-land-water/water/waterquality/water-quality-guidelines/approved-wqgs/bc_moe_se_wqg.pdf (accessed October 3, 2023).

(48) Hirsch, R. M.; Moyer, D. L.; Archfield, S. A. Weighted Regressions on Time, Discharge, and Season (WRTDS), with an application to Chesapeake Bay River inputs. Journal of the American Water Resources Association 2010, 46 (5), 857-880. DOI: 10.1111/j.1752-1688.2010.00482.x.

(49) Cruickshank, A. How pollution from Canadian coal mines threatens the fish at the heart of communities from B.C. to Idaho. The Narwhal (Vicoria, B.C.), 2022. https://thenarwhal.ca/teck-resources-coal-transboundary/ (accessed October 3, 2023).

(50) Lemly, A. D. Review of Environment Canada's Teck Coal environmental assessment and evaluation of selenium toxicology tests on Westslope Cutthroat in the Elk and Fording Rivers in Southeast British Columbia; 2014.

(51) Weber, B. U.S. wants Canada to join investigation of cross-border pollution from B.C. coal mines. The Canadian Press, 2022. https://www.cbc.ca/news/canada/british-columbia/us-canada-cross-border-pollution-investigation-bc-mines-1.6489348 (accessed Sept 27, 2023).

(52) Robbins, J. Tracing mining's threat to U.S. waters. New York Times, July 11, 2023, 1. https://www.nytimes.com/2023/07/11/science/us-canada-mining-pollution.html (accessed July 12, 2023).

(53) U.S. Army Corps of Engineers. Environmental statement: Libby Dam and Lake Koocanusa, Kootenai River, Montana Final Draft, U.S. Army Corps of Engineers, Seattle, Washington; 1972. https://usace.contentdm.oclc.org/digital/api/collection/p16021coll7/id/10891/download (accessed February 9, 2023).

(54) Chisholm, I.; Hamlin, P. Libby reservoir angler census: May 13-October 31, 1987 [i.e. 1985]: Interim Report; ON: DE88005200; Montana Department of Fish, Wildlife and Parks, Kalispell, Montana, 1987. DOI: 10.2172/5494223.

(55) British Columbia Ministry of Forests Lands Natural Resource Operations and Rural Development. B.C. Water Tool - Streamflow & Water Levels. 2023. https://kwt.bcwatertool.ca/streamflow (accessed June 6, 2023).

(56) British Columbia Ministry of Forests Lands Natural Resource Operations and Rural Development. Elk Valley Water Quality Hub - Website. 2023. https://elkvalleywaterquality.gov.bc.ca/ (accessed May 16, 2023).

(57) Clarke, G.; Northcote, B.; Katay, F.; Tombe, S. P. Exploration and mining in British Columbia, 2020: A summary. In Provincial Overview of Exploration and Mining in British Columbia, 2020, British Columbia Geological Survey Information Circular 2021-01, British Columbia Ministry of Energy, Mines and Low Carbon Innovation, 2021; pp 1-45.

(58) Teck Coal Limited. 2020 regional water quality model update report; 2021. https://www.teck.com/media/Teck-EVWQP-2020-RWQM-Update-Report.pdf (accessed December 2022).

(59) Golder Associates LTD. Elk Valley Water Quality Plan: Annex D.1 Water quality modelling methods; 2014. https://www2.gov.bc.ca/assets/gov/environment/waste-management/industrial-waste/industrial-waste/mining-smelt-energy/area-based-man-plan/annexes/d1_water_quality_modelling_methods.pdf (accessed June 1, 2023).

(60) Villeneuve, S. A.; Barbour, S. L.; Hendry, M. J.; Carey, S. K. Estimates of water and solute release from a coal waste rock dump in the Elk Valley, British Columbia, Canada. Science of the Total Environment 2017, 601-602, 543-555. DOI: 10.1016/j.scitotenv.2017.05.040.

(61) Province of British Columbia. Order of the Minister of Environment: section 89 environmental management act. 2013; Vol. ministerial order No. M113.

(62) Government of Canada. Columbia River basin long-term water quality monitoring data. 2023. https://open.canada.ca/data/en/dataset/c2adcb27-6d7e-4e97-b546-b8ee3d586aa4/resource/7bb8d1ff-f446-494f-8f3d-ad252162eef5 (accessed February 9, 2023).

(63) Hirsch, R. M. A comparison of four streamflow record extension techniques. Water Resources Research 1982, 18 (4), 1081-1088. DOI: 10.1029/WR018i004p01081.

(64) Moog, D. B.; Whiting, P. J.; Thomas, R. B. Streamflow record extension using power transformations and application to sediment transport. Water Resources Research 1999, 35 (1), 243-254. DOI: 10.1029/1998WR900014.

(65) Hirsch, R. M.; De Cicco, L. A. User guide to Exploration and Graphics for RivEr Trends (EGRET) and dataRetrieval: R packages for hydrologic data: U.S. Geological Survey Techniques and Methods 4-A10; Reston, VA, 2015. DOI: 10.3133/tm4A10.

(66) RStudio Team. RStudio: integrated development environment for R; RStudio, PBC, Boston, MA, 2021. http://www.rstudio.com/ (accessed January 12, 2023).

(67) Choquette, A. F.; Hirsch, R. M.; Murphy, J. C.; Johnson, L. T.; Confesor, R. B. Tracking changes in nutrient delivery to western Lake Erie: Approaches to compensate for variability and trends in streamflow. Journal of Great Lakes Research 2019, 45 (1), 21-39. DOI: 10.1016/j.jglr.2018.11.012.

(68) Helsel, D. R.; Hirsch, R. M.; Ryberg, K. R.; Archfield, S. A.; Gilroy, E. J. Statistical methods in water resources; Reston, VA, 2020. (accessed February 13, 2023). DOI: 10.3133/tm4A3.

(69) Rowland, F. E.; Stow, C. A.; Johnson, L. T.; Hirsch, R. M. Lake Erie tributary nutrient trend evaluation: Normalizing concentrations and loads to reduce flow variability. Ecological Indicators 2021, 125, 107601. DOI: 10.1016/j.ecolind.2021.107601.

(70) Hirsch, R. M.; Archfield, S. A.; De Cicco, L. A. A bootstrap method for estimating uncertainty of water quality trends. Environmental Modelling & Software 2015, 73, 148-166. DOI: 10.1016/j.envsoft.2015.07.017.

(71) Lee, C. J.; Hirsch, R. M.; Crawford, C. G. An evaluation of methods for computing annual water-quality loads: U.S. Geological Survey Scientific Investigations Report 2019-5084; Reston, VA, 2019. DOI: 10.3133/sir20195084.

(72) Zhang, Q.; Hirsch, R. M. River water-quality concentration and flux estimation can be improved by accounting for serial correlation through an autoregressive model. Water Resources Research 2019, 55 (11), 9705-9723. DOI: 10.1029/2019WR025338.

(73) Zinsser, L. M. Trends in concentration, loads, and sources of trace metals and nutrients in the Spokane River Watershed, northern Idaho, water years 1990–2018; 2020. http://pubs.er.usgs.gov/publication/sir20205096 (accessed March 22, 2023). DOI: 10.3133/sir20205096.

(74) Luoma, K.; Niemi, J. V.; Aurela, M.; Fung, P. L.; Helin, A.; Hussein, T.; Kangas, L.; Kousa, A.; Rönkkö, T.; Timonen, H.; et al. Spatiotemporal variation and trends in equivalent black carbon in the Helsinki metropolitan area in Finland. Atmospheric Chemistry and Physics 2021, 21 (2), 1173-1189. DOI: 10.5194/acp-21-1173-2021.

(75) Clow, D. W.; Drever, J. I. Weathering rates as a function of flow through an alpine soil. Chemical Geology 1996, 132 (1), 131-141. DOI: 10.1016/S0009-2541(96)00048-4.

(76) Knapp, J. L. A.; von Freyberg, J.; Studer, B.; Kiewiet, L.; Kirchner, J. W. Concentration–discharge relationships vary among hydrological events, reflecting differences in event characteristics. Hydrology and Earth System Sciences 2020, 24 (5), 2561-2576. DOI: 10.5194/hess-24-2561-2020.

(77) Clow, D. W.; Mast, M. A. Mechanisms for chemostatic behavior in catchments: Implications for CO2 consumption by mineral weathering. Chemical Geology 2010, 269 (1), 40-51. DOI: 10.1016/j.chemgeo.2009.09.014.

(78) Godsey, S. E.; Kirchner, J. W. Dynamic, discontinuous stream networks: Hydrologically driven variations in active drainage density, flowing channels and stream order. Hydrological Processes 2014, 28 (23), 5791-5803. DOI: 10.1002/hyp.10310.

(79) Godsey, S.; Kirchner, J.; Clow, D. Concentration discharge relationships reflect chemostatic characteristics of U.S. catchments. Hydrological Processes 2009, 23, 1844–1864.

(80) Exploration and Graphics for RivEr Trends (EGRET); USGS: 2023. https://pubs.usgs.gov/tm/04/a10/ (accessed Febuary 9, 2023).

(81) Murphy, S. F.; McCleskey, R. B.; Writer, J. H. Effects of flow regimes on stream turbidity and suspended solids after wildfire, Colorado Front Range, USA. In Wildfire and Water Quality: Processes, Impacts and Challenges, Vol. IAHS Publ. 354; IAHS Press, 2012; p 325.

(82) Murphy, J. C.; Hornberger, G. M.; Liddle, R. G. Concentration–discharge relationships in the coal mined region of the New River basin and Indian Fork sub-basin, Tennessee, USA. Hydrological Processes 2014, 28 (3), 718-728. DOI: 10.1002/hyp.9603.

(83) Katay, F. Exploration and mining in the Kootenay-Boundary Region, British Columbia. In: Exploration and Mining in British Columbia, 2014; Information Circular 2015-2; British Columbia Ministry of Energy and Mines, British Columbia Geological Survey, 2015. https://cmscontent.nrs.gov.bc.ca/geoscience/publicationcatalogue/InformationCircular/BCGS_IC2016-01-03.pdf (accessed February 9, 2023).

(84) British Columbia. Canada-B.C. Water Quality Monitoring Program. https://www.nrs.gov.bc.ca/ecms/CanadaBCWQReports/TrendReports/BC08NK0003_SiteReport.html (accessed Sept 27, 2023).

(85) British Columbia Ministry of Environment. Water quality guidelines for nitrogen (nitrate, nitrite, and ammonia); 2009. https://www2.gov.bc.ca/assets/gov/environment/air-land-water/water/waterquality/water-quality-guidelines/approved-wqgs/nitrogen-addendum.pdf#:~:text=For%20nitrate%20%28as%20N%29%2C%20the%2030-d%20average%20concentration,to%20protect%20marine%20aquatic%20life%203.7%2A%20mg%20L-1 (accessed June 28, 2023).

(86) British Columbia Ministry of Environment. Ambient water quality guidelines for sulphate; 2013. https://www2.gov.bc.ca/assets/gov/environment/air-land-water/water/waterquality/water-quality-guidelines/approved-wqgs/sulphate/bc_moe_wqg_sulphate.pdf#:~:text=Sulphate%20is%20a%20potentially%20harmful%20contaminant%20in%20freshwater,toxicity%20data%20to%20develop%20a%2030-day%20average%20guideline. (accessed June 28, 2023).

(87) Environment and Climate Change Canada. Canadian environmental protection act, 1999 federal environmental quality guidelines: Selenium; 2022. https://www.canada.ca/content/dam/eccc/documents/pdf/pded/feqg-selenium/Federal-environmental-quality-guidelines-selenium.pdf (accessed June 1, 2023).

(88) Teck Resources Limited. Water quality in the Elk Valley. 2023. https://www.teck.com/sustainability/sustainability-topics/water/water-quality-in-the-elk-valley/ (accessed February 9, 2023).

(89) Burri, N. M.; Weatherl, R.; Moeck, C.; Schirmer, M. A review of threats to groundwater quality in the anthropocene. Science of The Total Environment 2019, 684, 136-154. DOI: 10.1016/j.scitotenv.2019.05.236.

(90) Teck Coal Limited. 2020 annual report; 2020. https://www.teck.com/media/2020-Annual-Report.pdf (accessed February 9, 2023).

(91) Ganapathi, H.; Phukan, M. Environmental hazards of limestone mining and adaptive practices for environment management plan. In Environmental Processes and

Management: Tools and Practices, Singh, R. M., Shukla, P., Singh, P. Eds.; Springer International Publishing, 2020; pp 121-134.

(92) Conde, J. E.; Sanz Alaejos, M. Selenium concentrations in natural and environmental waters. Chemical Reviews 1997, 97 (6), 1979-2004. DOI: 10.1021/cr960100g.

(93) Pommen Water Quality Consulting. Water quality assessment of St. Mary River at Wycliffe (1973 – 2003); 2004. https://www2.gov.bc.ca/assets/gov/environment/air-land-water/water/waterquality/monitoring-water-quality/kootenay-wq-docs/wq_ko_stmary_river_wycliffe.pdf (accessed June 1, 2023).

(94) Huang, M.; Barbour, S. L.; Hendry, M. J. Simulating nitrate release from an unsaturated coal waste rock dump. Science of The Total Environment 2021, 779, 146429. DOI: https://doi.org/10.1016/j.scitotenv.2021.146429.

(95) Hendry, M. J.; Biswas, A.; Essilfie-Dughan, J.; Chen, N.; Day, S. J.; Barbour, S. L. Reservoirs of Selenium in Coal Waste Rock: Elk Valley, British Columbia, Canada. Environ Sci Technol 2015, 49 (13), 8228-8236. DOI: 10.1021/acs.est.5b01246.

(96) Day, S.; Kennedy, C.; Pumphrey, J. Interpretation of selenium release from coal mine waste rock dumps, Southeastern British Columbia, Canada; 2012.

(97) Read, E. K.; Carr, L.; De Cicco, L.; Dugan, H. A.; Hanson, P. C.; Hart, J. A.; Kreft, J.; Read, J. S.; Winslow, L. A. Water quality data for national-scale aquatic research: The Water Quality Portal. Water Resources Research 2017, 53 (2), 1735-1745. DOI: 10.1002/2016WR019993.

CHAPTER THREE

DIEL AND SEASONAL VARIATION IN SOLUTES: FEEDBACK AMONG NITRATE, PRIMARY PRODUCTION, AND WATER QUALITY IN AN ALPINE STREAM ECOSYSTEM

Contribution of Authors and Co-Authors

Manuscript in Chapter 3

Author: Meryl Storb
Contributions: Designed the study, collected data, trained technicians to collect data, conducted the analysis, wrote the manuscript.

Co-Author: Robert A. Payn
Contributions: Provided funding and resources, wrote the metabolism model used in the analysis, provided guidance on the study and design and analysis, provided mentorship and extensive editorial assistance with the manuscript.

Co-Author: Juliana D'Andrilli
Contributions: Provided significant assistance with data collection and study design, edited the manuscript, provided mentorship.

Co-Author: Stephanie A. Ewing
Contributions: Provided mentorship and guidance on interpretation and edited the manuscript.

Co-Author: Kristin Gardner
Contributions: Helped facilitate access and data collection, contributed to knowledge of the area, and edited the manuscript.

Co-Author: Wyatt Cross
Contributions: Assisted with interpretation and edited the manuscript.

Manuscript Information

M.B Storb, R.A. Payn, J. D'Andrilli, S.A. Ewing, K.K. Gardner, W.F. Cross

Freshwater Science

Status of Manuscript:
x Prepared for submission to a peer-reviewed journal
☐ Officially submitted to a peer-reviewed journal
☐ Accepted by a peer-reviewed journal
☐ Published in a peer-reviewed journal

Abstract

Nutrient pollution is now one of the most pervasive sources of impairment to streams and rivers, with significant contributions of pollutants originating from nonpoint sources that are the result of human influence on the landscape. Headwater streams are important locations to understand the consequences of human alterations to nutrient dynamics due to the potential for disproportionate effects from nutrients in a setting that would otherwise have lower natural nutrient contributions to the stream ecosystem. We examined how chronic, nonpoint source nitrate loading altered primary production in an alpine, headwater stream subject to urban and amenity development pressures. We then evaluated how autotrophic nutrient demand from fertilized primary production affected the variation in in-stream nutrient concentrations with diel and seasonal periodicity. Our study was located on the West Fork of the Gallatin River (WFG) in Big Sky, MT. We collected and compared data from two reaches on the WFG with known variation in chronic nitrate loading due to an increase in nitrate concentrations over a 3km section. We characterized the hourly variation in nitrate, chloride, and sulfate concentration at each site over 24-36 hour sampling events conducted monthly from May – October of 2016. Furthermore, we used two-station dissolved oxygen measurements over the study season to estimate daily gross primary production, and we collected benthic epilithon samples for characterizing ash free dry mass and chlorophyl a. Spatiotemporal relationships among combinations of solutes suggested wastewater contributions were a source of chronic nitrate loading to the downstream reach, which fueled much higher primary production and algal biomass growth over the growing season compared to the unaffected upstream reach. Autotrophic uptake from fertilized growth masked true nitrate loads entering the downstream

reach by reducing concentrations during the daytime relative to nighttime and during the algal growing season relative to colder months. This work shows that seasonal and diel variation in biogeochemical processes propagate to corresponding variation in nutrient concentrations and imply that characterizations of nutrient loads that do not consider diel variation in concentration may be underestimated.

Keywords: nutrients, solutes, primary production, nonpoint source, processing, TMDL

1. Introduction

Nonpoint source nutrient pollution from diffuse human activities is one of the most pervasive sources of impairment to freshwaters in the United States (U.S.) (US EPA 2013), but unlike other common impairments such as sediment and bacteria, the downstream propagation of nutrient contamination may be mitigated by biological activity. Many studies have focused on feedbacks between nutrient concentrations and biogeochemical processes in lotic ecosystems, advancing our understanding of coupled elemental cycles (e.g. C and N) and responses to chronic nutrient loading (Dodds and Welch 2000; Mulholland *et al.* 2001; Dodds 2007; Mulholland and Webster 2010; Appling and Heffernan 2014; Hensley and Cohen 2016; Chamberlin *et al.* 2019). Expanding on this understanding of how metabolic coupling of elemental cycles (e.g. C and N) influences both primary production and nutrient concentration dynamics at different timescales is critical to improved understanding of how stream ecosystems might react to increasing nonpoint sources of nutrient loading (Cross *et al.* 2005; Suberkropp *et al.* 2010; Rosemond *et al.* 2015). Similarly, better understanding of the sources of nutrient contamination and instream biogeochemical controls on stream water nutrient concentrations under higher loading conditions is needed to adequately inform current regulatory and management frameworks.

Analyses of spatial and temporal variation in the abundance of solutes in stream and rivers have provided perspective on the drivers of water quality (Lutz *et al.* 2012). Combined spatial and temporal patterns in concentration of multiple conservative and reactive solutes can help tease apart variation in mechanisms of solute delivery apart from the effect of biogeochemical processes occurring in the channel (O'Donnell and Hotchkiss 2019; Valett *et al.* 2022). Biologically important chemical species of nitrogen and phosphorus are well known to limit metabolism and growth of biota in streams (Mulholland and Webster 2010), so downstream propagation of contamination from these nutrients is subject to instream processing under many conditions. Conversely, patterns in conservative solutes that are not influenced by metabolic demand can help infer sources of contributed water because they are not subject to the same in-stream processing effects on their concentrations. Interpretations of coupled conservative and metabolically reactive solute signals over multiple spatial and temporal scales should reveal how feedbacks between variation in contamination sources and instream processing affect assessments of developing water quality issues.

Wastewater disposal is a major source of nutrients and other contaminants of concern to both surface water and groundwater systems globally. Wastewater from human infrastructure commonly has a distinct chemical composition relative to natural environmental waters, allowing potential identification of sources of wastewater from characteristic chemical signatures found in environmental samples (Richards *et al.* 2017; Ledford and Toran 2020). Chloride/bromide ratios are commonly used to look for evidence of septic influence in groundwater (Katz *et al.* 2011).

More recent studies have demonstrated effective tracking of sources of wastewater effluent in streams and rivers using the ratio of a conservative element such as chloride (Cl^-) with other characteristic wastewater indicators (Ledford and Toran 2020). Techniques for using chemistry to identify wastewater contributions to environmental waters are critical for assessment of the mechanisms of potential increases in nutrient loading from increasing human infrastructure.

Chronic nutrient contributions to stream ecosystems from wastewater commonly leads to fertilization, generating excessive primary production and eutrophication (Burns *et al.* 2019; Ledford and Toran 2020), which propagates to an array of changes in ecosystem function (Dodds and Smith 2016; Arroita *et al.* 2019). The strong coupling between oxygen concentrations and diel cycles in primary production suggests that diel variation in other limiting elements (e.g., N) are mediated by the stoichiometry of autotrophic demand (Hall and Tank 2003a; Mulholland *et al.* 2006a; Roberts and Mulholland 2007; Nimick *et al.* 2011; Chamberlin *et al.* 2019). Thus, increases in nutrient sources have implications related to C cycling by inducing autotrophic growth through reduction in a nutrient limitation (Appling and Heffernan 2014; Chamberlin 2020). Furthermore, increases in nutrients have been shown to increase processing of terrestrial carbon sources (Rosemond *et al.* 2015) and secondary production (Cross *et al.* 2005; Suberkropp *et al.* 2010) resulting in changes to energy flow through stream ecosystems and increased inorganic C losses. The propagation of chronic nutrient loading to downstream systems therefore depends strongly on the changes in the productivity of the ecosystem that feedback on changes in the demand for that nutrient.

Past work has shown that light and disturbance are first order constraints on primary production in streams, but nutrient supply is most likely to influence metabolism if the influence of light is constant and disturbance is limited (Hill *et al.* 2009; Hucks Sawyer *et al.* 2009; Bernhardt *et al.* 2018; Arroita *et al.* 2019). Bernhardt et al. (2018), suggested that nutrient pollution resulting from land use change may have less of an effect on stream metabolism than other anthropogenic effects. While this may be the case across the entire stream and river continuum, we expect chronic nutrient loading from human activity is a common cause of eutrophication in previously undeveloped headwaters that would otherwise have low nutrient input. We also expect that the strength in both seasonal and diel variation in nutrient concentrations in these headwaters may therefore provide information about eutrophication states driven by chronic nutrient loading.

Nutrient loads are particularly important to productivity in most alpine, headwater systems because natural higher elevation landscapes generally export lower nutrient loads to the stream (Rattray and Sievering 2001; Bundi and Brittain 2010). Because of this limitation, headwater streams tend to be important sites of temporary nitrogen retention or removal (Grimm 1987; Peterson *et al.* 2001; Alexander *et al.* 2007; Mulholland and Webster 2010; Gardner *et al.* 2011), and are known to integrate chemical signals from adjacent terrestrial ecosystems. High-elevation watersheds are sensitive to climate and land-use influence, providing a unique opportunity to study the response of coupled stream elemental cycles to the changes in land use associated with the growth of amenity communities (Hansen *et al.* 2002). In particular, changes in land use in developing alpine amenity communities may be altering nutrient loads to stream ecosystems due to wastewater management practices (Gardner and McGlynn 2009; Schade and Kusnierz 2010; Gardner *et al.* 2011).

We suggest that patterns in nutrient concentrations in alpine streams subject to amenity land use pressures provide a natural experiment for exploring the consequences of chronic nitrate loading on aquatic ecosystems. The known effects of biological processes on nutrients allow ecosystem behavior to be inferred or compared based on variation in loads or concentration in space and time (Appling and Heffernan 2014; Chamberlin *et al.* 2019). Many studies have explored the influence of nitrate on steam ecosystems (Vitousek *et al.* 1997; Hall and Tank 2003b; Mulholland *et al.* 2006b; Heffernan and Cohen 2010b; Manning *et al.* 2018) with notable contributions from manipulative experiments demonstrating effects of long-term enrichment of nutrients on increasing allochthonous C processing rates (Rosemond *et al.* 2015), increases in secondary production (Slavik *et al.* 2004; Cross *et al.* 2006; Suberkropp *et al.* 2010) and improved understanding of uptake dynamics over gradients of enrichment from limitation to saturation (Earl *et al.* 2006). Contrasting the ecosystem behavior for reaches on the same alpine headwater stream that experience substantially different magnitudes of anthropogenic loading (despite otherwise being similar), presents a unique opportunity to expand understanding of the consequences of chronic nutrient loading.

The goal of this study was to develop a better understanding of the influence of chronic nitrate loading on diel and seasonal variation in the biogeochemical processing of nutrients in streams. We took advantage of a natural experiment in a mountain headwater stream running through a resort community in southwest Montana, where there is a known increase in nitrate concentration along a 3-km section of river likely attributable to wastewater from nonpoint source human infrastructure (Figure 1). Our primary questions were: (1) How does the resulting chronic nitrate loading influence the metabolic regimes controlling diel variation in nitrate concentrations in an otherwise nutrient-limited alpine stream ecosystem? and (2) How does fertilization from chronic nitrate loading alter the distribution of metabolic demand for nitrogen throughout the day and over the algal growing season? We hypothesized that chronic nitrate loading in a mountain headwater stream will have a fertilization effect on primary producers by reducing nutrient limitation. We anticipated greater autotrophic biomass and higher rates of gross primary production (GPP) within stream reaches that receive higher nitrate loads (Figure 2). In stream reaches where nutrient limitation no longer inhibits production (i.e. biomass growth) we hypothesized that oscillating patterns in nitrate concentration would reflect the uptake associated with autotrophic demand. We therefore predict oscillating patterns in diel nitrate concentrations, with lower concentrations during the day and higher concentrations at night in comparison to low-nutrient sites (Heffernan and Cohen 2010a; Nimick *et al.* 2011; Appling and Heffernan 2014; Chamberlin *et al.* 2019) (Figure 2). Similarly, we predicted that the higher amplitudes of diel fluctuations in nitrate concentrations would occur later in the growing season, when nutrient concentrations were generally higher than those at higher flow conditions and more demand from photosynthetic biomass has accumulated (Figure 2). This work shows that chronic nitrate loads effect seasonal and diel variation in biogeochemical processes and propagate corresponding variation in solute concentrations. Strong temporal variations in nitrate concentration imply that stream nutrient assessments that are conducted at times of higher biological demand and do not consider seasonal or diel variation may be underestimating the severity of chronic loading.

2. Methods

Our study took advantage of a unique field setting on the WFG that allowed assessment of two stream reaches in close proximity but with strongly contrasting nitrate loads. We compared two stream reaches to evaluate patterns in solutes associated with treated wastewater and the effects of chronic nitrate loading on biogeochemical cycles. Methods relied on extensive field data collection including deployment of dissolved oxygen sensors and 24-36 hour high-frequency sampling campaigns conducted monthly across a growing season. Analysis methods were focused on exploration of spatiotemporal relationships among conservative and biogeochemically reactive solutes and seasonal patterns in diel solute signals, ecosystem primary production, and autotrophic growth.

2.1 Study Area and Site Selection

The WFG drains an area of 212 km2 and is a fourth order tributary of the Gallatin River, which joins the Jefferson and Madison Rivers to form the Missouri River north of the study area. The WFG drainage area includes the Big Sky Ski Resort and surrounding community. The WFG runs through the main population center in Big Sky, MT (Figure 1). The Big Sky community on the WFG has developed a typical "New West" amenity community development pattern (Hansen et al. 2002) due to resort development driving land use change in an alpine environment. The area has been monitored extensively for the consequences of changes in water quality by community groups (Gallatin River Task Force) and past academic research (Gardner and McGlynn 2009; Campos *et al.* 2011; Gardner *et al.* 2011; Covino *et al.* 2012; Montross *et al.* 2013). Resort development began in Big Sky in the 1970's (Figure 1). The watershed has transitioned from forest and ranching land uses to ski resort development, including a subsequent transition to a landscape dominated by vacation homes ranging from luxury condominiums to mansions. Development was relatively moderate but constant from 1976 until the mid-1990's. With an increasing rate of development over the past three decades, the unincorporated community is facing growing concerns about water resources related to supply, water quality degradation, and wastewater treatment for the expanding population.

The high-relief mountain watershed draining to the study reaches includes regions well above tree line, and the generally shallow soils are located at the lower elevations with exposed bedrock and talus at higher elevations. Bedrock in the watershed is composed of Cretaceous through Upper Jurassic marine and non-marine shales. Bedrock has been uplifted and tilted by local intrusions and regional faulting. The shale bedrock contains thin interbeds of siltstone, mudstone, sandstone, and limestone. Glacial till, glacial outwash, debris flows, landslide deposits, alluvium, and colluvium cover much of the land surface. Bedrock is exposed on steep hillsides. The study area is in a relatively lower gradient and more depositional stretch of the river valley (Figure 1) such that the study reaches flow over relatively thick unconsolidated sediment that has accumulated over shale bedrock (Rose and Waren 2022).

The watershed elevation ranges between 1800 m at the lowest elevation at the confluence with the main stem of the Gallatin River to 3400 m at the summit of Lone Peak. The variation in elevation has a strong influence on the precipitation regime across the watershed. Average annual precipitation is approximately 50 cm at lower elevations and often exceeds 125 cm at higher elevations. Most of the annual precipitation across the watershed falls in the form of snow (Gardner and McGlynn 2009; Montross *et al.* 2013).

Within the WFG, the algal (and terrestrial) growing season is relatively short and associated with lower flows in a snowmelt dominated hydrologic regime. Peak flows typically scour the benthic algal community in ca. June, and the growing season progresses from the return to base flow in ca. July through the return of freezing temperatures and ice formation in ca. November. For most of the winter, WFG streams are partially to completely covered with snow and ice, severely limiting the solar radiation necessary for photosynthesis. In addition, stream temperatures are near 0 °C, which is likely to influence metabolic processes (Brown *et al.* 2004; Yvon-Durocher *et al.* 2010).

Nutrient pollution, primarily in the form of dissolved nitrate, has resulted in nuisance algae growth on several sections of the WFG, and more recently nuisance algal growth has expanded to the receiving main stem of the Gallatin River. Seasonal changes in nitrate concentrations and the locations of elevated nitrate concentrations are well documented from past studies (Gardner and McGlynn 2009; Schade and Kusnierz 2010) and also via a local non-profit watershed group ("Gallatin River Task Force" 2024). In 2010, a TMDL was developed for the entire WFG watershed, as well as composite reaches and tributaries with varying levels of impairment. The TMDL development process identified water quality issues, including sediment, nutrients (both N and P based solutes), and E. Coli, with a particular concern related to nitrate on a smaller section of the WFG through the low-lying Meadow Village area (Figure 1) (Waren *et al.* 2021; Rose and Waren 2022).

Spatial patterns of nitrate concentrations in streams across the WFG have suggested that human activities are strong predictors of nitrate loading from the landscape. The links with land development have been most evident in the dormant season for algae in the winter (Gardner and

McGlynn 2009; Gardner *et al.* 2011), suggesting the potential for stream ecosystem retention of nutrients to mask summertime assessments of the sources of water quality impairments. Previous work has shown that summer and fall algal growth within the WFG streams is elevated above natural background levels (Gardner and McGlynn 2009; Schade and Kusnierz 2010), and a sharp decrease in nitrate concentrations during the growing season suggests that N may be a limiting nutrient within the stream ecosystem (Gardner and McGlynn 2009).

Within the Big Sky Water and Sewer District (BSWSD), treated wastewater is stored in ponds until it is applied as irrigation to the golf course and adjacent fields. Irrigation is limited to the relatively short terrestrial growing season of 75–90 frost-free days from mid-June to mid-September (Covino *et al.* 2012). This source of nitrate dispersed across the landscape was considered in the development of the TMDL (MTDEQ, 2010) and has been linked to nuisance algae growth in the Meadow Village area and other lower sections of the WFG (Gardner and McGlynn 2009; Gardner *et al.* 2011; Covino *et al.* 2012; Rose and Waren 2022). Our data collection targeted the algal growing season that coincides with the timing of the application of treated wastewater to the adjacent landscape (Figure 2). However, more recent studies have suggested that septic wastewater and fertilizer runoff may also be sources of nitrate within this stretch of the WFG (Rose and Waren 2022).

To differentiate the effects of chronic loading, we selected two WFG study reaches in the Meadow Village area that are known to be subject to markedly lower (upstream) and higher (downstream) nitrate loading. Reaches were selected to be as similar as possible in terms of geomorphic and physical setting, while exploiting their locations on a known strong nitrate loading gradient as a natural experimental treatment relative to chronic nutrient inputs (Schade and Kusnierz 2010). The Above Golf Course (AGC) reach has a history of lower nitrate concentrations and is located on the western edge of the Meadow Village Golf Course (Figure 1). While it intersects some of golf course property, the AGC reach is relatively unaffected by drainage from the golf course. The Below Golf Course (BGC) reach has a history of much higher nitrate concentrations and is located ca. 1 km downstream from the eastern edge of the golf course (Gardner and McGlynn 2009; Schade and Kusnierz 2010). The AGC reach is ca. 650 m long and the BGC reach is ca. 800 m long (Figure 1). Both reaches consist of single meandering channels with lower slopes compared to the surrounding alpine systems. The AGC reach was mostly open canopy with limited shading from conifers on the banks in some areas, while the bank vegetation on the BGC reach was dominated by scrub willows with little shading of the channel.

2.2 Field Sampling and Data Collection

In 2016, several high frequency water sampling campaigns intended to characterize diel variation in water chemistry were conducted concurrently at the upstream end of the AGC reach and at the downstream end of the BGC reach. These campaigns were conducted monthly from June through October and consisted of hourly sample collection for 24-36 hours centered around a photoperiod. A shorter campaign just prior to peak flow was conducted in May, where 5 samples were collected approximately every 2 hours.

Temperature, dissolved oxygen (DO), conductivity, and pH of in-situ stream water were measured at each sampling time and location using a handheld probe (YSI). Water samples were collected and filtered in the field using 50 mL rinsed plastic syringes and 0.45-micron filters. A portion of each sample was frozen prior to analysis and was analyzed on a Dionex ion chromatograph for nitrate, chloride, and sulfate concentrations. These analyses were completed in the Environmental Analytical Laboratory at Montana State University.

Four PME miniDOT loggers were used to record DO and water temperature at 10-minute intervals at the upstream and downstream ends of each of the AGC and BGC reaches. Loggers were mounted to the streambed in the thalweg at locations presumed to represent well-mixed channel water. Each logger was checked against saturated conditions for measurement drift and downloaded monthly.

A stage discharge relationship was established at a cross-section near the downstream end of the BGC reach. This site was chosen to complement an existing long-term gauging station that was maintained by the Gallatin River Task Force, where stage was recorded every 10 minutes by an acoustic doppler sensor. Additionally, this work coincided with a Montana Bureau of Mines and Geology (MBMG) Groundwater Investigations Program study that installed an additional pressure transducer near this location, though it was removed on 15 September 2016. Discharge and travel time for each stream reach were measured 5 times. Modal travel time was determined by introducing an instantaneous release of NaCl at the top of the reach and identifying the timing of peak in electrical conductivity measured every 30 seconds at the downstream of the reach (Payn *et al.* 2009). Discharge was measured via velocity-area gauging using a 2-D acoustic doppler flow meter (SonTek FlowTracker) and additional discharge measurements collected by MBMG were incorporated into stage discharge relationships (MBMG 2024).

Biomass samples were collected one to two days after each diel sampling campaign was completed. Five to ten rocks were selected haphazardly from each reach, to capture roughly 150 cm^2 of surface area across a range of representative substrate sizes. Rocks were scrubbed in the laboratory to detach all epilithic biomass from the upward facing rock surface and collect it in a suspension. The rock surface area was subsequently measured using digital image analysis (Analyzing Digital Images). The resulting suspension of epilithon was then filtered onto multiple pre-weighed glass fiber filters (GFF, 0.7µm) for chlorophyl a (chl a) and ash free dry mass (AFDM) measurements. Chl a samples were frozen prior to measurement, extracted with 90% buffered acetone solution, and analyzed on a Perkin Elmer Lambda35 spectrophotometer. AFDM samples were dried, weighed, combusted at 500° C, and re-weighed to provide estimates of total biomass.

2.3 Data Analysis

2.3.1 Wastewater Signal We examined relationships between nitrate, chloride, and sulfate at both stream reaches to explore evidence of wastewater loading. In the well-oxygenated headwater setting of the WFG, sulfate and chloride are effectively conservative tracers that can help inform understanding of sources of water entering the stream. Sulfate is present in groundwater in the WFG with origins related to shale bedrock (Rose and Waren 2022). Dissolved sulfate in stream water may be derived from lithospheric, atmospheric, or soil origins (Mayer *et al.* 2010). We assumed that variation in sulfate in the WFG channel is primarily a signal of groundwater contribution to the stream. This assumption is reasonable if shallow soils generally limit the influence of chemical weathering of sulfate from soils and if the catchment has a limited contributing area for atmospheric deposition of sulfate. Chloride also occurs naturally in groundwater, where concentrations reflect the dissolution of salts in bedrock, especially from marine sediments (Rose and Warrant 2022). In the WFG, we expected that elevated chloride relative to sulfate was indicative of a wastewater signal, because chloride is present in urine, it is commonly added to water in the area via water softeners, and chloride is not removed in the BSWSD treatment process. Where nitrate and chloride concentrations both occur above natural background levels in groundwater and surface water, they may indicate the presence of wastewater effluent (Rose and Warren, 2022). We therefore interpret high chloride concentrations relative to sulfate concentrations as an indicator of the influence of wastewater. Furthermore, we interpret correlation of nitrate concentrations with chloride to sulfate ratios as an indicator that nitrate was originating from wastewater sources.

2.3.2 Metabolism We estimated stream metabolism and air-water gas exchange using inversion of a two-station dissolved oxygen model. Estimates were generated by fitting the Lagrangian model to dissolved oxygen data from the downstream end of each reach, using the upstream oxygen data as input for the model. The two-station method quantifies the effects of metabolism on the parcels of water traveling a defined reach between the upstream and downstream DO sensors,

$$C_{DO,t+\Delta t} = C_{DO,t} + \Delta t P_{GPP} + \Delta t R_{ER} + \Delta t \overline{K}_{g,DO,\Delta t} \frac{\left(C^*_{DO,t} - C_{DO,t}\right) + \left(C^*_{DO,t+\Delta t} - C_{DO,t+\Delta t}\right)}{2}$$

where $C_{DO,t}$ is the concentration of oxygen in a parcel of water passing the upstream end of the reach, $C_{DO,t+\Delta t}$ is the concentration in a parcel of water passing the downstream end of the reach after travel time Δt, P_{GPP} is the effect of GPP on the oxygen concentration in parcels of water, R_{ER} is the effect of aerobic ecosystem respiration (ER) on the oxygen concentration in parcels of water, $\overline{K}_{g,DO,\Delta t}$ is the air-water gas exchange coefficient for DO, and C^* denotes the saturation concentration for a parcel of water passing either the upstream or downstream end of the reach. A model for the downstream concentration $C_{DO,t+\Delta t}$ is derived from solving the equation above.

$$C_{DO,t+\Delta t} = \frac{C_{DO,t} + \Delta t P_{GPP} + \Delta t R_{ER} + \Delta t \overline{K}_{g,DO,\Delta t} \frac{\left(C^*_{DO,t} - C_{DO,t}\right) + C^*_{DO,t+\Delta t}}{2}}{1 + \frac{\Delta t}{2} \overline{K}_{g,DO,\Delta t}}$$

An estimate of the average depth of the stream channel ($\bar{z}$) was then used to convert the effect of GPP on concentration (g m^{-3} day^{-1}) to the more conventional reporting of a mass flux (P^*_{GPP}, g m^{-2} day^{-1}):

$$P^*_{GPP} = \bar{z} P_{GPP}$$

The relative distribution of solar radiation through the day was used to constrain the distribution of GPP through the day, assuming a linear relationship. Exchange of gas with the atmosphere was not measured independently, so the gas exchange coefficient was estimated from the DO data along with the metabolism parameters (Hall *et al.* 2016). The model was fit to downstream DO observations using a maximum likelihood estimate (MLE) approach. We fit each daytime period separately starting at 04:00 and ending 24hrs later. We focused our interpretations on GPP with limited consideration of NEP, due to potential complications of accurately estimating ER in the absence of independent information about gas exchange rates. Average depths were estimated from 5 cross sections for each reach that were repeated three times over the growing season and interpolated over time based on a regression relationship with discharge.

We attempted local monitoring of solar radiation, but data proved unreliable and provided unreasonable fits for the metabolism models, so estimates of metabolism used models of incident solar radiation based on the location of the stream reaches and time of year (Hall *et al.* 2016). The use of modeled solar radiation is likely to bias metabolism estimates on variably cloudy days, but we do not expect that this bias systematically occurred on enough days to influence general interpretation of patterns in GPP between sites or over time.

2.3.3 Diel and Seasonal Patterns in Nitrate and Primary Production Comparisons of higher nitrate concentrations at night were assumed to be the most representative of variation in nitrate loading to the stream because of minimal algal processing. To avoid the influence of outliers, we used the 95^{th} percentile concentrations instead of maximum values from a sampling campaign as representative of the minimally processed loading to the stream. We used the 5^{th} percentile concentrations as representative concentrations during maximum biologic processing. We estimated nitrate loads using 95^{th} percentile concentrations and discharge inferred from stage at the BGC site.

To estimate the degree of instream biological processing relative to loading, we compared the 95^{th} ('high') percentiles of the nitrate concentrations to the 5^{th} ('low') percentiles from each sampling campaign. May samples were not included because they did not span a full 24hr. cycle. June samples were included but spanned two partial nighttime periods, while all other months spanned a single nighttime period. We interpreted the ratio of the differences in the 95th and 5th percentiles to the 95th percentile as a relative fractional metric of the efficiency of the stream in reducing the loading available before export. Ratios closer to 1 suggested that instream processing removes a higher fraction of loading and ratios closer to 0 indicated instream processing removes a lower fraction of loading.

We used linear mixed-effects models to assess the confidence with which patterns in ash free dry mass over the growing season could be explained by nitrate loading (represented by 95^{th} percentile concentrations). We evaluated several linear mixed-effects models to estimate biomass growth while accounting for repeated measures at the same sites over multiple sampling events (R software version 4.3.3, "lme4" package version 1.1-35.1). In our final model, which was slected based on our study design and objectives we assigned month and site as random effects to account repeated measures, and daily mean discharge, 95th percentile concentrations, and number of days since initial sampling as fixed effects. The natural log of AFDM was used as the response variable to improve assumption of normality in the residuals for the model. $\hat{\beta}$ are the estimated coefficents associated with each fixed effect model parameter, which included site $D_{site=MFCP}$, daily discharge $\cdot\, dQ_i$, and the 95th percentile concentration $\cdot\, C95_i$. Coefficients for random effects ($\hat{u}$) were estimated for both site and month.

$$\mathrm{Log}(\widehat{\mathrm{AFDM}}) = \beta_0 + \hat{\beta}_1 \cdot D_{site=MFCP} + \hat{\beta}_2 \cdot dQ_i + \hat{\beta}_3 \cdot C95_i + \hat{\beta}_4 \cdot days_i + \hat{u}_1 \cdot site_i + \hat{u}_2 \cdot month_i + \varepsilon_{ij} ,$$

We calculated an autotrophic index (AI) as the ratio of AFDM to chl a to distinguish the relative autotrophic vs heterotrophic structure of epilithic communities at each site. Epilithic communities that support large populations of bacteria, fungi and other non-chlorophyll bearing organisms, or when more detritus was present should have larger values of AI. Elevated AI values indicate that heterotrophs and organic detritus comprise a larger percentage of epilithic AFDM than autotrophs. AI can vary by over three orders of magnitude, with values >400 typical of organically polluted conditions and ratios around 250 being typical for streams enriched in inorganic nutrients with existing or potential eutrophication problems (US EPA 2018).

3. Results

Patterns in sulfate, chloride, and nitrate concentrations in the BGC reach were very different from those of the AGC reach during our sampling events. Higher nitrate loading present in the BGC reach corresponded with more epilithic biomass (AFDM and chl a) and higher gross primary production compared to the AGC reach. Diel variation in nitrate concentrations were observed at both sites, with the BGC site exhibiting a higher magnitude of uptake but the AGC site exhibiting higher apparent efficiency in processing the input load.

3.1 Diel and Seasonal Patterns in Solute Concentrations

Chloride and sulfate concentrations were similar at the AGC and BGC study reaches in May, followed by decreases in June except for three episodically high Cl values at the BGC site (Figure 3 row c). Mean chloride and sulfate concentrations subsequently increased through July and August at both sites, with a higher rate of increase for chloride relative to sulfate at the BGC site. Chloride concentrations at AGC remain relatively consistent after August at around 5 mg L^{-1} while BGC chloride concentrations continue to increase (e.g. September, mean AGC = 5.60, mean BGC = 10.71 mg L^{-1}) each month until a decrease between September in October. Sulfate concentrations continue to increase gradually for both sites through October (Figure 3 row c and d, Figure 4 b). Sulfate concentrations were somewhat higher (0.1-0.2 mg S L^{-1}) at the BGC reach compared to the AGC reach except for May and August (Figure 3 row d). Sulfate and chloride concentrations at both sites did not exhibit consistent cyclic diel variation (Figure 3 row c and d).

Seasonal patterns from July through October show that nitrate and chloride concentrations were higher and more strongly correlated at the BGC site compared to the AGC site (Figures 3 row b and c and Figure 4a). Chloride to sulfate ratios at the BGC site were an even stronger predictor of nitrate concentrations (Figure 4c). At each time of day and across seasons, concentrations of nitrate below the golf course (BGC) were always higher than concentrations above the golf course (AGC), except for a single measurement in August (Figure 3 row b).

When compared on the same scale, patterns in diel oscillation of nitrate concentrations at the AGC site are less obvious in comparison to those at the BGC site, but both sites exhibit variation in nitrate concentrations throughout the day (Figure 3 row b, Figure 5a). The highest nitrate concentrations generally occur during nighttime hours and lower concentrations generally occur during the afternoon hours (Figure 3 row b). Clear diel oscillations with daytime minima appeared across all months at the BGC site but were the most pronounced during the months of July, August, and September. Diel fluctuations in nitrate with the largest amplitude occurred in August at the BGC site, where daytime to nighttime nitrate concentrations nearly tripled from 0.096 during the day to 0.264 mg N L^{-1} at night (Figure 3 row b, Figure 5 a and b). The largest 95^{th} percentile nitrate concentration at the BGC site was observed in September (0.322 mg N L^{-1}) and the largest 95^{th} percentile AGC concentration was observed in August (0.11 mg N L^{-1}) (Figure 3). With the exception of the high flow conditions in June, the amplitude of the diel variation in nitrate concentrations was always greater at the BGC site (Figure 5b). However, the AGC site exhibited higher efficiency than the BGC site because the amplitude of the diel variation was a larger fraction of the available nitrate concentration (Figure 5 b and c).

3.2 Seasonal Patterns in Loads, Biomass, and Production

In general, discharge (Figure 6a) was more important than concentration in determining variation in the nitrate load, as evidenced by higher loads at the BGC site when concentrations were lower (Figures 3 row a and b and 5b). However, the loads increased at the BGC site in September due to increasing concentrations, despite the recession in streamflow that drove the decrease in loads in September at the AGC site (Figure 5b). Load at the AGC site continued to decrease into October despite an increase in stream discharge. Daily loads were most similar between sites during the late June sampling event, when stream flow was still relatively high and concentrations of nitrate were more uniform (Figure 3 row b, 5b). Across all months, loads at the BGC site were greater, especially in October when the daily load at the BGC site (7.13 kg day $^{-1}$) was 11 times greater than the load at the AGC site (0.64 kg day $^{-1}$, Figure 5b).

All metrics for ecosystem production and algal growth exhibited similar seasonal patterns, with the lowest GPP estimates and the lowest AFDM and chl a measurements at each site occurring in early July and increasing over the growing season through late September. A gradual decline in GPP from September to October was more pronounced than declines in AFDM or chl at both the AGC and BGC sites (Figure 6). Relative temporal patterns in AFDM and chl a were similar between sites across the growing season, though the BGC site had a much larger magnitude of seasonal variation (Figure 6). The AGC reach generally showed less primary production with higher relative GPP occurring later in the growing season (Figure 6). The mean autotrophic index (AI) values for both sites indicated a much larger amount of biomass relative to photosynthetic pigment in epilithic materials (>200). AI was highest early in the season at the BGC reach then generally decreased with no clear pattern but variation in the AGC reach (Table 1).

Results from the mixed effects model suggest that the 95th percentile nitrate concentration provided the most confident predictions of variation in log AFDM (β = 0.363, p = 3×10^{-5}). Days since the first sampling event was the second most meaningful variable in the model in terms that of confidence that it had an effect (β = 0.171, p = 0.171), followed by discharge (β = 1.012, p = 0.244).

4. Discussion

Patterns in the changes in natural abundance of conservative and reactive solutes from AGC to BGC reveal how increases in nitrate concentrations along the West Fork of the Gallatin are likely tied to inputs from treated wastewater. We discuss how chronic loading of nitrate between the study reaches is influencing ecosystem metabolic dynamics, and how the resulting seasonal and diel variation in metabolism is feeding back on observed nitrate concentrations and load dynamics. Understanding of these dynamic controls on nitrate concentrations where chronic loading is causing eutrophication may also have effects on diel concentration dynamics, which are often overlooked in sampling schemes assessing the potential for nutrient impairment.

4.1 Wastewater Signals and Chronic Loading

The relationship between nitrate concentrations and chloride to sulfate ratios below the golf course suggested an influence of wastewater that was not observed above the golf course (Figure 4a and c). Subsequent increases in nitrate and chloride that are disproportionate to the increases in sulfate downstream of the golf course (Figure 3, 4) strongly suggest a meaningful input of wastewater derived sources over the intervening ca. 3 km reach. No clear patterns between nitrate and chloride to sulfate ratios were evident upstream of the golf course (Figure 4c), which would be expected for natural waters unless weathering products from a common upstream geologic source included both nitrate and chloride. Past work in other areas of the WFG have shown some geologic bedrock formations are possible sources of nitrate weathering products (Montross *et al.* 2013). However, the covariance of nitrate and chloride with respect to sulfate is unlikely to be attributable to a natural source, considering the lack of confluences with major tributaries between the AGC and BGC study reaches. This interpretation corroborates other research in the area (Montross *et al.* 2013; Rose and Waren 2022). Rose and Warren (2022) concluded that septic and fertilizer may be more important sources of nitrate to the stream than irrigation with treated wastewater, but interpretation of our results would not likely be able to distinguish between the influence of septic effluent or the distributed application of treated wastewater. The timing of increases in sulfate and chloride (Figure 4) suggest the potential for rapid transport of solutes to the stream from the application of irrigation, but further investigation is necessary for conclusive evidence of specific wastewater sources.

Wastewater likely enters the stream reach primarily via groundwater contributions between the AGC and BGC reaches and potentially via rapid transport in tile drains from the golf course. If groundwater is the source of increases in sulfate concentrations between the AGC and BGC reaches, then consistency in the magnitude of these increases suggest that lateral groundwater inflows along the stream adjacent to the golf course scale with discharge. However, general increases in sulfate concentrations through the growing season suggest that a larger proportion of stream flow is sourced from groundwater later in the baseflow recession (Figure 3 row d). Our interpretation of groundwater inflow corroborates past work that suggests this section of the WFG has some reaches that demonstrate localized net groundwater gains, but the net change in flow between the upstream end of AGC reach and the downstream end of the BGC reach is likely small (Waren *et al.* 2021). Taken together, our results join past research in suggesting that the lateral inputs from groundwater over the Meadow Village section of the West Fork of the Gallatin are a strong control on longitudinal variation in solute concentrations tied to wastewater in the late summer through the winter.

4.2 Influence of Chronic Loading on Metabolic Processing.

Patterns in biomass between reaches show that additional loading of nitrate between the AGC and BGC reach likely had a fertilization effect in fueling additional autotrophic production below the golf course. Results from the mixed linear model suggested epilithic biomass production responded to both availability of nutrients and the length of the growing season. The confidence in the nitrate explanatory variable in the mixed effects model provides evidence that the higher relative biomass growth in the BGC reach is caused by the higher available nitrate present in that reach, as more clearly evident in the 95th percentile concentrations relative to the 5th percentile concentrations. The influence of additional loading is further supported by differences in the epilithic biomass AFDM, and chl a, and GPP estimates between the AGC and BGC reaches. Areal flux of oxygen due to gross primary production generally followed patterns exhibited by biomass and provided additional evidence of fertilization fueled growth. Generally, evidence of chronic nutrient loading on increases in algal production and AFDM in excess of chl a is consistent with previous work on long term nutrient additions (Slavik *et al.* 2004; Rosemond *et al.* 2015; Burns *et al.* 2019), and we observed this pattern consistently through the growing season in the BGC reach in contrast with less growth and production in the AGC reach.

Relatively high epilithic biomass (AFDM) with respect to photosynthetic potential (chl a) at both AGC and BGC sites suggest detritus and or bacterial and fungal assemblages fueled by algal by-products may be an additional component of metabolic activity influenced by chronic nutrient loading (Cross *et al.* 2006; Rosemond *et al.* 2015). Mean AI values for both sites were commonly higher than 250 (Table 2), which is more typical for streams with high abundance of inorganic nutrients and eutrophic conditions (Allan and Castillo 2007). These higher AI values are consistent with the propagation of the effects of nutrient pollution to the heterotrophic community, and is consistent with past work that has shown long-term nutrient loading enhances processing of organic C introduced to the stream from terrestrial sources (Rosemond *et al.* 2015). Nutrient enrichment thus enhances carbon (or energy) flow to secondary production (Slavik *et al.* 2004; Cross *et al.* 2006; Suberkropp *et al.* 2010). Organic matter utilized by microbes and heterotrophic organisms is often the most important component of the energy that moves through an aquatic ecosystem (Wetzel 1995) and high AI values in these stream reaches are consistent with N loading influencing C processing beyond primary production.

4.3 Influence of Nutrient Limitation on Diel Nitrate Concentration Signals

Feedbacks between nutrient loading and ecosystem production are the likely cause of differences in diel variation of nitrate concentrations between the AGC and BGC reaches. Specifically, the BGC site shows signs of less nitrogen limitation or more nitrogen saturation than the AGC site. The differences in nutrient limitation between the AGC and BGC reaches is perhaps most evident in the differences in the apparent efficiency with which the nitrate load is being removed (Figure 5c). Uptake rates of nutrients are often described as a saturating function of availability, to account for other factors becoming limiting as nutrients become more abundant (Dodds *et al.* 2002b; Earl *et al.* 2006). The decrease in efficiency with a decrease in limitation (Figure 5c) are consistent with analyses like Earl et al. (2006) that describe how fertilization of aquatic ecosystems might push aquatic ecosystems toward saturation, resulting in higher absolute uptake rates but lower uptake efficiencies. Past work using data from 2011 has suggested that the WFG was not yet experiencing strong nitrate saturation (Covino *et al.* 2012), and thus may exhibit further decrease in efficiencies with further increases in loading from the landscape.

The difference in amplitudes of daily swings in nitrate concentration between the AGC and BGC sites may also be related to the severity of the physiological response of photoautotrophs to nutrient limitation (Appling and Heffernan 2014; Chamberlin *et al.* 2019). Appling and Heffernan (2014) predicted that diel oscillations in nutrient concentration should only occur when systems are not strongly nutrient limited, because strongly limited systems are more likely to be taking up nutrients outside daylight hours. This prediction was supported by mesocosm experiments by Chamberlin et al. (2019), but limited evidence for this effect has been supported by field experiments. The lower amplitudes of daily swings in nitrate concentration at the AGC site may in part be explained by nutrient limitation driving higher nitrate uptake during the nighttime at this site, in contrast to the clear oscillations and large magnitude changes between day a night concentrations at the BCG site (Figure 3).

The strong diel variation that develops between the AGC and BGC reach suggest highly localized processes that are better explained by stream metabolism than other potential drivers of diel variation in nitrate concentrations. Propagation of a diel signal can be influenced by dispersion, diffusion, transient storage, tributary inputs, groundwater inputs, or tile drainage, all of which may diminish or create lags between peak photosynthesis and observed solute responses (Hensley *et al.* 2014; Hensley and Cohen 2016). We also acknowledge that hydrodynamic effects of residence time can create time lags between nutrient concentrations and primary productivity (Hensley and Cohen 2016). However, because we are working near an upstream section with lower concentrations and diel signals align with daytime minima, we assume that any potential convolution of the nitrate signal in the BGC reach was limited.

4.4 Implications

Differences in diel patterns of nitrate concentration between AGC and BGC suggest that accurate inference of nutrient loading from in-stream concentrations requires consideration of how fertilization from elevated nutrient concentrations translates to diel variation in uptake. Current regulations on nonpoint source pollution are commonly based on limitations of the Total Maximum Daily Load (TMDL) in stream transport, which implies the need to estimate variation in the load of a nutrient over a 24hr period to accurately integrate the observed daily load (Elshorbagy *et al.* 2005; US EPA 2015b). Data collection schemes are typically based on samples taken at a much lower frequency (weekly to monthly) than that which would be necessary to consider temporal variation within a typical 24hr period. More specifically, sampling needs to be at sufficient frequency to understand the feedback effects of algal production on diel variation. For example, relatively low nitrate concentrations measured at a conventional sampling time during a standard workday may be the result of either low inputs (e.g. the AGC reach) or high inputs that are masked by a higher stimulated uptake rate (i.e. the BGC reach in August, Figure 3 b-4). This work suggests that the same daytime concentrations may be achieved via multiple nutrient loading and algal production regimes. Higher resolution information about seasonal transitions in diel variation in concentration is needed to parse the level of biological influence on data backing TMDL determination or any need for estimating daily nutrient loads.

Relatively recent derivations of nitrate TMDL recommendations for the West Fork of the Gallatin may have been biased by under-sampling of the daily concentration signal (Schade and Kusnierz 2010). Potential underestimates can be illustrated by the August diel fluctuations in nitrate concentration at the BGC site, where concentration varied over a 24 hr period by 275%

from a daytime minimum of 0.096 mg NO_3^--N L^{-1} to a nighttime maximum of 0.264 mg NO_3^--N L^{-1}. If we assume similar seasonal and diel dynamics were at play during the TMDL development, loads and concentration targets for the lower WFG are likely to have been underestimated. Montana DEQ has recently (2022) listed the middle section of the Gallatin River main stem as impaired due to severe algal blooms, though it was not listed as impaired by nutrients because water quality monitoring did not reflect consistent exceedances of nutrient criteria. Diel variation observed in the West Fork of the Gallatin illustrates how the outcomes of this TMDL determination may have been different if sampling was designed to provide data when loading would have been the strongest control on concentrations.

5. Conclusion

The results from this work provide better understanding of the influence of chronic nitrate loading on diel variation in the biogeochemical processing of nutrients in streams. Spatiotemporal patterns in stream water chemistry coupled with measurements of ecosystem production illustrate that fertilization from a chronic, nonpoint wastewater source affected ecosystem function, with feedbacks on concentration dynamics at multiple timescales. Wastewater loading to the stream between the study sites appears to be chronically reducing nutrient limitation of the autotrophic community below the golf course. The removal of nutrient limitation stimulated biomass growth and primary production below the golf course over the duration of the 2016 growing season. Increased biomass had a feedback effect on concentrations of nitrate in the stream, where additional demand induced larger magnitude changes in concentration. However, as would be suggested by saturating kinetics, this larger magnitude of nutrient uptake stimulated by higher primary production is associated with a less efficient use of nutrient inputs. This work demonstrates that recognition of the biotic signatures embedded within concentration measurements of metabolically important solutes is critically important to understand temporal variation in those concentrations when they are used to infer loads. Seasonal and diel variation in biogeochemical processes that lead to corresponding variation in solute concentrations are critical for TMDL derivations or regulatory criteria that reflect the true threat to a beneficial use.

References

Alexander, R. B., E. W. Boyer, R. A. Smith, G. E. Schwarz, and R. B. Moore. 2007. The Role of Headwater Streams in Downstream Water Quality1. JAWRA Journal of the American Water Resources Association 43:41–59.

Allan, J. D., and M. M. Castillo. 2007. Stream Ecology: Structure and function of running waters. Springer Science & Business Media.

Appling, A., and J. Heffernan. 2014. Nutrient Limitation and Physiology Mediate the Fine-Scale (De)coupling of Biogeochemical Cycles. The American Naturalist 184:384–406.

Arroita, M., A. Elosegi, and R. O. Hall Jr. 2019. Twenty years of daily metabolism show riverine recovery following sewage abatement. Limnology and Oceanography 64:S77–S92.

Bernhardt, E. S., J. B. Heffernan, N. B. Grimm, E. H. Stanley, J. W. Harvey, M. Arroita, A. P. Appling, M. J. Cohen, W. H. McDowell, R. O. Hall, J. S. Read, B. J. Roberts, E. G. Stets, and C. B. Yackulic. 2018. The metabolic regimes of flowing waters: Metabolic regimes. Limnology and Oceanography 63:S99–S118.

Brown, J. H., J. F. Gillooly, A. P. Allen, V. M. Savage, and G. B. West. 2004. Toward a metabolic theory of ecology. Ecology 85:1771–1789.

Bundi, U., and J. E. Brittain (Eds.). 2010. Alpine waters. Springer, Heidelberg.

Burns, D. A., B. A. Pellerin, M. P. Miller, P. D. Capel, A. J. Tesoriero, and J. M. Duncan. 2019. Monitoring the riverine pulse: Applying high-frequency nitrate data to advance integrative understanding of biogeochemical and hydrological processes. WIREs Water 6:e1348.

Campos, N., R. Lawrence, B. McGlynn, and K. Gardner. 2011. Using Quickbird and Landsat imagery to analyze temporal changes in mountain resort development: Big Sky, Montana 1990–2005. Journal of Applied Remote Sensing 5:053541-053541–14.

Chamberlin, C. 2020. The Role of Ecology in Creating Diel Nitrate Concentration Patterns in Streams and Rivers. Ph.D., Duke University, United States -- North Carolina.

Chamberlin, C. A., E. S. Bernhardt, E. J. Rosi, and J. B. Heffernan. 2019. Stoichiometry and daily rhythms: Experimental evidence shows nutrient limitation decouples N uptake from photosynthesis. Ecology 100:e02822.

Covino, T., B. McGlynn, and R. McNamara. 2012. Land use/land cover and scale influences on in-stream nitrogen uptake kinetics. Journal of Geophysical Research: Biogeosciences 117:G02006.

Cross, W. F., J. P. Benstead, P. C. Frost, and S. A. Thomas. 2005. Ecological stoichiometry in freshwater benthic systems: Recent progress and perspectives. Freshwater Biology 1895–1912.

Cross, W. F., J. B. Wallace, A. D. Rosemond, and S. L. Eggert. 2006. Whole-system nutrient enrichment increases secondary production in a detritus-based ecosystem. Ecology 87:1556–1565.

Dodds, W. K. 2007. Trophic state, eutrophication and nutrient criteria in streams. Trends in Ecology & Evolution 22:669–676.

Dodds, W. K. K., and E. B. Welch. 2000. Establishing nutrient criteria in streams. Journal of the North American Benthological Society 19:186–196.

Dodds, W. K., A. J. López, W. B. Bowden, S. Gregory, N. B. Grimm, S. K. Hamilton, A. E. Hershey, E. Martí, W. H. McDowell, J. L. Meyer, D. Morrall, P. J. Mulholland, B. J. Peterson, J. L. Tank, H. M. Valett, J. R. Webster, and W. Wollheim. 2002. N uptake as a function of concentration in streams. Journal of the North American Benthological Society 21:206–220.

Dodds, W. K., and V. H. Smith. 2016. Nitrogen, phosphorus, and eutrophication in streams. Inland Waters 6:155–164.

Earl, S. R., H. M. Valett, and J. R. Webster. 2006. Nitrogen Saturation in Stream Ecosystems. Ecology 87:3140–3151.

Elshorbagy, A., R. S. V. Teegavarapu, and L. Ormsbee. 2005. Total maximum daily load (TMDL) approach to surface water quality management: Concepts, issues, and applications. Canadian Journal of Civil Engineering 32:442–448.

Gallatin River Task Force. 2024, January 17. Gallatin River Task Force. (Available from: https://gallatinrivertaskforce.org/)

Gardner, K. K., and B. L. McGlynn. 2009. Seasonality in spatial variability and influence of land use/land cover and watershed characteristics on stream water nitrate concentrations in a developing watershed in the Rocky Mountain West: human impacts on spatial N patterns. Water Resources Research 45:n/a-n/a.

Gardner, K. K., B. L. McGlynn, and L. A. Marshall. 2011. Quantifying watershed sensitivity to spatially variable N loading and the relative importance of watershed N retention mechanisms: watershed sensitivity to N loading. Water Resources Research 47:n/a-n/a.

Grimm, N. B. 1987. Nitrogen Dynamics During Succession in a Desert Stream. Ecology 68:1157–1170.

Hall, R. Jr. O., and J. L. Tank. 2003a. Ecosystem metabolism controls nitrogen uptake in streams in Grand Teton National Park, Wyoming. Limnology and Oceanography 48:1120–1128.

Hall, R. O., J. L. Tank, M. A. Baker, E. J. Rosi-Marshall, and E. R. Hotchkiss. 2016. Metabolism, gas exchange, and carbon spiraling in rivers. Ecosystems 19:73–86.

Hansen, A. J., R. Rasker, B. Maxwell, J. J. Rotella, J. D. Johnson, A. W. Parmenter, U. Langner, W. B. Cohen, R. L. Lawrence, and M. P. V. Kraska. 2002. Ecological Causes and Consequences of demographic change in the new west. BioScience 52:151–162.

Heffernan, J. B., and M. J. Cohen. 2010a. Direct and indirect coupling of primary production and diel nitrate dynamics in a subtropical spring-fed river. Limnology and Oceanography 55:677–688.

Hensley, R. T., and M. J. Cohen. 2016. On the emergence of diel solute signals in flowing waters. Water Resources Research 52:759–772.

Hensley, R. T., M. J. Cohen, and L. V. Korhnak. 2014. Inferring nitrogen removal in large rivers from high-resolution longitudinal profiling. Limnology and Oceanography 59:1152–1170.

Hill, W. R., S. E. Fanta, and B. J. Roberts. 2009. Quantifying phosphorus and light effects in stream algae. Limnology and Oceanography 54:368–380.

Hucks Sawyer, A., M. Bayani Cardenas, A. Bomar, and M. Mackey. 2009. Impact of dam operations on hyporheic exchange in the riparian zone of a regulated river. Hydrological Processes 23:2129–2137.

Katz, B. G., S. M. Eberts, and L. J. Kauffman. 2011. Using Cl/Br ratios and other indicators to assess potential impacts on groundwater quality from septic systems: A review and examples from principal aquifers in the United States. Journal of Hydrology 397:151–166.

Ledford, S. H., and L. Toran. 2020. Downstream evolution of wastewater treatment plant nutrient signals using high-temporal monitoring. Hydrological Processes 34:852–864.

Lutz, B. D., P. J. Mulholland, and E. S. Bernhardt. 2012. Long-term data reveal patterns and controls on stream water chemistry in a forested stream: Walker Branch, Tennessee. Ecological Monographs 82:367–387.

Manning, D. W. P., A. D. Rosemond, V. Gulis, J. P. Benstead, and J. S. Kominoski. 2018. Nutrients and temperature additively increase stream microbial respiration. Global Change Biology 24:e233–e247.

Mayer, B., J. B. Shanley, S. W. Bailey, and M. J. Mitchell. 2010. Identifying sources of stream water sulfate after a summer drought in the Sleepers River watershed (Vermont, USA) using hydrological, chemical, and isotopic techniques. Applied Geochemistry 25:747–754.

MBMG. 2024. Montana Bureau of mine and Geology- Ground Water Investigations Program. (Available from: https://mbmg.mtech.edu/WaterEnvironment/GWIP/ProjectUpdate.asp?projectid=BWIPBS&#gsc.tab=0)

Montross, G. G., B. L. McGlynn, S. N. Montross, and K. K. Gardner. 2013. Nitrogen production from geochemical weathering of rocks in southwest Montana, USA: nitrogen from geochemical weathering. Journal of Geophysical Research: Biogeosciences 118:1068–1078.

Mulholland, P. J., C. S. Fellows, J. L. Tank, N. B. Grimm, J. R. Webster, S. K. Hamilton, E. Martí, L. Ashkenas, W. B. Bowden, W. K. Dodds, W. H. Mcdowell, M. J. Paul, and B. J. Peterson. 2001. Inter-biome comparison of factors controlling stream metabolism. Freshwater Biology 46:1503–1517.

Mulholland, P. J., S. A. Thomas, H. M. Valett, J. R. Webster, and J. Beaulieu. 2006a. Effects of light on NO_3^- uptake in small forested streams: Diurnal and day-to-day variations. Journal of the North American Benthological Society 25:583–595.

Mulholland, P. J., S. A. Thomas, H. M. Valett, J. R. Webster, and J. Beaulieu. 2006b. Effects of light on NO_3^- uptake in small forested streams: Diurnal and day-to-day variations. Journal of the North American Benthological Society 25:583–595.

Mulholland, P. J., and J. R. Webster. 2010. Nutrient dynamics in streams and the role of *J-NABS*. Journal of the North American Benthological Society 29:100–117.

Nimick, D. A., C. H. Gammons, and S. R. Parker. 2011. Diel biogeochemical processes and their effect on the aqueous chemistry of streams: A review. Chemical Geology 283:317.

O'Donnell, B., and E. R. Hotchkiss. 2019. Coupling concentration- and process-discharge relationships integrates water chemistry and metabolism in streams. Water Resources Research 55:10179–10190.

Payn, R. A., M. N. Gooseff, B. L. McGlynn, K. E. Bencala, and S. M. Wondzell. 2009. Channel water balance and exchange with subsurface flow along a mountain headwater stream in Montana, United States. Water Resources Research 45.

Peterson, B. J., W. M. Wollheim, P. J. Mulholland, J. R. Webster, J. L. Meyer, J. L. Tank, E. Martí, W. B. Bowden, H. M. Valett, A. E. Hershey, W. H. McDowell, W. K. Dodds, S. K. Hamilton, S. Gregory, and D. D. Morrall. 2001. Control of nitrogen export from watersheds by headwater streams. Science 292:86–90.

Rattray, G., and H. Sievering. 2001. Dry deposition of ammonia, nitric acid, ammonium, and nitrate to alpine tundra at Niwot Ridge, Colorado. Atmospheric Environment 35:1105–1109.

Richards, S., P. J. A. Withers, E. Paterson, C. W. McRoberts, and M. Stutter. 2017. Potential tracers for tracking septic tank effluent discharges in watercourses. Environmental Pollution 228:245–255.

Roberts, B. J., and P. J. Mulholland. 2007. In-stream biotic control on nutrient biogeochemistry in a forested stream, West Fork of Walker Branch: BIOTIC CONTROL ON STREAM NUTRIENT UPTAKE. Journal of Geophysical Research: Biogeosciences 112:n/a-n/a.

Rose, J., and K. Waren. 2022. Hydrogeology and groundwater availability at Big Sky, Montana. Montana Bureau of Mines and Geology Open-File Report 747 98.

Rosemond, A. D., J. P. Benstead, P. M. Bumpers, V. Gulis, J. S. Kominoski, D. W. P. Manning, K. Suberkropp, and J. B. Wallace. 2015. Experimental nutrient additions accelerate terrestrial carbon loss from stream ecosystems. Science 347:1142–1145.

Schade, P., and L. Kusnierz. 2010. The west fork gallatin river watershed total maximum daily loads (TMDLS) and framework watershed water quality improvement plan. Montana Department of Environmental Quality.

Slavik, K., B. J. Peterson, L. A. Deegan, W. B. Bowden, A. E. Hershey, and J. E. Hobbie. 2004. Long-Term Responses of the Kuparuk River Ecosystem to Phosphorus Fertilization. Ecology 85:939–954.

Suberkropp, K., V. Gulis, A. D. Rosemond, and J. P. Benstead. 2010. Ecosystem and physiological scales of microbial responses to nutrients in a detritus-based stream: Results of a 5-year continuous enrichment. Limnology and Oceanography 55:149–160.

US EPA, O. 2013, February 22. History of the Clean Water Act. US EPA. Overviews and Factsheets. (Available from: https://www.epa.gov/laws-regulations/history-clean-water-act)

US EPA, O. 2015, October 7. TMDL Support Documents. Reports and Assessments. (Available from: https://www.epa.gov/tmdl/tmdl-support-documents)

US EPA, O. 2018, October 24. Nutrient Criteria Technical Guidance Manuals. US EPA. Reports and Assessments. (Available from: https://www.epa.gov/nutrient-policy-data/nutrient-criteria-technical-guidance-manuals)

Valett, H. M., M. Peipoch, and G. C. Poole. 2022. Nutrient processing domains: Spatial and temporal patterns of material retention in running waters. Freshwater Science 41:195–214.

Vitousek, P. M., J. D. Aber, R. W. Howarth, G. E. Likens, P. A. Matson, D. W. Schindler, W. H. Schlesinger, and D. G. Tilman. 1997. Human Alteration of the Global Nitrogen Cycle: Sources and Consequences. Ecological Applications 7:737–750.

Waren, K., J. Rose, and R. Breitmeyer. 2021. Groundwater model of the meadow village aquifer at Big Sky, Montana.

Wetzel, R. G. 1995. Death, detritus, and energy flow in aquatic ecosystems. Freshwater Biology 33:83–89.

Yvon-Durocher, G., J. I. Jones, M. Trimmer, G. Woodward, and J. M. Montoya. 2010. Warming alters the metabolic balance of ecosystems. Philosophical Transactions of the Royal Society B: Biological Sciences 365:2117–2126.

Acknowledgements

Thank you to the Gallatin River Task Force, for sharing data and knowledge of the area and for helping to facilitate access to stream sites. Thank you to Big Sky Resort, The Meadow Village Golf Course, and local landowners for permitting access to the stream and supporting our study – including in the middle of the night. Thank you, to the Big Sky Water and Sewer District, for answering questions and providing historical information. Thank you to MBMG for sharing data and information. Thank you for the abundance of field and lab help. This was a very field data intensive project which would not have been completed without the help of many individuals standing in the stream in the middle of the night and scrubbing rocks back in the lab including: Rebecca McNamara, Anna Price, Benjamin Farrick, Taylor Zabel, Emily Hultin, Rose Valor, Stephanie Lynn, Eric Scholl, Jim Junker and Forrest Vogel. Thank you to the Montana State University Environmental Analytical Lab and Jane Klassen for sample analysis. Funding and support was provided by Montana State University College of Agriculture and the Montana Institute on Ecosystems, with analytical support from Montana State University Environmental Analytical Lab.

Tables

C3 Table 1. Mean autotrophic index (ratio of ash free dry mass to chlorophyll a) for each site during each sampling event.

Site	Sample Date	Autotrophic Index
AGC	2016-06-25	297.19
AGC	2016-07-16	473.86
AGC	2016-08-17	259.93
AGC	2016-09-16	313.36
AGC	2016-10-27	67.35*
BGC	2016-06-25	318.47
BGC	2016-07-16	285.36
BGC	2016-08-17	292.58
BGC	2016-09-16	226.34
BGC	2016-10-27	187.91

*Value is based on only one sample, due to instrument failure.

Figures

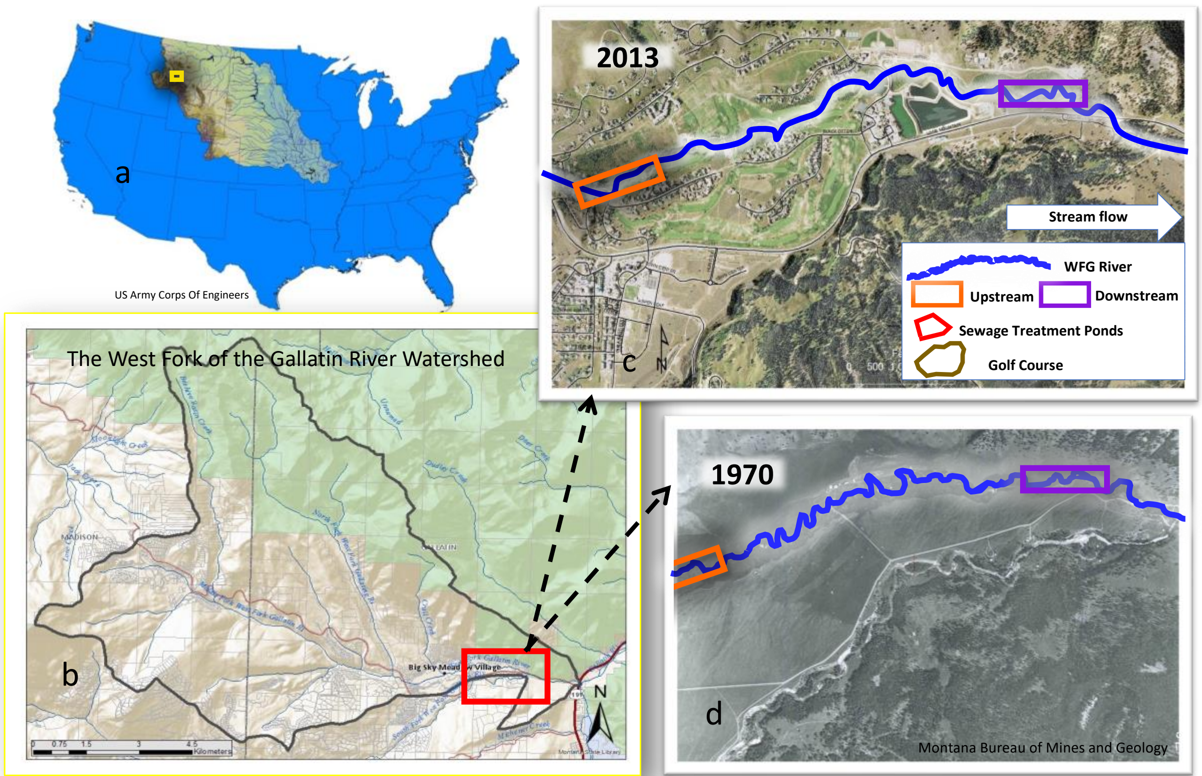

C3 Figure 1. (a) Map of the 48 contiguous United States showing a DEM of the Missouri River Basin and the area of the West Fork of the Gallatin River framed in yellow. (b) Shaded hillslope map of the West Fork of the Gallatin watershed with the area near the study reaches framed in red. (c-d) Aerial or satellite imagery of the area near the study reaches from the years (c) 2013 and (d) 1970. The AGC study reach is framed in orange and the BGC study reach is framed in purple. Historical 1970 aerial photo from the Montana Bureau of Mines and Geology.

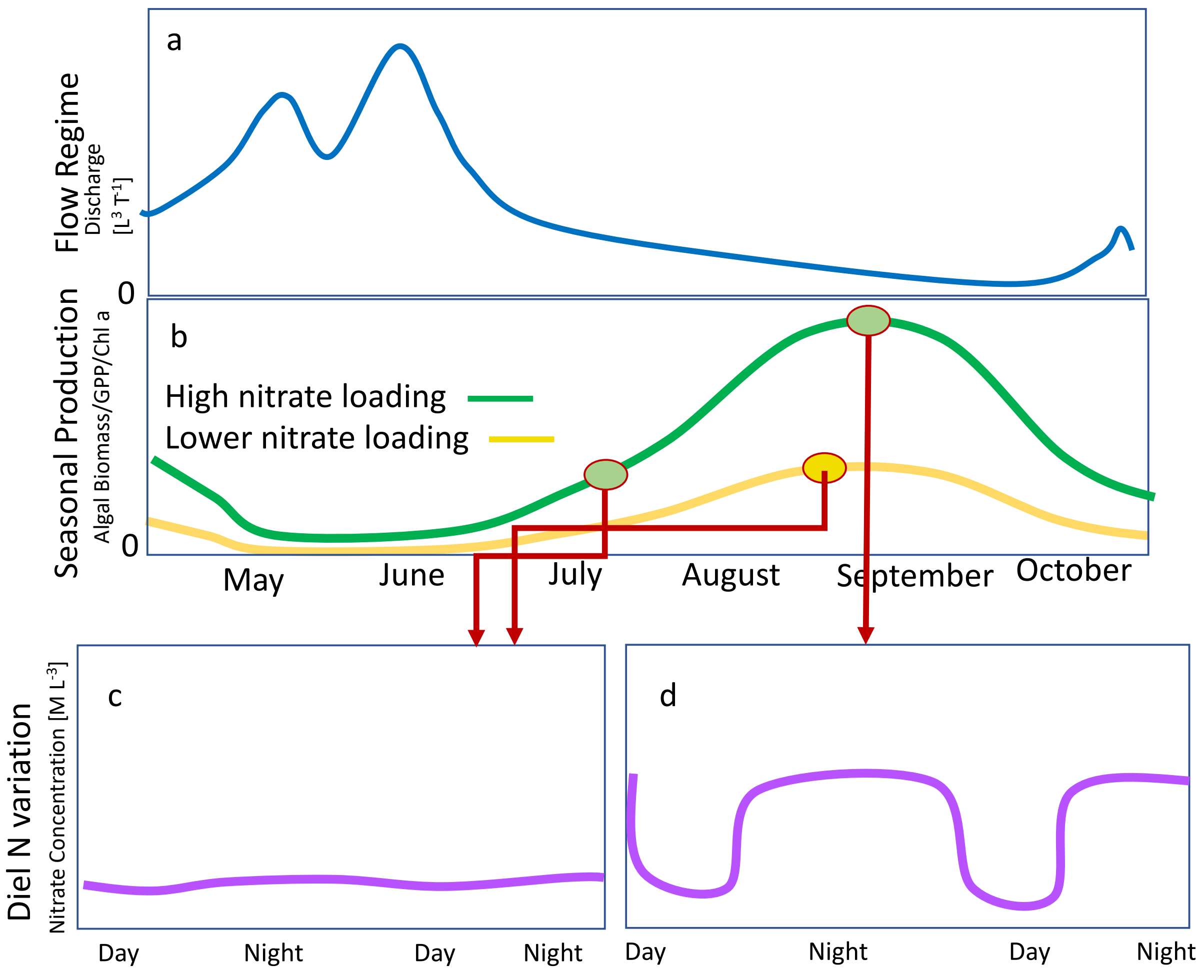

C3 Figure 2. Conceptual model of the response of limiting nutrient concentration dynamics to a snowmelt driven hydrologic regime and the algal growing season during low flow conditions. (a) A typical stream hydrograph for a snowmelt driven hydrologic regime. (b) The hypothesized response of algal production to stream flow associated with higher (green) and lower (yellow) chronic nitrate loading. (c-d) Hypothesized diel response in nitrate concentrations from fertilized biomass growth, where (c) diel swings in concentration are lower when concentrations are lower due to less loading or more dilution at higher flows, and (d) diel swings in concentration are higher during the growing season in reaches where chronic loading is apparent.

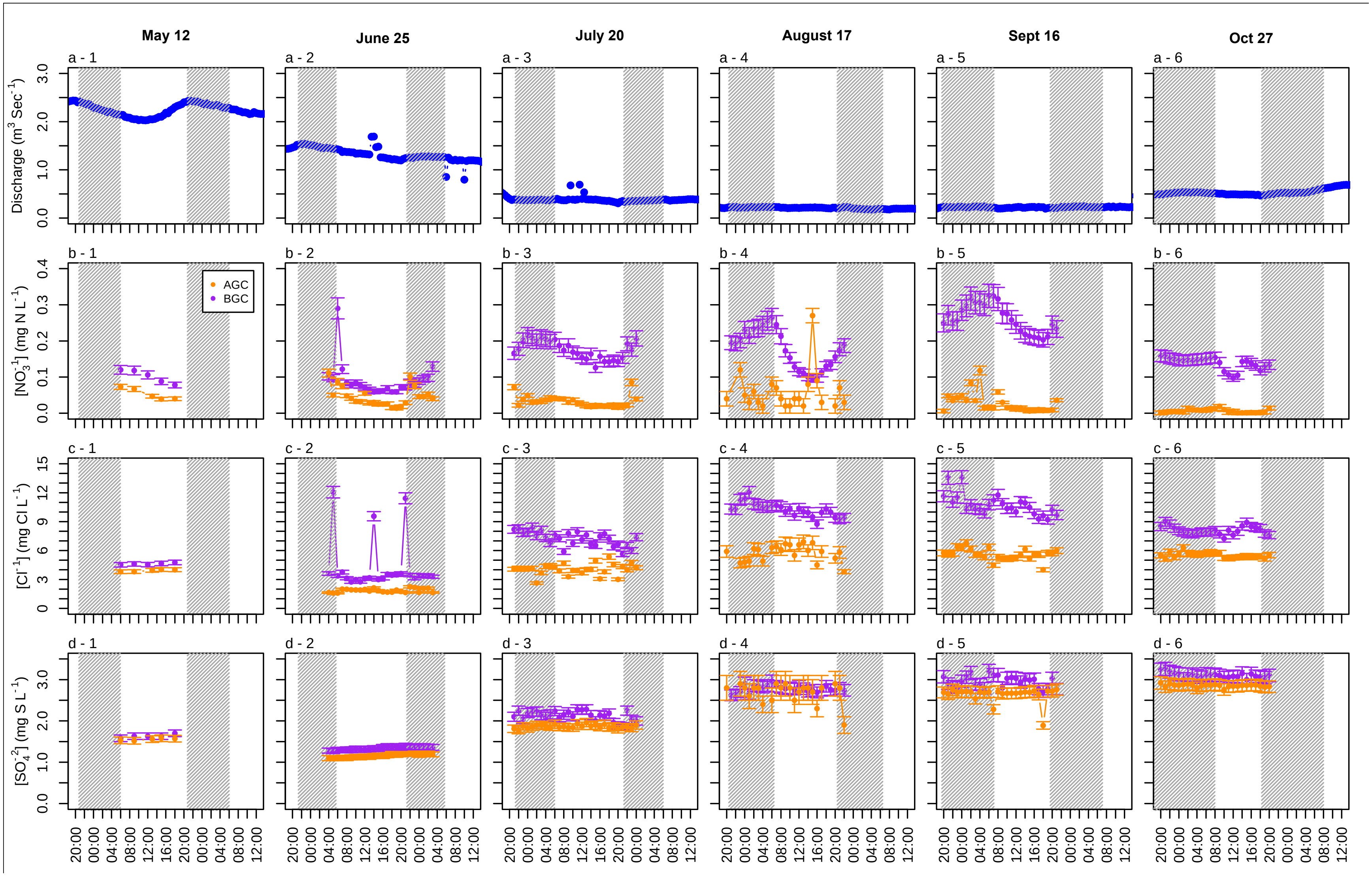

C3 Figure 3. Daily discharge and dissolved solute concentration measurements for each sampling event. Samples were collected hourly, except for May what samples were collected every 2 hrs. Lettered rows refer to pots of (a) discharge, (b) nitrate concentration, (c) chloride concentration, and (d) sulfate concentration. Numbered columns refer to plots from sampling events on (1) 12 May, (2) 25 June, (3) 20 July, (4) 17 August, (5) 16 September, and (6) 27 October 2016. Concentrations measured at the Above Golf Course (AGC) location are shown in orange and Below Golf Course (BGC) are shown in purple. Nighttime periods are shaded in gray. Error bars show analytical uncertainty in the measurement

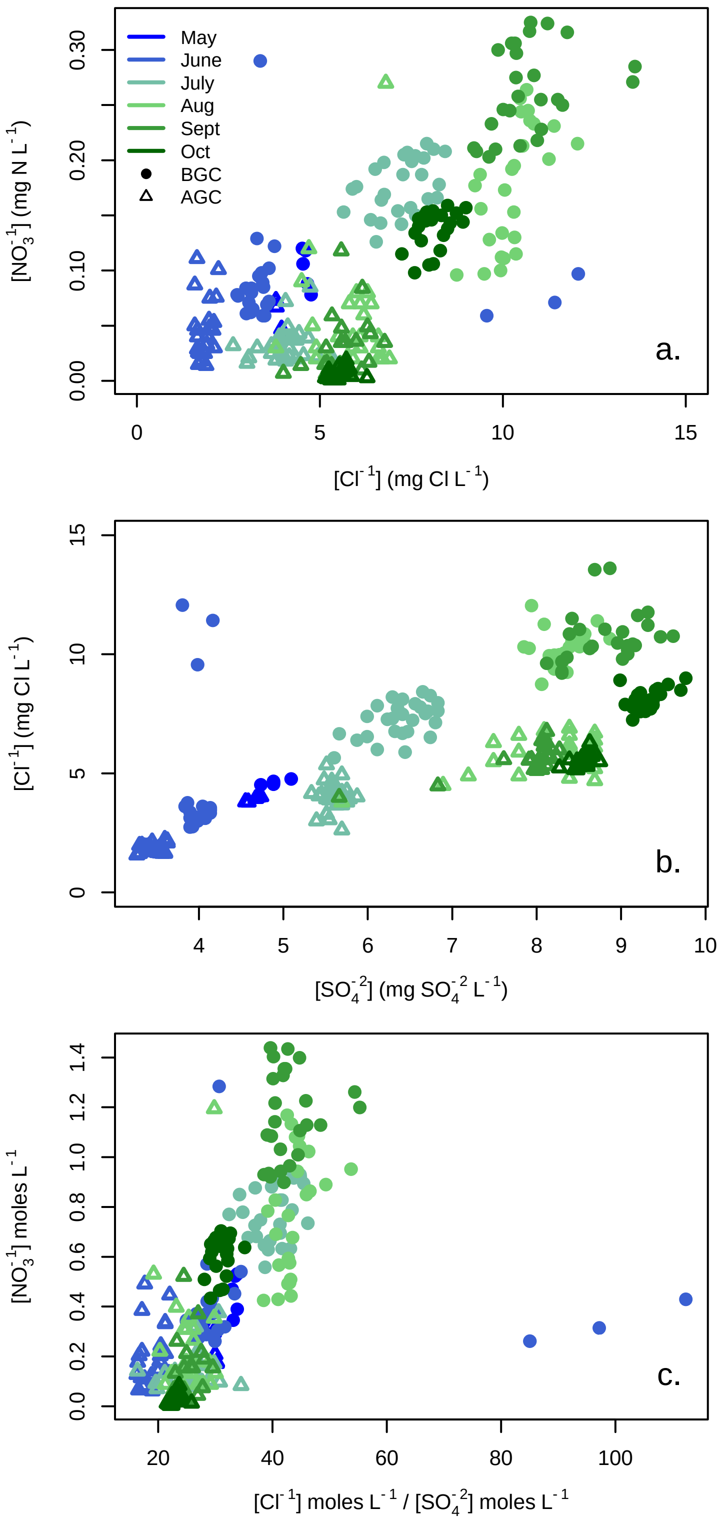

C3 Figure 4. Comparisons among measurements of nitrate, chloride, and sulfate for all samples collected during hourly diel sampling events at the AGC and BGC study reaches, including; (a) nitrate vs chloride concentrations; (b) chloride vs. sulfate concentration; (c) nitrate molarity vs. the chloride to sulfate molar ratio.

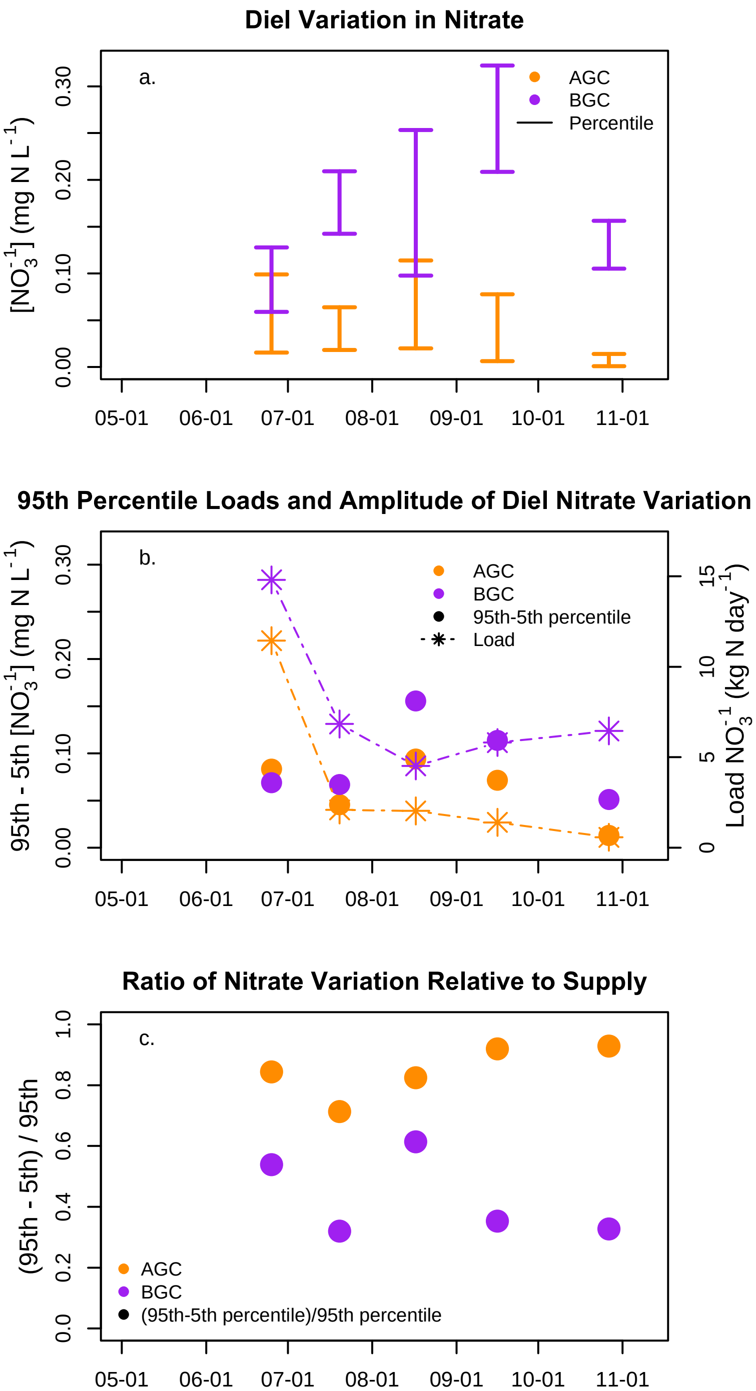

C3 Figure 5. (a) Diel variation in nitrate concentrations from each diel sampling event where the bars represent the 5^{th} and 95^{th} percentiles of the variation during each sampling event. (b) The amplitude of diel variation in nitrate concentration represented by the difference between the 95^{th} and 5^{th} percentiles and daily nitrate loads based on the 95^{th} percentile concentration for each diel sampling event (c) The amplitude of the diel variation in nitrate concentration as a ratio of the

95th percentile concentration, which we interpret as a metric of efficiency in processing the nitrate load.

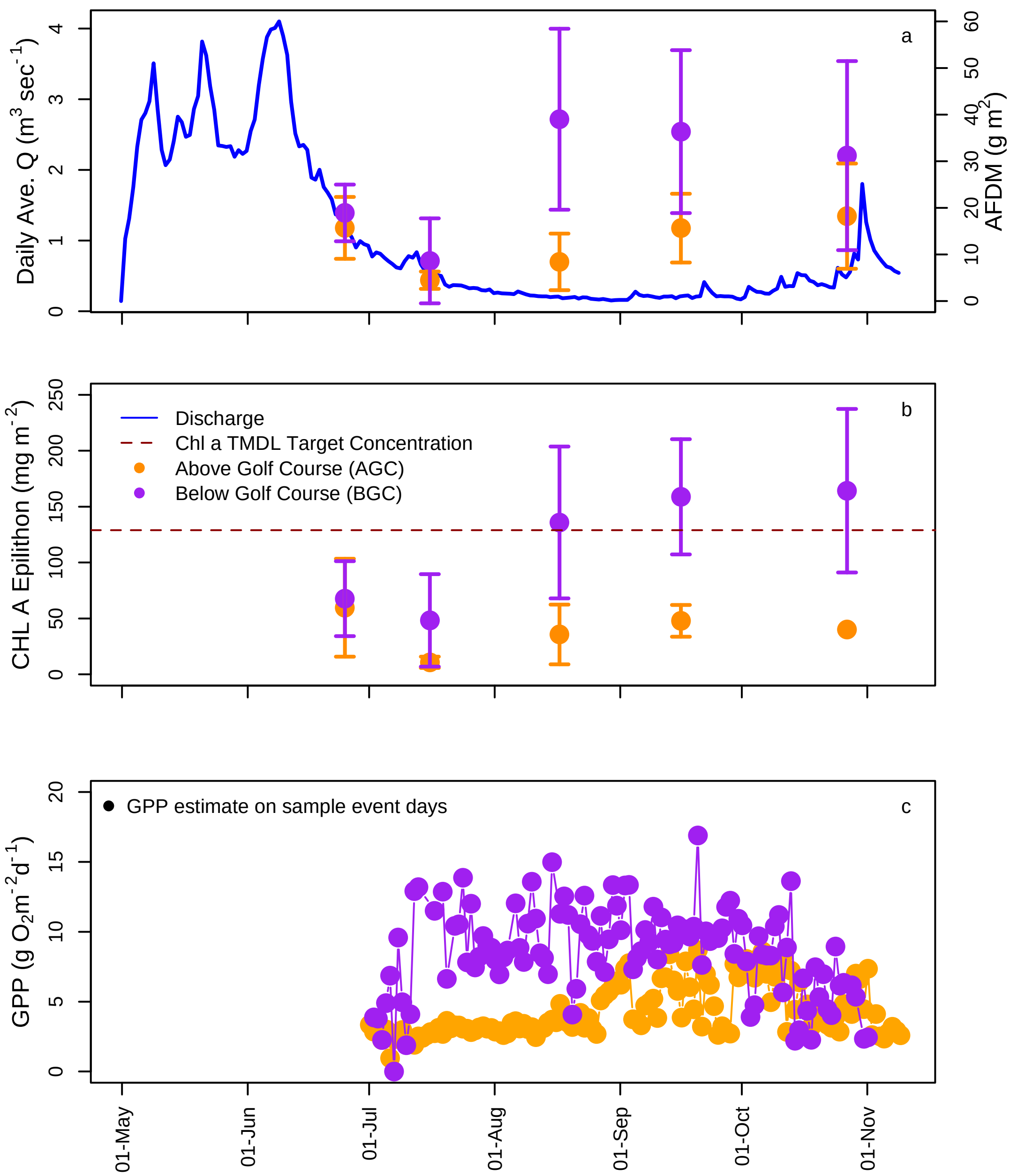

C3 Figure 6. Epilithic growth and primary production for the AGC and BGC stream reaches over the 2016 growing season. (a) Stream flow (blue line) and ash free dry mass (AFDM) measurements for each site over time, including the mean AFDM for each site (dots) and standard deviation (whiskers). (b) Chlorophyll a (chl a) plotted over time for each site. (c) daily estimates of gross primary production (GPP) from dissolved oxygen modeling for each site. Samples collected or measured at AGC are shown in orange, and samples collected or measured at BGC are shown in purple. The red dotted line is the target chl a concentration based on the

Total Maximum Daily Load for the West Fork of the Gallatin River. Error bars in panels (a) and (b) indicate the standard deviations of 5 samples collected at each site.

CHAPTER FOUR

QUANTIFYING THE TIMING OF KEY HYDROLOGIC INFLECTIONS IN SNOWMELT DOMINATED STREAMS AND EVALUATION OF CHANGES IN INFLECTION TIMING OVER THE PAST CENTURY

Contribution of Authors and Co-Authors

Manuscript in Chapter 4

Author: Meryl Storb
Contributions: Collected the data, helped conceptualize the analysis, and implemented the analysis, wrote the manuscript.

Co-Author: Robert A. Payn
Contributions: Provided substantial help with coding and analysis methods, aided in study design, provided extensive mentoring and editorial review.

Co-Author: Mark Greenwood
Contributions: Suggested the method used for analysis, provided guidance on statistical methods and interpretation.

Manuscript Information

M.B. Storb, R.A. Payn, M.C. Greenwood

Journal of Hydrology

Status of Manuscript:
X Prepared for submission to a peer-reviewed journal
☐ Officially submitted to a peer-reviewed journal
☐ Accepted by a peer-reviewed journal
☐ Published in a peer-reviewed journal

Abstract

Hydrologic and stream metabolic regimes in the northern Rocky Mountains (NRM) are primarily controlled by the timing of accumulation and melt of snow. The timing of hydrologic cycles in high elevation watersheds like many in the NRM are known to be in transition with the global changes in climate. Thus, identifying shifts in timing of hydrograph inflections may illustrate effects of climate change on hydrologic and biogeochemical regimes via changes in snowmelt runoff timing that control the length of the aquatic ecosystem growing season. We developed a novel application of an existing statistical smoothing and differentiation technique (SiZer) to determine the timing of key hydrologic inflections related to peak flows and the transition from snowmelt to groundwater dominated stream flow generation. We developed an algorithm to identify optimally smoothed hydrographs and then calculate the first and second derivatives to objectively quantify timing of transitions in annual hydrographs. We used this algorithm to assess changes in the timing of snowmelt for the period of record (77-112 yrs) for 15 USGS gauge locations in the northern Rocky Mountains of Idaho and western Montana. We also explored variation in the timing of inflections adjusted for the influence of total snow volume, providing a rough assessment of the timing of meteorological drivers of snowmelt independent of total annual precipitation. Timing of inflections in annual hydrographs shifted to earlier in the year for 9 out of 15 sites, where 6 sites showed high confidence in negative slope estimates. For the sites that had higher confidence (90% CI did not contain 0) the shifts in timing ranged between 1.3 – 3.3 days earlier for every 25 years of record. Higher elevations stream gages exhibited larger shifts to earlier inflection points compared to lower elevation gauges, and these strong shifts appeared to be more common at lower latitudes among the sites analyzed. This

work provides a new approach to objectively identifying key inflections in hydrographs and demonstrates how the approach may be used to understand the shifts in timing of inflections important to stream ecosystems in snowmelt driven hydrologic regimes.

1. Introduction

Undammed streams and rivers often follow predictable physical, chemical, and ecological patterns dictated by annual hydrologic regimes (Poff *et al.* 1997) that are undoubtedly being gradually altered by global climate change (Milly *et al.* 2008; Yarnell *et al.* 2010b). Hydrologic regimes often control ecological regimes in streams, including disturbance and seasonal flow patterns that dictate life stages for primary and secondary producers (Power *et al.* 1995; Poff *et al.* 1997; Doyle *et al.* 2005; Poff and Zimmerman 2010; Patterson *et al.* 2020b) and influence solute concentrations and loads (Chapters 2 and 3). The timing of seasonal flow transitions (some of which may be identified by hydrograph inflections) are particularly important for understanding ecological processes such as establishment and senescence of the photosynthetic community (i.e. algal and macrophyte), macroinvertebrate life cycles, and fish migration or spawning (Power *et al.* 1995; Poff and Zimmerman 2010; Yarnell *et al.* 2010a).

In mountainous high elevation systems, spring runoff driven by snowmelt represents an annual disturbance that mobilizes bed sediment and dictates the nature of ecological succession in the riparian and aquatic ecosystems. The inflection in the seasonal streamflow recession indicating the transition of stream flow generation from melt-driven flow to groundwater-driven baseflow provides a predictable annual delineation between the end of disturbance and the reestablishment of epilithic and riparian production (Poff and Zimmerman 2010; Yarnell *et al.* 2010a). Many studies within the western United States (U.S.) and elsewhere provide evidence that climate change is causing meaningful shifts in the timing of snowmelt runoff (Stewart *et al.* 2004; Rood *et al.* 2008; Yarnell *et al.* 2010a; Clow 2010; Whitlock *et al.* 2017; Blöschl *et al.* 2019b; Xu *et al.* 2021). Shifts in timing of ecologically important hydrograph inflections will have direct and indirect effects on streams through alteration of both biotic and abiotic components of ecosystem structure and function (Yarnell *et al.* 2010a). The near certainty of continued changes in the behavior of snowmelt dominated systems suggests characterizations of trends in ecologically important hydrograph inflections are critical to evaluating potential effects of climate change on stream ecosystems (Yarnell *et al.* 2010a; Patterson *et al.* 2020b).

In alpine catchments of the northern Rocky Mountains (NRM), the seasonal accumulation and melt of the snowpack play a critical role in the hydrologic regime (Adam *et al.* 2009), and the timing of snow accumulation and melt are changing with the climate. Precipitation from late fall through early spring is primarily stored as snow in the higher elevations of these catchments, and the water stored in the snowpack is released by melt starting in late spring through early summer. The volume of stream flow during the snowmelt season constitutes up to 50-80% of total annual runoff in these basins (Dettinger and Cayan 1995; Stewart *et al.* 2004) and snow constitutes ca. 65% of annual precipitation (Serreze *et al.* 1999). Therefore, total annual runoff volume and annual snowpack accumulation tend to be strongly correlated in these watersheds (Moore *et al.* 2007). The importance of climate change to snowmelt dominated hydrologic systems has been recognized for decades (Rood *et al.* 2008; Adam *et al.* 2009), with studies in the late 1980s and early 1990s showing that increasing temperatures could affect the timing of runoff in mountainous watersheds in the western US

(Gleick 1987; Lettenmaier and Gan 1990; Adam *et al.* 2009). In particular, studies have provided evidence of a shift in snowmelt-driven peak flows to earlier in the year (Adam *et al.* 2009).

Understanding the potential for trends in key transitions in mechanisms of hydrologic storage from the shapes of hydrographs requires an understanding of how timing of the accumulation, volume, extent, and melt of mountain snowpack are linked to seasonal variability in weather and longer-term climate change (Luce 2018). Within montane regions of the NRM, climate change will have multiple pathways of influence on the hydrologic cycle. Earlier and smaller snowmelt pulses will manifest via warming temperatures that cause changes to the form of precipitation and the timing of melt. Several studies have suggested that the volume of water stored in snowpack is decreasing and snowmelt runoff is occurring earlier due to warming temperatures (McCabe and Clark 2005; Stewart *et al.* 2005). Altered precipitation regimes may influence the timing of snowmelt through several pathways. Both the change in the timing of initiation of melt and the overall decrease in the amount of water stored in the snowpack have potential to shift the timing of the snowmelt pulse to earlier in the year (Stewart *et al.* 2004; Stewart 2009; Pederson *et al.* 2011, 2013; Stahle *et al.* 2020). These shifting snowmelt drivers are likely to alter timing of key inflections along a hydrograph related to both peak flow and the return to base flow.

Any gradual long-term trends in the timing of peaks or inflections in hydrogeologic regimes are likely difficult to detect within the noise from interannual variation in precipitation and snowpack volume that commonly occurs in snowmelt dominated watersheds (Moore *et al.* 2007; Stewart 2009). Moore *et al.* 2007, found that snowmelt runoff timing has changed within snowmelt dominated systems, but that change is better explained by the variation in discharge than by an independent trend over time. Precipitation has a more direct influence on hydrologic processes than temperature. However, global climate models have shown that potential changes in precipitation in a warming climate are more uncertain, and a wide range of changes to annual snowpack water volume in the northern Rockies has been projected (+30 to -20%) (Luce 2018). Research specific to Montana has provided evidence that total annual stream flow discharges may increase, but summer low flows are expected to decrease because of reductions in snowpack and recharge of groundwater (Whitlock et al. 2017; Luce 2018). Timing of key inflections along a hydrograph will be affected by the amount of water available in any given year, in addition to changes in the timing of meteorological drivers of snowmelt.

Another challenge to detecting long-term trends in timing of snowmelt is confidently and objectively identifying key hydrograph features within each year in the presence of high-frequency noise generated by episodic melt events. Recent analyses based on detecting differential transitions in smoothed hydrographs (Patterson *et al.* 2020a) may provide a useful technique for more objective approaches to identifying changes in timing of general seasonal drivers of snowmelt runoff. These techniques filter out high-frequency noise in the hydrograph introduced by episodic behavior in temperature or rainfall to focus on the more general information available about the seasonal hydrologic regime.

The overarching goal of this research was to explore novel hydrograph interpretation methods for objective assessment of how climate change might be shifting snowmelt dominated flow regimes. Specific objectives necessary to achieve this goal were: (1) refine the methods for identifying key transitions in the storage behavior of snowmelt dominated systems from annual hydrographs and (2) evaluate whether timing of those transitions in watersheds of the NRM have shifted over the past century. Refinement of the hydrograph analysis methods required designing an automated technique for finding an optimally smoothed unimodal hydrograph, followed by finding key locations along the first and second numerical derivatives of that smoothed hydrograph for quantifying the timing of peak flow and inflections in the summer recession. We applied these refined techniques to historical daily stream flow time series data from 15 stream gauges in the NRM representative of snowmelt driven hydrologic regimes unaffected by impoundment or diversion. We then evaluated shifts in timing of hydrograph inflections to address the following questions: (1) How has timing of the annual peak flow (derived from first derivative) and the transition to baseflow (derived from the second derivative) changed over the past century? and (2) How have the meteorological drivers of snowmelt that are independent of the total annual snowfall shifted over the past century? We hypothesize that higher elevation watersheds will show disproportionate changes in the hydrologic regime due to the stronger effects of climate changes at higher elevations and latitudes, and we predict this will result in finding stronger trends toward early snowmelt at higher elevations in NRM watersheds. This work contributes refined hydrograph signal processing methods for identifying hydrologic inflections in snowmelt-driven hydrologic regimes. Furthermore, we use these techniques to contribute to understanding of the effects of climate change on temporal trends in hydrologic processes likely to affect stream ecosystems in the northern Rocky Mountains of the USA.

2. Methods

We designed a specialized application of the “significant zero crossings” (SiZer) statistical analysis (Chaudhuri and Marron 1999) to detect the timing of inflections in smoothed hydrographs from across the NMR, while minimizing the influence of episodic variation in flow.

We then explored long-term time series of the annual timing of snowmelt-related hydrograph inflections for any trends associated with climate change. We repeated this analysis after adjusting the timing of inflections to account for the influence of total annual flow to assess trends in the timing of meteorological influences on snowmelt.

2.1 Study Catchments and Gauge Data

We used USGS stream and river gauge data from the NRM region comprised of western Montana and portions of eastern and central Idaho (Figure 1). These data are therefore from the northern most region of the Rocky Mountains within the United States (US) and contains the largest contiguous area of designated wilderness in the US, outside of Alaska. Climate in the NRM varies considerably with elevation and location relative to the Continental Divide, but catchments are generally expected to have snowmelt dominated hydrologic regimes. Maximum elevations generally range between 3,000 to 4,000 m and elevations for gauges used in this study range between 442 to 2020 m (Table 1). Precipitation type and amount vary strongly with elevation, with higher elevations receiving more snow than lower elevations (Luce 2018). Streams and rivers on the western side of the Continental Divide drain into the Columbia River basin, while streams and rivers on the eastern side drain either to Hudson Bay or to the Missouri River Basin (Figure 1).

We selected only streams and rivers without evidence of major impoundments or extensive withdrawals to isolate trends due to climate change rather than more direct human influence. Data were obtained for 15 different USGS gauge locations in western Montana and eastern Idaho (Table 1). Selection criteria for gauges generally followed those of Moore et. al (2007), where selection of a gauge required: a minimum of 75 complete water years (1 October through 30 September) of daily average discharge data; all sites drain mountainous catchments with snowmelt driven hydrologic regimes; and sites showed no evidence of influence from human withdrawal or impoundment (Moore *et al.* 2007). Locations were also selected to span a range of latitudes and elevations within the region (Figure 1, Table 1). The periods of record analyzed for each gauge ranged between 77 and 117 years, starting between 1890 and 1941 and ending between 2022 and 2023. The median duration of the periods of record analyzed was 93 years (Table 1).

2.2 Detection of hydrograph inflections

SiZer (Chaudhuri and Marron 1999) is a statistical R package (Sonderegger 2011) (version 0.1-8) used to explore structures within smoothed curves that can be identified via numerical differentiation. We used SiZer to derive first and second derivatives with respect to time for smoothed annual hydrographs, generating a matrix of results by iterating the differentiations using multiple window sizes for smoothing (i.e., multiple threshold frequencies for low-pass filtering) (Figure 3). SiZer applies a non-parametric localized kernel-weighted regression to smooth the data before performing numerical differentiation, and then repeats the smoothing and differentiation across a range of window sizes (or bandwidths) for the kernel weighting function. The window size of the sliding localized regression along the timeline is based on the width of the Gaussian distribution used to describe the weighting kernel. For each pass over the hydrograph at a given window size, the first and second derivatives of the smoothed data are calculated numerically, and variation in the values of the derivatives are classified over time as either positive, negative, or zero, within a tolerance determined by the confidence intervals of the localized regression. Derivatives are considered unavailable if insufficient information is available to estimate a confidence interval (Sonderegger *et al.* 2009). For a given size of the smoothing kernel, identifying transitions in the sign of the first and second derivatives (often through a period of zero values) is the key to objectively identifying key inflections. For example, the timing of hydrograph peaks or troughs are indicated by the change in sign of the first derivative and the timing of transitions between concavity and convexity are indicated by the change in sign of the second derivative.

The selection of the window size or bandwidth for smoothing can influence the interpretation of the timing of inflection points. For this analysis, we defined an objective optimum smoothing level as the smallest window size (i.e., least amount of smoothing) necessary to produce a unimodal hydrograph (e.g., Figure 2). We assessed unimodality with an algorithm designed to determine if the first derivative of the smoothed hydrograph had a single transition from positive to negative (i.e., a single peak) in the snowmelt runoff period (Table 1, Figure 3).

The first and second derivatives of the optimally smoothed hydrographs from each water year were used to identify the timing of two key hydrograph inflections indicative of key transitions in timing of snowmelt runoff. The peak time (PT) was identified as a change from positive to negative sign in the first derivative during the snowmelt period of the smoothed annual hydrograph (Figure 3). We interpret PT as the transition where stream flow generation driven by snowmelt starts to decrease after the sustained increase through the initiation of the influence of snowmelt. Storage transition time (ST) was identified as the time when the influence of sustained contributions from groundwater storage became more evident in the hydrograph relative to the decreasing contributions from storage in the snowpack, as indicated by a transition from a convex curve to a concave curve. ST was thus identified as a change from a positive to a negative sign in the second derivative of the smoothed curve through the seasonal flow recession from the peak (Figure 3). Additional details and code for completing the analysis will be available via Hydroshare (CUAHSI, 2024).

2.3 Normalizing the Timing of Inflections to Variation Caused by Annual Snowpack

The variation in total annual precipitation and snowpack accumulation is often the primary control on the timing of hydrograph features in snowmelt driven hydrologic regimes (Moore *et al.* 2007; Clow 2010). To assess trends in the drivers of snowmelt that are independent of the total annual snowpack volume, we explored adjustments to the timing of hydrograph inflections aimed at removing the variation explained by total annual precipitation. We used total annual discharge volume as a surrogate for total annual snowpack based on clear relationships between the two (Dettinger and Cayan 1995; Stewart *et al.* 2004; Kormos *et al.* 2016) and because long-term snowpack data were not readily available for all study catchments.

We adjusted the timing of inflections in the hydrograph relative to the degree to which a given year's total runoff volume was higher or lower than the median annual flow volume. The relative annual flow (Q^*_{annual}) used to determine the magnitude of adjustment was calculated by dividing the total annual discharge for a given year by the median annual discharge from the period of record for the associated gauge. Values greater than one indicate a year where inflections may be happening later due to higher than typical annual precipitation, and values less than one indicate a year where inflections would be happening sooner due to less than typical annual precipitation.

We then fit a linear regression model to describe the relationship between PT or ST and Q^{*}_{annual} over the entire period of record to determine how much the timing of the inflection should be adjusted to account for the effect of higher or lower than normal flow.

$$PT = b_{PT} + m_{PT} \cdot Q^{*}_{annual}$$

$$ST = b_{ST} + m_{ST} \cdot Q^{*}_{annual}$$

where b and m are the intercepts and slopes inferred from linear regressions. Adjusted timing of the peak time PT_{adj} and storage transition ST_{adj} inflections were calculated as follows.

$$PT_{adj} = PT + m_{PT}(1 - Q^{*}_{annual})$$

$$ST_{adj} = ST + m_{ST}(1 - Q^{*}_{annual})$$

Patterns in the adjusted inflections times no longer reflect the variation directly attributable to annual precipitation, thus providing a perspective on other meteorological drivers of melt that may show long term trends with climate change.

2.4 Analysis of Long-Term Trends and Relationships to Elevation

Long-term trends in PT and ST were assessed over the full period of record for each gauge using linear regressions with year as the independent variable. Regressions were completed for both adjusted and unadjusted inflection times, and slope estimates with associated p values were compared among models. The p values of slope estimates were used to assess the confidence in the detection of trends, and to assess if removing variation due to annual discharge changes confidence in trends. Relationships to elevation were also evaluated with linear regressions for adjusted and unadjusted PT and ST timing for both gauge elevation and mean basin elevation (USGS, 2024). Mean basin elevation was unavailable for two sites, so the Moyie

River and Basin Creek sites were excluded from the mean basin elevation regression. We also looked for evidence of trends in total annual stream flow to understand to what degree any trend in unadjusted metrics might be explained by trends in annual stream flow - linear regressions were completed for each site between total annual discharge volume and year to look for any potential trends in total annual stream flow.

3. Results

Examples of smoothed hydrographs and visualizations of the SiZer analysis for determining optimal smoothing are provided (Figure 2 and 3). The process for identifying the optimum smoothing and corresponding inflection points was semi-automated in that a graph was generated to allow a human to quickly double check the results. Our automated algorithm for objectively identifying an optimal smoothing window size failed to identify a bandwidth twice and selected inappropriate bandwidths (e.g,, over- or under-smoothed based on a single identifiable PT) for about 4% of the annual hydrographs. The algorithm tended to fail when peak runoff was long in duration or when many episodic flow events occurred on the rising or falling limbs of the hydrograph. For about 11% of the annual hydrographs, the optimal smoothing for PT resulted in multiple inflections in the recession after the peak that complicated an objective identification of ST (SI Figure 1). ST misidentifications, like PT misidentifications, were also typically associated with wide peaks or when many episodic high flow events occurred on the falling limb. Misidentifications or failures resulted in manual corrections to the data used in further analysis. The bandwidth selected by the algorithm varied among the sites and among the water years for a given site, with averages across the individual periods of record ranging from

8.3 to 13.5 (Table 2). The standard deviation of bandwidths across the years for a given gauge ranged between 2.8 and 5.38 (Table 2).

Adjusted and unadjusted PT values ranged from water year day 183 (1 April) to water year day 275 (2 July) across all sites. Median PT over the period of record ranged from water year day 222 (10 May) to water year day 260 (17 June) across sites (Figure 4). Ranges in timing for ST were larger than those for PT and spanned from water year day 203 (21 April) to water year day 310 (6 August). Median ST over the period of record ranged between water year day 250 (7 June) and water year day 285 (12 July) across the sites (Figure 4).

Total annual discharge volumes demonstrated little evidence of a trend over time for all study sites except perhaps the Gallatin River (SI Table 1). However, regressions from 9 of the 15 study watersheds suggested a trend of PT or ST shifting to earlier in the water year (negative slopes), with 8 showing a trend toward earlier dates for both PT and ST (Table 2). Data from five watersheds demonstrated at least 90% confidence of non-zero negative slopes for PT and ST (Table 2). For sites with 90% confidence in a trend toward earlier PT, timing shifted between a maximum of 2.3 days every 25 years for the Yellowstone River watershed draining to the Corwin Springs site and a minimum of 1.3 days every 25 years for the Boise River watershed draining to the gauge near Twin Springs Idaho. Shifts of ST to earlier in the year occurred at a maximum rate of 3.3 days every 25 years for the Yellowstone River at Corwin Springs and a minimum rate of 1.5 days every 25 years for the Gallatin River at Gallatin Gateway (Table 2). The Swan River watershed draining to the gauge near Big Fork produced the only hydrograph with greater than 90% confidence in a shift in ST to later in the year.

Where stronger trends were more evident, the adjusted PT and ST generally demonstrated more rapid shifts to earlier timing relative to the unadjusted PT and ST. This pattern was the strongest for trends in the timing of PT (Table 2, SI Figure 2). Regional differences were evident in both confidence and magnitude of a trend toward earlier snowmelt, with lower latitude sites showing both higher confidence in trends and a larger magnitude in trends (Figure 5, Table 2). Boundary Creek catchment near Porthill ID is an exception to this pattern due to high confidence in a larger negative trend despite being the farthest north (Table 1).

Trends in timing of inflection points also appeared to be related to elevation, where higher elevations tended to be associated with more negative slopes (Figure 6 and SI Figure 3). Again, the Boundary Creek watershed appears to be an outlier from the general trends (Figure 6). Relationships of trends in snowmelt timing and elevation were consistent between adjusted PT (slope = -4.4×10^{-5}) and unadjusted PT (slope = -4.1×10^{-5}) or between adjusted ST (slope = -7.4×10^{-5}) and unadjusted ST (slope = -7.1×10^{-5}, Figure 6). Relationships were stronger for the mean basin elevations (SI Figure 3) compared to the gauge elevation (Figure 6). In addition to having larger regression slopes, elevation described more of the variation in timing of ST ($R^2 = 0.34$) and adjusted ST ($R^2 = 0.32$) than the variation in timing of PT ($R^2 = 0.24$) and adjusted PT ($R^2 = 0.23$) (Figure 6).

4. Discussion

Analyses of trends in climate based on inflections in smoothed hydrographs allow assessment of changes in the timing of key transitions within snowmelt-driven hydrologic regimes. Use of the timing of these inflections allows characterization of specific transitions in watershed storage dynamics that cannot be assessed by conventional flow metrics based on summaries of the distribution of annual flow. Conventional flow metrics lose information about the shape of a hydrograph, but the timing of specific inflections in that shape allow interpretation of the influence of storage and runoff generation mechanisms (Surkan 1969).

Our approach to identifying hydrograph inflections builds on work by Patterson et al. (2020), who applied a similar feature identification method based on hydrograph smoothing to identify timing of 4 different 'functional flow' transitions of hydrologic regimes across several different stream types (Lane *et al.* 2017) in California. We add to this approach by demonstrating the utility of considering the inflections identified by both the first and the second derivative of the hydrograph and by demonstrating long-term trend analysis in hydrograph inflections associated with snowmelt flow regimes. Our refined approach to identifying optimal smoothing using the results from SiZer analyses also provides a more objective and automated approach to finding hydrograph features across large datasets.

We observed trends toward earlier occurrence in the timing of inflections in the hydrologic regimes, but the magnitude and confidence in trends of both unadjusted and adjusted PT and ST were not consistent across NRM watersheds. Many other studies have found shifts to earlier occurrence in several measures of runoff timing (Stewart *et al.* 2004, 2005; McCabe and Clark 2005; Moore *et al.* 2007; Arrigoni *et al.* 2010; Kormos *et al.* 2016; Gordon *et al.* 2022), but evidence of earlier snowmelt is not consistent across all conditions (Arrigoni *et al.* 2010; Gordon *et al.* 2022). A common theme across these studies is that trends toward earlier snowmelt attributable to climate change were small in the context of natural interannual variation (Maurer *et al.* 2007; Moore *et al.* 2007; Arrigoni *et al.* 2010). Variation in timing of hydrograph inflections may be large among regional catchments and across years for individual catchments in part due to different individual catchment responses to changes in both temperature and precipitation regimes. Physical variation such as watershed elevation and area also influence runoff and thus hydrograph inflection timing in snowmelt dominated catchments (Luce 2018). Additionally, high natural variation occurs on a multitude of timescales from local weather to decadal-scale climate patterns (e.g. El Nino, Pacific Decadal Oscillation), resulting in potentially low signal-to-noise ratios when attempting to identify gradual trends, even over relatively long periods of record (Moore *et al.* 2007; Stewart 2009). Thus, evaluating trends in timing of snowmelt-derived streamflow with statistical confidence is a multifaceted problem. Despite these challenges, our results provide some evidence of a shift to earlier timing of snowmelt-related inflections for many of our study watersheds.

Strong confidence in trends toward later inflections in the hydrologic regime were only evident in the ST metric for one watershed (Table 2). In the Swan watershed, this trend was accompanied by an increase in the size of the smoothing window required over time. An increase in the amount of high frequency noise (e.g. frequency of flashier flow events) may have necessitated additional smoothing, resulting in an apparent trend toward later timing of ST. The Swan may be an example where climate change is influencing snowmelt dynamics in the watershed, but not via conventional mechanisms underlying our original hypotheses. Climate change may leading to "noisier" snowmelt hydrographs (McCabe and Clark 2005; Fritze *et al.* 2011), which may be more evident in the optimal smoothing window size than the timing of inflections.

The timing of PT and ST are inherently tied to variation in the total annual volume of snowpack, such that trends in the values of these metrics provided directly by our feature identification algorithm cannot be separated from the potential influence of trends in total annual flow in a snowmelt driven hydrologic regime (Moore *et al.* 2007). Total annual snowpack would also be expected to be a primary control on the more conventional methods of identifying the timing of snowmelt. Therefore, interpretation of patterns in the timing of hydrograph inflections that are adjusted for the influence of variation in annual flow provide perspective on potential trends in other controls on key transitions in the hydrologic regime. In contrast to the unadjusted values, variation in the adjusted PT and ST values are more likely to reflect variation in how much of the total annual runoff was associated with rain vs. snow, or variation in the time of year when the energy budget of the snowpack allows for melt (Adam *et al.* 2009; Luce and Holden 2009; Arrigoni *et al.* 2010; Pederson *et al.* 2011; Luce 2018). Future work with a multivariate statistical analysis may help explore the relative importance of total annual precipitation vs. other factors controlling the timing of snowmelt, but for the purposes of this study we suggest that a direct characterization of adjusted timing helps conceptualize the potential meteorological mechanisms behind any trends detected in the adjusted data. Variation in snowmelt timing has an inherent connection with variation in flow in snowmelt dominated hydrologic regimes (Nejadhashemi *et al.* 2007; Moore *et al.* 2007; Cho *et al.* 2021), and we suggest that comparisons of the unadjusted and adjusted trends together help parse which mechanisms of earlier snowmelt trends may be important across watersheds of differing landscape position.

Higher confidence in trends toward earlier adjusted PT and ST in several study watersheds (relative to the unadjusted metrics) and a general lack of detectable trends in total annual precipitation suggest that meteorological controls on snowmelt other than total annual snowpack may be important to the effects of climate change on snowmelt timing (Table 2, SI

Table 1). We add to other research on streamflow in the western US that has found evidence that both changes in temperature and annual snowpack are significant drivers of spring snowmelt runoff timing (Kormos *et al.* 2016). Much of the current body of literature surrounding climate change effects to snowmelt timing highlight temperature driven effects on runoff (Stewart *et al.* 2004; Knowles and Cayan 2004; Mote *et al.* 2005; Maurer *et al.* 2007). The potential for shifts in the timing of hydrograph inflections due to seasonal temperature or precipitation phase changes at our sites is consistent with common findings from climate models where the changes in the temperature regime are more consistent than changes in the precipitation regime (Luce 2018).

Spatial variation in the magnitude and confidence in trends across our study watersheds suggest that shifts to earlier melt conditions may be related to watershed size, latitude, and elevation (Figure 5, 6). Form and amount of precipitation are intrinsically linked to temperature, but how that relationship manifests depends on latitude and elevation (Stewart 2009). Precipitation in general has a more direct effect on hydrologic processes than temperature (Stewart 2009), but potential changes in both the physical state and timing of precipitation in a warming climate are more uncertain (Luce 2018). Like the findings in Patterson et al (2020), the least significant trends occurred in the largest watersheds, with the exception of the Yellowstone River. Less evidence of trends in larger basins may be in part because they span a larger range of elevations. Variation in precipitation mechanisms, and specifically less dramatic climate change effects at lower elevations, may have more attenuated effects in snowmelt related runoff response (Lundquist et al., 2004; Stewart, 2008). In our data set, higher elevation watersheds show some evidence of experiencing larger magnitude shifts to earlier snowmelt. This pattern is contradictory to some findings that higher elevations are likely to see temporary increases in snowpack from increasing precipitation (Stewart 2009), but aligns with evidence that mountainous areas have warmed more than lower elevation areas over the last century due to enhanced longwave radiation from warming surfaces and albedo feedback (Luce 2018). Furthermore, projections of future conditions suggest that the influence of this amplified warming on both temperature and precipitation regimes is expected to continue at high elevations (Luce 2018).

The value of characterizing timing of hydrograph inflections rather than calculating temporal summary statistics of the entire hydrograph is illustrated by considering the implications of earlier ST on stream organisms and ecosystems (Poff *et al.* 1997; Poff and Zimmerman 2010). Earlier end to scouring flows from snowmelt runoff likely translates into longer growing season lengths, which has implications for the role of streams in carbon cycling (Knowles and Cayan 2004; Yarnell *et al.* 2010a; Bernhardt *et al.* 2017), biogeochemical processing of N and P (Bernhardt *et al.* 2017), and water quality (Chapter 2 and 3). Shifts in the magnitude of snowmelt runoff are likely to influence abiotic conditions in the channel (e.g. sediment and solute transport) but shifts in timing will have multiple cascading effects to biological response to the changes in habitat (Poff and Zimmerman 2010; Yarnell *et al.* 2020). Ultimately, understanding shifts in ecological integrity and controls on water quality through climate change will be inseparable from understanding the shifts in hydrological regimes.

5. Conclusion

This analysis demonstrates how numerical differentiation of smoothed hydrographs allows identification and evaluation of trends in the timing of inflections in snowmelt-driven hydrologic regimes. Our results from the northern Rocky Mountains corroborate many other studies suggesting that snow melt runoff has been progressively occurring earlier in the year for some snowmelt driven watersheds since before the 1940's. Results varied geographically, but for the southernmost sites we observed a change in the inflection associated with the transition to baseflow of up to 3.0 days every 25 years. Elevation appears to have some role with higher rates of change occurring in the watersheds with higher elevations, which aligns with some findings suggesting higher elevation systems may be more susceptible to climate change (Luce 2018). Our findings also suggest that the mechanisms underlying earlier snowmelt are not only tied to the total annual snowpack, but also related to changes in the timing of seasonal transitions in meteorological conditions. Alterations to the hydrologic regime have implications for water resource management and stream ecosystem function because of alteration to storage mechanisms and timing within a watershed. Shifts in the timing of flow transitions are likely to affect biotic conditions (Yarnell *et al.* 2010a) and we have shown evidence for shifts in timing attributed to climate change that have occurred in over half of the streams within our study area. This study implies that climate change is likely to influence hydrologic regimes via alterations to snowmelt runoff timing with varied responses that are in part related to location and elevation. Consideration of these shifts in timing may be important to resource management and ecosystem function moving forward.

References

Adam, J. C., A. F. Hamlet, and D. P. Lettenmaier. 2009. Implications of global climate change for snowmelt hydrology in the twenty-first century. Hydrological Processes 23:962–972.

Arrigoni, A. S., M. C. Greenwood, and J. N. Moore. 2010. Relative impact of anthropogenic modifications versus climate change on the natural flow regimes of rivers in the Northern Rocky Mountains, United States. Water Resources Research 46:W12542.

Bernhardt, E. S., J. B. Heffernan, N. B. Grimm, E. H. Stanley, J. W. Harvey, M. Arroita, A. P. Appling, M. J. Cohen, W. H. McDowell, R. O. Hall, J. S. Read, B. J. Roberts, E. G. Stets, and C. B. Yackulic. 2017. The metabolic regimes of flowing waters: Metabolic regimes. Limnology and Oceanography.

Blöschl, G., J. Hall, A. Viglione, R. A. P. Perdigão, J. Parajka, B. Merz, D. Lun, B. Arheimer, G. T. Aronica, A. Bilibashi, M. Boháč, O. Bonacci, M. Borga, I. Čanjevac, A. Castellarin, G. B. Chirico, P. Claps, N. Frolova, D. Ganora, L. Gorbachova, A. Gül, J. Hannaford, S. Harrigan, M. Kireeva, A. Kiss, T. R. Kjeldsen, S. Kohnová, J. J. Koskela, O. Ledvinka, N. Macdonald, M. Mavrova-Guirguinova, L. Mediero, R. Merz, P. Molnar, A. Montanari, C. Murphy, M. Osuch, V. Ovcharuk, I. Radevski, J. L. Salinas, E. Sauquet, M. Šraj, J. Szolgay, E. Volpi, D. Wilson, K. Zaimi, and N. Živković. 2019. Changing climate both increases and decreases European river floods. Nature 573:108–111.

Chaudhuri, P., and J. S. Marron. 1999. SiZer for exploration of structures in curves. Journal of the American Statistical Association 94:807.

Cho, E., R. R. McCrary, and J. M. Jacobs. 2021. Future Changes in snowpack, snowmelt, and runoff potential extremes over North America. Geophysical Research Letters 48:e2021GL094985.

Clow, D. W. 2010. Changes in the timing of snowmelt and streamflow in Colorado: A Response to recent warming. Journal of Climate 23:2293–2306.

CUAHSI. 2024. Find, Analyze and Share Water Data | CUAHSI HydroShare. (Available from: https://www.hydroshare.org/)

Dettinger, M. D., and D. R. Cayan. 1995. Large-scale atmospheric forcing of recent trends toward early snowmelt runoff in California. Journal of Climate 8:606–623.

Doyle, M. W., E. H. Stanley, D. L. Strayer, R. B. Jacobson, and J. C. Schmidt. 2005. Effective discharge analysis of ecological processes in streams. Water Resources Research 41.

Fritze, H., I. T. Stewart, and E. Pebesma. 2011. Shifts in Western North American Snowmelt runoff regimes for the recent warm decades. Journal of Hydrometeorology 12:989–1006.

Gleick, P. H. 1987. The development and testing of a water balance model for climate impact assessment: Modeling the Sacramento Basin. Water Resources Research 23:1049–1061.

Gordon, B. L., P. D. Brooks, S. A. Krogh, G. F. S. Boisrame, R. W. H. Carroll, J. P. McNamara, and A. A. Harpold. 2022. Why does snowmelt-driven streamflow response to warming vary? A data-driven review and predictive framework. Environmental Research Letters 17:053004.

Knowles, N., and D. R. Cayan. 2004. Elevational dependence of projected hydrologic changes in the San Francisco estuary and watershed. Climatic Change 62:319–336.

Kormos, P. R., C. H. Luce, S. J. Wenger, and W. R. Berghuijs. 2016. Trends and sensitivities of low streamflow extremes to discharge timing and magnitude in Pacific Northwest mountain streams. Water Resources Research 52:4990–5007.

Lane, B. A., H. E. Dahlke, G. B. Pasternack, and S. Sandoval-Solis. 2017. Revealing the diversity of natural hydrologic regimes in California with relevance for environmental flows applications. JAWRA Journal of the American Water Resources Association 53:411–430.

Lettenmaier, D. P., and T. Y. Gan. 1990. Hydrologic sensitivities of the Sacramento-San Joaquin River Basin, California, to global warming. Water Resources Research 26:69–86.

Luce, C. H. 2018. Effects of Climate Change on Snowpack, Glaciers, and Water Resources in the Northern Rockies. Pages 25–36 *in* J. E. Halofsky and D. L. Peterson (editors). Climate change and Rocky Mountain ecosystems. Springer International Publishing, Cham.

Luce, C. H., and Z. A. Holden. 2009. Declining annual streamflow distributions in the Pacific Northwest United States, 1948–2006. Geophysical Research Letters 36:L16401.

Maurer, E. P., I. T. Stewart, C. Bonfils, P. B. Duffy, and D. Cayan. 2007. Detection, attribution, and sensitivity of trends toward earlier streamflow in the Sierra Nevada. Journal of Geophysical Research: Atmospheres 112.

McCabe, G. J., and M. P. Clark. 2005. Trends and variability in snowmelt runoff in the western United States. Journal of Hydrometeorology 6:476–482.

Milly, P. C. D., J. Betancourt, M. Falkenmark, R. M. Hirsch, Z. W. Kundzewicz, D. P. Lettenmaier, and R. J. Stouffer. 2008. Stationarity is dead: Whither water management? Science 319:573–574.

Moore, J. N., J. T. Harper, and M. C. Greenwood. 2007. Significance of trends toward earlier snowmelt runoff, Columbia and Missouri Basin headwaters, western United States. Geophysical Research Letters 34:L16402.

Mote, P. W., A. F. Hamlet, M. P. Clark, and D. P. Lettenmaier. 2005. DEclining mountain snowpack in western North America*. Bulletin of the American Meteorological Society 86:39–49.

Nejadhashemi, A. P., J. M. Sheridan, A. Shirmohammadi, and H. J. Montas. 2007. Hydrograph separation by incorporating climatological factors: Application to small experimental watersheds 1. JAWRA Journal of the American Water Resources Association 43:744–756.

Patterson, N. K., B. A. Lane, S. Sandoval-Solis, G. B. Pasternack, S. M. Yarnell, and Y. Qiu. 2020a. A hydrologic feature detection algorithm to quantify seasonal components of flow regimes. Journal of Hydrology 585:124787.

Patterson, N. K., B. A. Lane, S. Sandoval-Solis, G. B. Pasternack, S. M. Yarnell, and Y. Qiu. 2020b. A hydrologic feature detection algorithm to quantify seasonal components of flow regimes. Journal of Hydrology 585:124787.

Pederson, G. T., J. L. Betancourt, and G. J. McCabe. 2013. Regional patterns and proximal causes of the recent snowpack decline in the Rocky Mountains, U.S. Geophysical Research Letters 40:1811–1816.

Pederson, G. T., S. T. Gray, T. Ault, W. Marsh, D. B. Fagre, A. G. Bunn, C. A. Woodhouse, and L. J. Graumlich. 2011. Climatic controls on the snowmelt hydrology of the northern Rocky Mountains. Journal of Climate 24:1666–1687.

Poff, N. L., J. D. Allan, M. B. Bain, J. R. Karr, K. L. Prestegaard, B. D. Richter, R. E. Sparks, and J. C. Stromberg. 1997. The Natural Flow Regime. BioScience 47:769–784.

Poff, N. L., and J. K. H. Zimmerman. 2010. Ecological responses to altered flow regimes: A literature review to inform the science and management of environmental flows. Freshwater Biology 55:194–205.

Power, M. E., A. Sun, G. Parker, W. E. Dietrich, and J. T. Wootton. 1995. Hydraulic Food-Chain Models: An approach to the study of food-web dynamics in large rivers. BioScience 45:159–167.

Rood, S. B., J. Pan, K. M. Gill, C. G. Franks, G. M. Samuelson, and A. Shepherd. 2008. Declining summer flows of Rocky Mountain rivers: Changing seasonal hydrology and probable impacts on floodplain forests. Journal of Hydrology 349:397–410.

Serreze, M. C., M. P. Clark, R. L. Armstrong, D. A. McGinnis, and R. S. Pulwarty. 1999. Characteristics of the western United States snowpack from snowpack telemetry (SNOTEL) data. Water Resources Research 35:2145–2160.

Sonderegger, D. 2011. Package 'SiZer.'

Sonderegger, D. L., H. Wang, W. H. Clements, and B. R. Noon. 2009. Using SiZer to detect thresholds in ecological data. Frontiers in Ecology and the Environment 7:190–195.

Stahle, D. W., E. R. Cook, D. J. Burnette, M. C. A. Torbenson, I. M. Howard, D. Griffin, J. V. Diaz, B. I. Cook, A. P. Williams, E. Watson, D. J. Sauchyn, N. Pederson, C. A. Woodhouse, G. T. Pederson, D. Meko, B. Coulthard, and C. J. Crawford. 2020. Dynamics, Variability, and Change in Seasonal Precipitation Reconstructions for North America. Journal of Climate 33:3173–3195.

Stewart, I. T. 2009. Changes in snowpack and snowmelt runoff for key mountain regions. Hydrological Processes 23:78–94.

Stewart, I. T., D. R. Cayan, and M. D. Dettinger. 2004. Changes in snowmelt runoff timing in western North America under abusiness as usual'climate change scenario. Climatic Change 62:217–232.

Stewart, I. T., D. R. Cayan, and M. D. Dettinger. 2005. Changes toward Earlier Streamflow Timing across Western North America. Journal of Climate 18:1136–1155.

U.S. Geologic Survey. 2024. (Available from: https://streamstats.usgs.gov/ss/)

Surkan. 1969. Synthetic Hydrographs: Effects of Network Geometry. Water Resources Research.

Valett, H. M., R. F. de Lima, M. Peipoch, and R. C. Engstrom. 2023. Bloom succession and nitrogen dynamics during snowmelt in a mid-order montane river. Biogeochemistry 166:227–246.

Whitlock, C., W. Cross, B. Maxwell, N. Silverman, and A. A. Wade. 2017. 2017 Montana Climate Assessment. (Available from: http://scholarworks.montana.edu/xmlui/handle/1/13584)

Xu, D., V. Y. Ivanov, X. Li, and T. J. Troy. 2021. Peak runoff timing is linked to global warming trajectories. Earth's Future 9:e2021EF002083.

Yarnell, S. M., E. D. Stein, J. A. Webb, T. Grantham, R. A. Lusardi, J. Zimmerman, R. A. Peek, B. A. Lane, J. Howard, and S. Sandoval-Solis. 2020. A functional flows approach to selecting ecologically relevant flow metrics for environmental flow applications. River Research and Applications 36:318–324.

Yarnell, S. M., J. H. Viers, and J. F. Mount. 2010a. Ecology and management of the spring snowmelt recession. BioScience 60:114–127.

Tables

C4 Table 1. Information about the gauges, watersheds, and periods of record for the stream flow hydrographs analyzed in this study. Note, -- indicates mean basin elevation was not available (USGS 2024).

Site ID	USGS Gage Site #	Complete Years in Record	Initial Year	Final Year	Mean annual flow ($m^3 s^{-1}$)	Gauge Elevation (m amsl)	Mean Basin Elevation (m amsl)
Boise River near Twin Springs ID	13185000	112	1912	2023	118.75	1018	6416
Boulder Creek at Maxville MT	12330000	77	1940	2023	6.88	1447.8	6934
Boundary Creek near Porthill ID	12321500	93	1931	2023	34.04	539.1	--
Gallatin River near Gallatin Gateway	06043500	91	1890	2023	100.64	1577.6	7893
Johnson Creek near Yellowpine ID	13313000	95	1929	2023	57.98	1419.1	7135
Lochsa River near Lowel ID	13337000	93	1930	2023	347.77	442.6	5197
Madison River near West Yellowstone	06037500	94	1914	2023	19.96	2026.9	7900
MF Flathead River nr West Glacier	12358500	83	1941	2023	393.36	953.4	5649
MF Rock Creek nr Phillipsburg	12332000	83	1939	2023	18.49	1072.6	7132
Moyie River at Eastport ID	12306500	94	1930	2023	105.34	799.8	--
NF Flathead River near Columbia Falls MT	12355500	92	1912	2023	381.16	958.78	5398
Selway River near Lowel ID	13336500	93	1930	2022	478.77	467.4	5512
St Joe River at Calder ID	12414500	104	1912	2023	240.69	663.1	4546
Swan River near Bigfork MT	12370000	101	1923	2023	107.00	933.48	5011
Yellowstone River at Corwin Springs MT	06191500	117	1890	2023	379.19	1548.1	8343

C4 Table 2. Summary of the results of the smoothing bandwidth selection and the subsequent regression analysis of trends in the PT and ST timings for each study watershed. Both adjusted and unadjusted slopes and p values for associated slope estimates are shown.

Site Name	Ave. Optimal Bandwidth	Standard Deviation of Bandwidth	PT slope (day yr^{-1})	*p* value	Adjusted PT slope (day yr^{-1})	*p* value	ST slope (day yr^{-1})	*p* value	Adjusted ST slope (day yr^{-1})	*p* value
Boise River nr Twin Springs ID	13.36	4.46	-0.049	0.104	-0.053	0.065	-0.007	0.857	-0.010	0.767
Boulder Creek at Maxville MT	9.76	4.69	-0.042	0.302	-0.027	0.44	-0.065	0.158	-0.050	0.261
Boundary Creek near Porthill ID	10.09	4.44	-0.071	0.096	-0.090	0.018	-0.061	0.175	-0.080	0.041
Gallatin River nr Gallatin Gateway	9.24	2.80	-0.025	0.501	-0.056	0.085	-0.031	0.443	-0.062	0.09
Johnson Creek nr Yellowpine ID	8.30	3.73	-0.053	0.168	-0.066	0.058	-0.041	0.366	-0.054	0.193
Lochsa River nr Lowel ID	13.33	5.38	0.003	0.942	0.007	0.853	0.009	0.837	0.013	0.754
Madison River nr West Yellowstone	11.62	4.74	-0.051	0.168	-0.050	0.126	-0.051	0.202	-0.050	0.161
MF Flathead River nr West Glacier	10.24	3.80	0.002	0.97	0.016	0.702	0.023	0.708	0.037	0.479
MF Rock Creek nr Phillipsburg	10.13	4.48	-0.061	0.128	-0.060	0.124	-0.015	0.742	-0.013	0.76
Moyie River at Eastport ID	10.98	4.93	0.010	0.778	0.021	0.544	0.009	0.827	0.020	0.607
NF Flathead River near Columbia Falls MT	9.25	3.29	0.029	0.432	0.027	0.415	0.010	0.809	0.008	0.833
Selway River near Lowel ID	13.50	5.24	0.022	0.581	0.010	0.779	0.046	0.316	0.034	0.429
St Joe River at Calder ID	13.12	5.29	-0.007	0.881	0.001	0.973	0.070	0.105	0.077	0.056
Swan River near Bigfork MT	11.84	4.57	0.034	0.41	0.027	0.48	0.099	0.012	0.092	0.011
Yellowstone River at Corwin Springs MT	9.77	3.98	-0.085	0.002	-0.092	<0.001	-0.123	<0.001	-0.130	<0.001

Slope -0.10 to -0.05	(red)
Slope -0.049 to 0	(orange)
Slope 0 to 0.05	(light green)
Slope 0.051 to 0.10	(dark green)
unadjusted p value is smaller than adjusted p value	(light yellow)

Figures

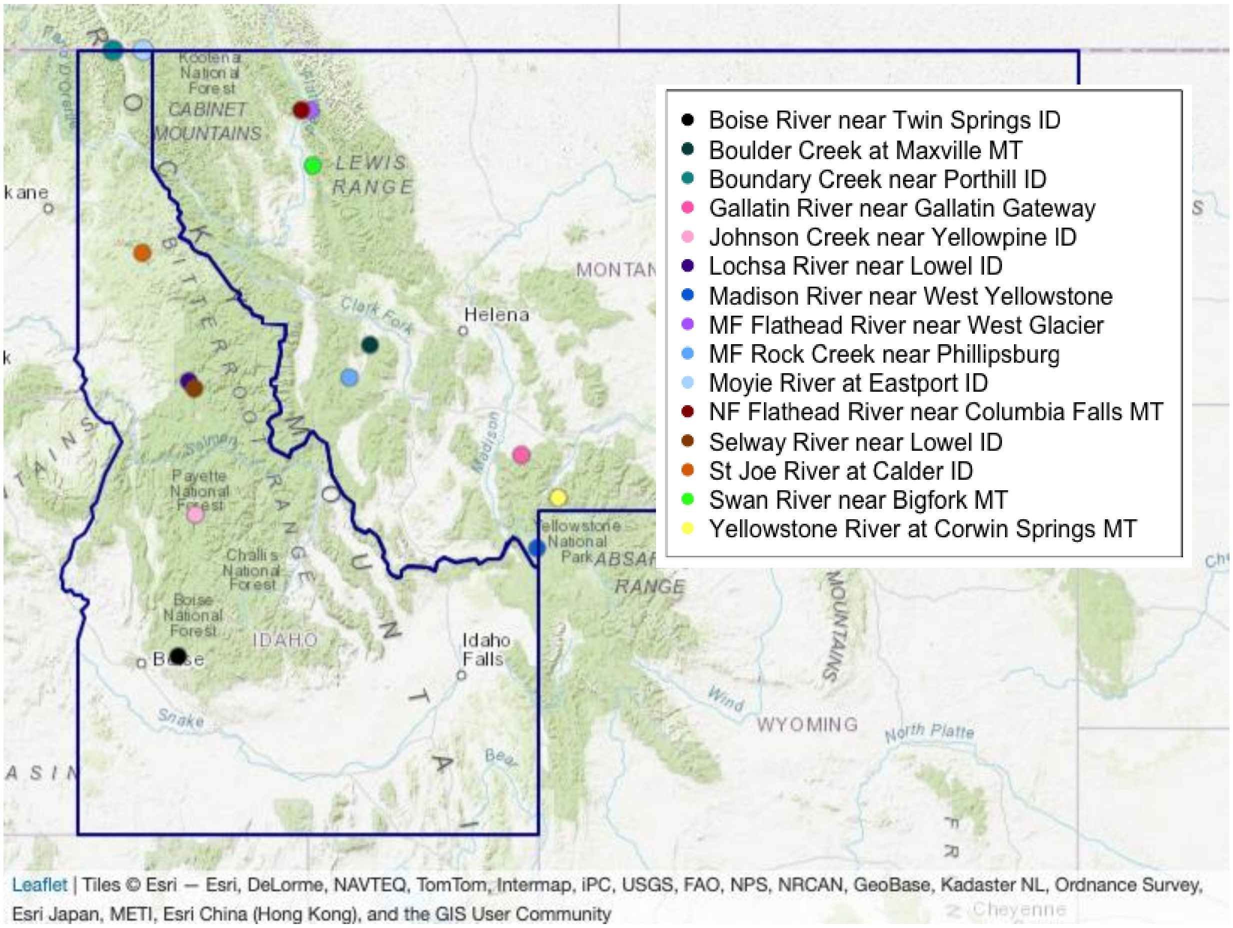

C4 Figure 1. Map of the location of study watersheds indicated by their USGS gauge locations within Montana and Idaho. Background hillshade map provided by Esri (2024).

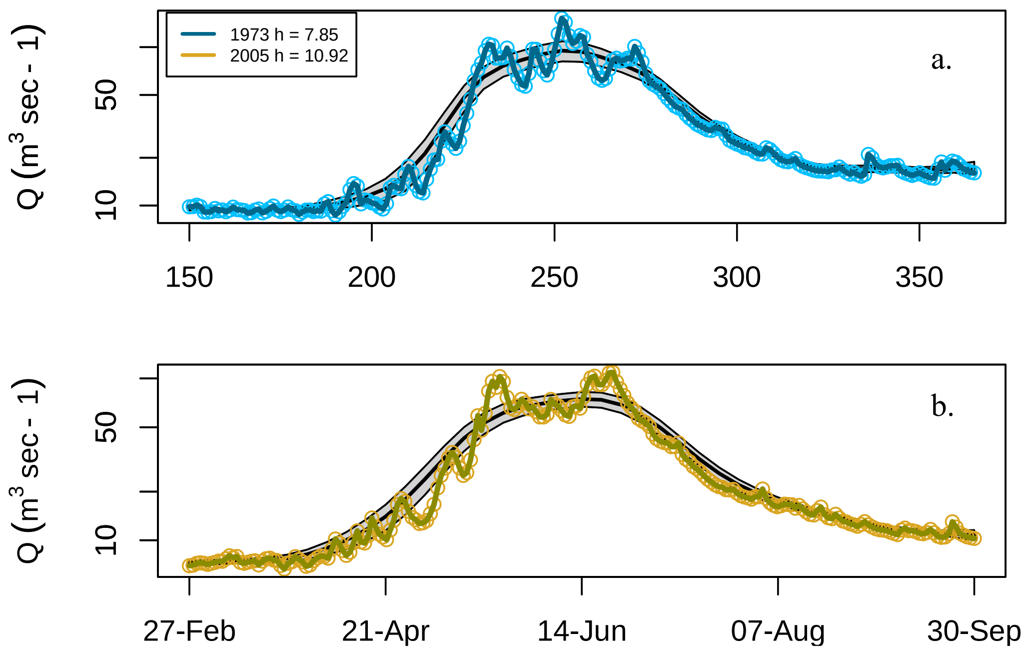

C4 Figure 2. An example of optimal bandwidth smoothing for two snowmelt season hydrographs (colored lines) from the Gallatin River at Gallatin Gateway: (a) data from 1973 and (b) data from 2005.

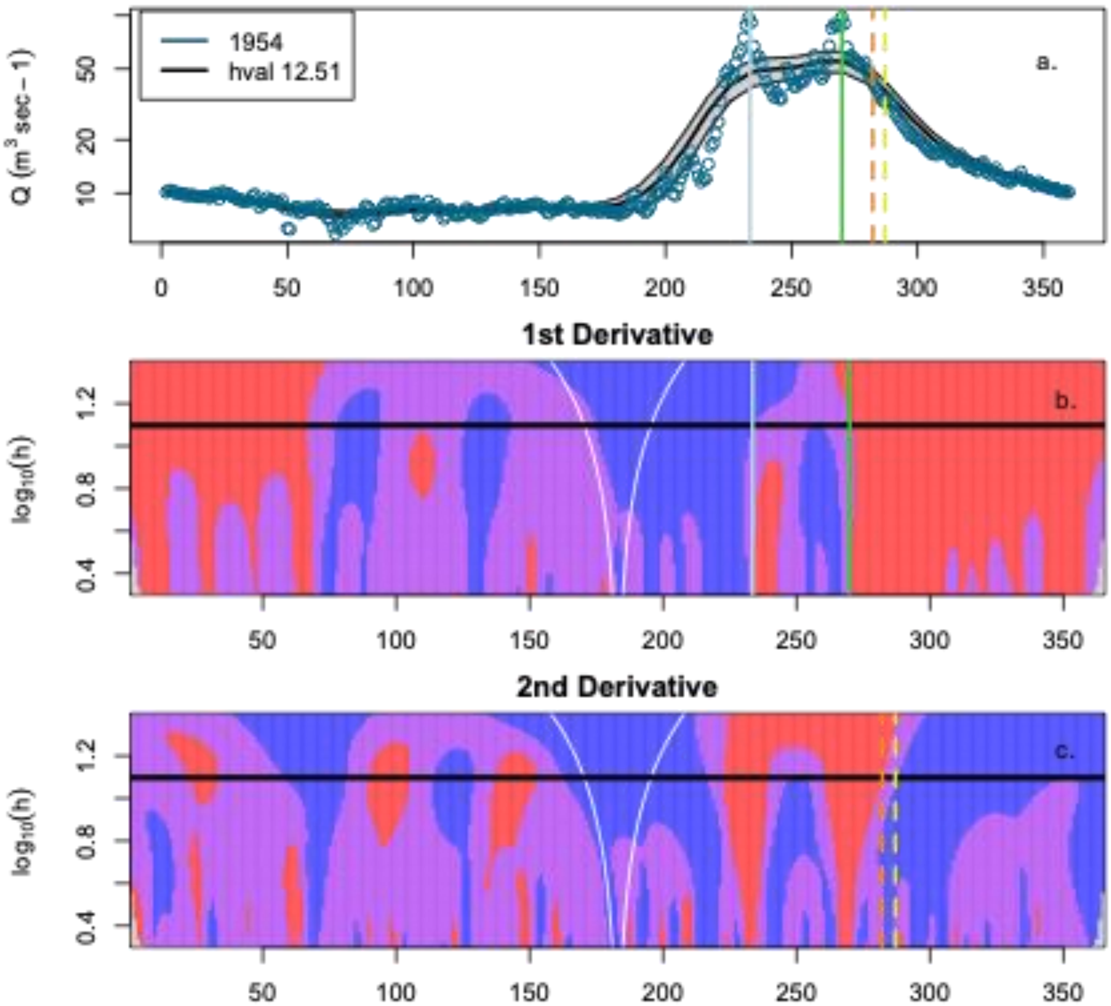

C4 Figure 3. An example of a SiZer map for the 1954 water year annual hydrograph for the Gallatin River at Gallatin Gateway. (a) Plot of the raw hydrograph, and a smoothed hydrograph based on the optimal bandwidth (h) for smoothing to a unimodal peak. (b) The 1st derivative SiZer map. (c.) The 2nd derivative SiZer map. The horizontal black line indicates the optimal smoothing for generating a unimodal peak. Colored vertical lines correspond to the edges of the zero values constraining the PT inflection in the first derivatives (light blue and lime green solid lines) and the ST inflection in the second derivative (orange and yellow dashed lines) of the smoothed hydrograph. PT and ST timing is calculated as the midpoint between these zero bounds for each metric.

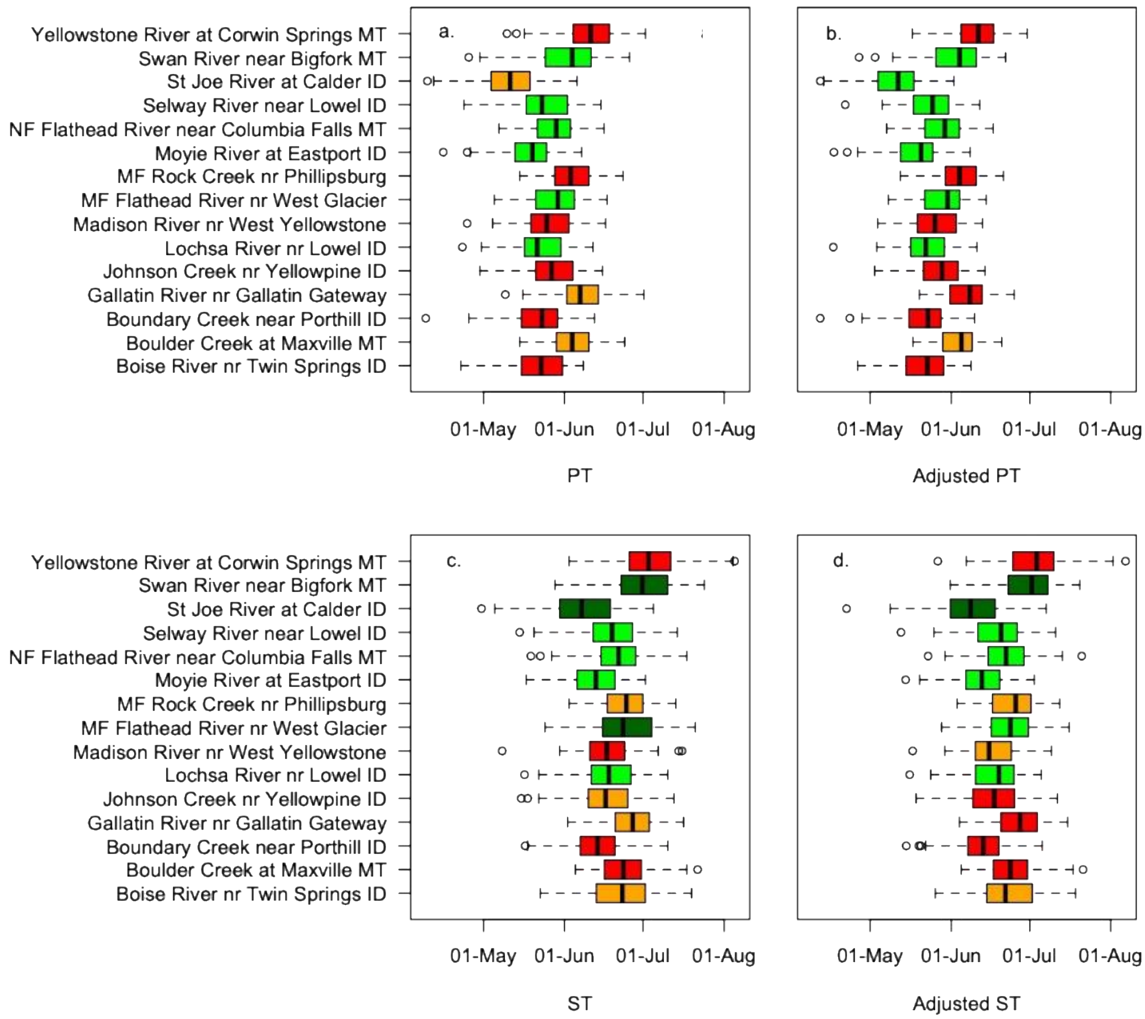

C4 Figure 4. Summary of results from SiZer analysis of the timing of PT and ST hydrograph inflection points, including: (a) PT timing, (b) adjusted PT timing, (c) ST timing, and (d) adjusted ST timing. The color of each box plot illustrates the binned magnitude of the trend (i.e. slope estimate) in timing for the linear model associated with each site (Table 2), where red indicates a slope between -0.10 and -0.05, orange indicates a slope between -0.049 and 0, light green indicates a slope between 0 and 0.05, and dark green indicates a slope between 0.05 and 0.10.

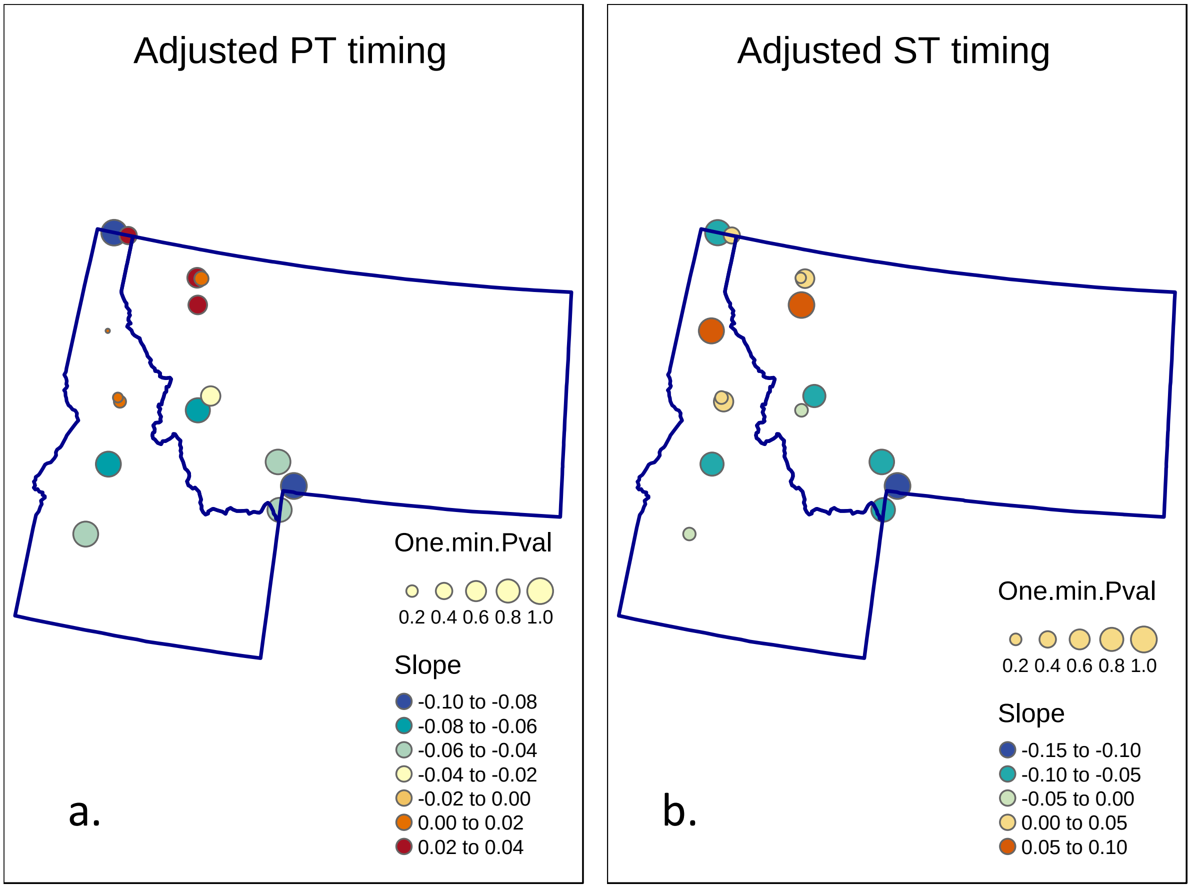

C4 Figure 5. The binned values of the magnitude of trends in timing of (a) PT and (b) ST hydrograph inflections. The size of each point corresponds to the confidence in detecting a trend as indicated by one minus the p-value.

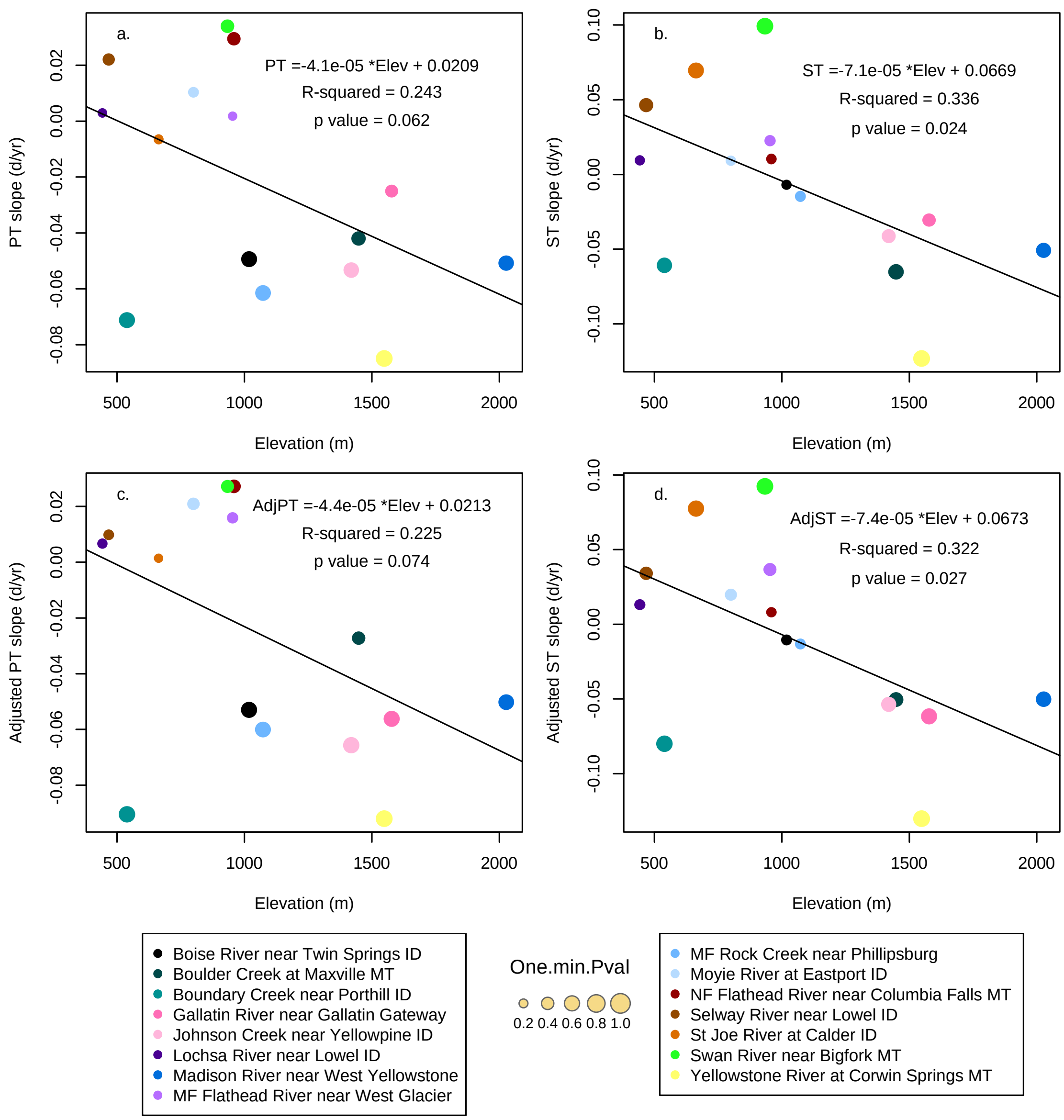

C4 Figure 6. Relationships between elevation and long-term trends in (a) PT, (b) ST, (c) adjusted PT, and (d) adjusted ST. The sizes of symbols are scaled by the confidence that associated data are indicating a long-term trend, based on one minus the p-value of the linear regression.

Supporting Information

Code for Algorithm that Completes Analysis of PT and ST.

Code runs for each individual site and requires individual csv files with daily discharge for each year:

```
lgth <- length(years)

###Determine H value based on uni-modality
#crate a data frame to store h-values for each year
hValues <- data.frame(year = years,
                      hVal = numeric(length = lgth),
                      loghVal = numeric(length = lgth),
                      SZ1.pkL= numeric(length = lgth),
                      SZ1.pkR= numeric(length = lgth),
                      SZ2.fallL = numeric(length = lgth),
                      SZ2.fallR = numeric(length = lgth))
#for loop or function to calculate h-values for each year

#i <- 7
for(i in 1:lgth){ #galatin
  #for(i in 50:length(years)){
  #load sixer object for 1 year
  load(file = paste0("../03_incremental/", site, "/Sizer Objects/",
years[i],"/",years[i],"obj1",".RData", sep="") )
  load(file = paste("../03_incremental/", site, "/Sizer Objects/",
years[i],"/",years[i],"obj2",".RData", sep="") )

  #identify the range for the rising limb for the most smoothed curve
  zeroR <- NaN
  zeroL <- NaN
  oneR <- NaN
  oneL <- NaN
  negoneL <- NaN

  #store year in dataframe
  hValues$year[i] <- years[i]

  # look from right to left for the first zero
  for(column in 265:1){
    if( is.nan(zeroR) && szGal.1$slopes[300, column] == 0 ){
      zeroR <- column
      negoneL <- column + 1
    }
    #after you find the first 0 then find the oneR
    if( !is.nan(zeroR) ){
      if( is.nan(oneR) && szGal.1$slopes[300, column] == 1  ){
        zeroL <- column + 1
        oneR <- column
      }
    }
    #after you find oneR keep looking for oneL
    if( !is.nan(oneR) && is.nan(oneL) && szGal.1$slopes[300, column] != 1 ){
      oneL <- column + 1
      break
    }
  }

  #now you have the x bounds (columns) you can start moving down (rows) to look for the h-value
with 2 peaks
```

```
  #look for -1 or 1's inbetween 0's to identify the first point with a 2nd peak
  for(row in 300:1){
    if( length(which(szGal.1$slopes[row, zeroL:zeroR] != 0 )) > 0){
      hindex <- row + 1 ### this is what we are trying to get out of the loops ###but i think
this needs to come from the h.grid
      break
    }
    if( length(which(szGal.1$slopes[row, oneL:oneR] != 1)) > 0){
      hindex <- row + 1 ### this is what we are trying to get out of the loops ###but i think
this needs to come from the h.grid
      break
    }

    #if loop doesn't break by finding changes in slope then start moving down rows.
    nextrow <- row - 1

    if( szGal.1$slopes[nextrow, oneL ] != 1){
      #look right for the first 1
      for(col in (oneL+1):zeroL ){
        if(szGal.1$slopes[nextrow, col] == 1 ){
          oneL <- col
          break
        }
      }
    } else {
      #start looking left ##or start looking down at the next row
      for(col in (oneL-1):0 ){
        if(szGal.1$slopes[nextrow, col] != 1 ){
          oneL <- col + 1
          break
        }
      }
    }

    if( szGal.1$slopes[nextrow, oneR ] == 1){
      # this loop is look right for the first 1
      for(col in (oneR+1):300 ){
        if(szGal.1$slopes[nextrow, col] != 1 ){
          oneR <- col-1
          zeroL <- col
          break
        }
      }
    } else {
      #start looking left ##or start looking down at the next row
      for(col in (oneR-1):oneL ){
        if(szGal.1$slopes[nextrow, col] == 1 ){
          oneR <- col
          zeroL <- col + 1
          break
        }
      }
    }

    #look R to see if negoneR changed
    if( szGal.1$slopes[nextrow, zeroR ] == 0){
      #look right
      for(col in (zeroR+1):299 ){
        if(szGal.1$slopes[nextrow, col] == -1 ){
          negoneL <- col
          zeroR <- col -1
          break
        }
      }

    } else {
      #start looking left ##or start looking down at the next row
      for(col in (zeroR-1):oneR ){
```

```
        if(szGal.1$slopes[nextrow, col] == 0 ){
          negoneL <- col + 1
          zeroR <- col
          break
        }
      }
    }
  }

  #Store optimal h value and inflection points for each year in a CSV

  hValues$hVal[i] <- szGal.1$h.grid[hindex]
  hValues$loghVal[i] <- log10(szGal.1$h.grid[hindex])
  hValues$SZ1.pkL[i] <- szGal.1$x.grid[oneR]
  hValues$SZ1.pkR[i] <- szGal.1$x.grid[zeroR]

  ##### 2nd derivative
  peak <- round((zeroL + zeroR)/2)
  zeroR2 <- NaN
  oneL2 <- NaN
  zeroL2 <- NaN

  ### after the peak, look right to find the first positive 1. ##column -1 is zeroR2
  for(column in zeroR:300){   ####!!! CONSIDER CHANGING PEAK TO zeroR
    if( is.nan(zeroR2) && szGal.2$slopes[hindex, column] == 1 ){
      oneL2 <- column
      zeroR2 <- column -1
      break
    }
  }

  #then look left to find the first negative one
  #column +1 is zerol2
  for(column in (zeroR2-1):150){
    if( is.nan(zeroL2) && szGal.2$slopes[hindex, column] == -1 ){
      zeroL2 <- column
      break
    }
  }
  hValues$SZ2.fallL[i] <- szGal.2$x.grid[zeroL2]
  hValues$SZ2.fallR[i] <- szGal.2$x.grid[zeroR2]

  ###### MAKE 1 FIGURE WITH 4 PLOTS
  fp <- paste0("../03_incremental/",site, "/OptimalH/plots/", paste("1st_deriv_opt_h",years[i],
sep=""))

  quartz(width =8 , height = 10 , file = paste0(fp,"_groupPlot.jpg"), type = "jpg")
  par(mfrow=c(4,1))
  #jpeg(filename = fp, width = 900, height = 600, units = "px", pointsize = 16, quality = 100)

  #plot hydrograph
  #load hydrograph data
  galdata <- read.csv(paste("../03_incremental/",site,"/annual data/",years[i],".csv", sep=""))


  plot(galdata$dayofwateryr[1:365], galdata$DayFlow.m3s[1:365], type = "l", cex = 2, main = site,
ylab = "Q (CFS)", xlab = "Day of Water Year", col = "deepskyblue4", lwd = 3, log = "y")
  #lines(gmean$dayofwateryr, gmean$meanQ, lwd = 3, log = "y")
  legend("topleft", legend = years[i], col = "deepskyblue4", lwd = 2, inset = 0.01)

  #plot smoothed curve
  modellargeh <- locally.weighted.polynomial(galdata$dayofwateryr [2:360],
                                             galdata$DayFlow.m3s [2:360],
                                             degree = 1,
                                             kernel.type = "Normal",
                                             h =  hValues$hVal[i]) #

  plot(modellargeh, xlab= "day of water year", ylab= "Q (CFS)", log = "y",
```

```
      col = "deepskyblue4", use.ess = F)
  mh <- paste("hval", round(hValues$hVal[i],2))
  legend("topleft", legend = c(years[i], mh), col = c("deepskyblue4", "black"),
         lwd = 2, inset = 0.01)

  #Plot SZ 1st deriv
  #par(mar=c(4, 4, 3, 1))
  plot(szGal.1, main = paste (site, years[i]) )
  abline(h = log10(szGal.1$h.grid[hindex]), col="black")
  abline(v = hValues$SZ1.pkR[i], col = "yellow", lwd = 2 )
  abline(v = hValues$SZ1.pkL[i], col = "pink", lwd = 2 )
  #
  # plot SZ 2nd deriv
  par(mar=c(4, 4, 3, 1))
  plot(szGal.2, main = paste(site, years[i], "2nd Deriv"))
  abline(h = log10(szGal.1$h.grid[hindex]), col="black", lwd = 3 )
  abline(v = hValues$SZ2.fallR[i], col = "yellow", lwd = 2 )
  abline(v = hValues$SZ2.fallL[i], col = "pink", lwd = 2 )
  #
  dev.off()

}
```

Supporting Information Figures

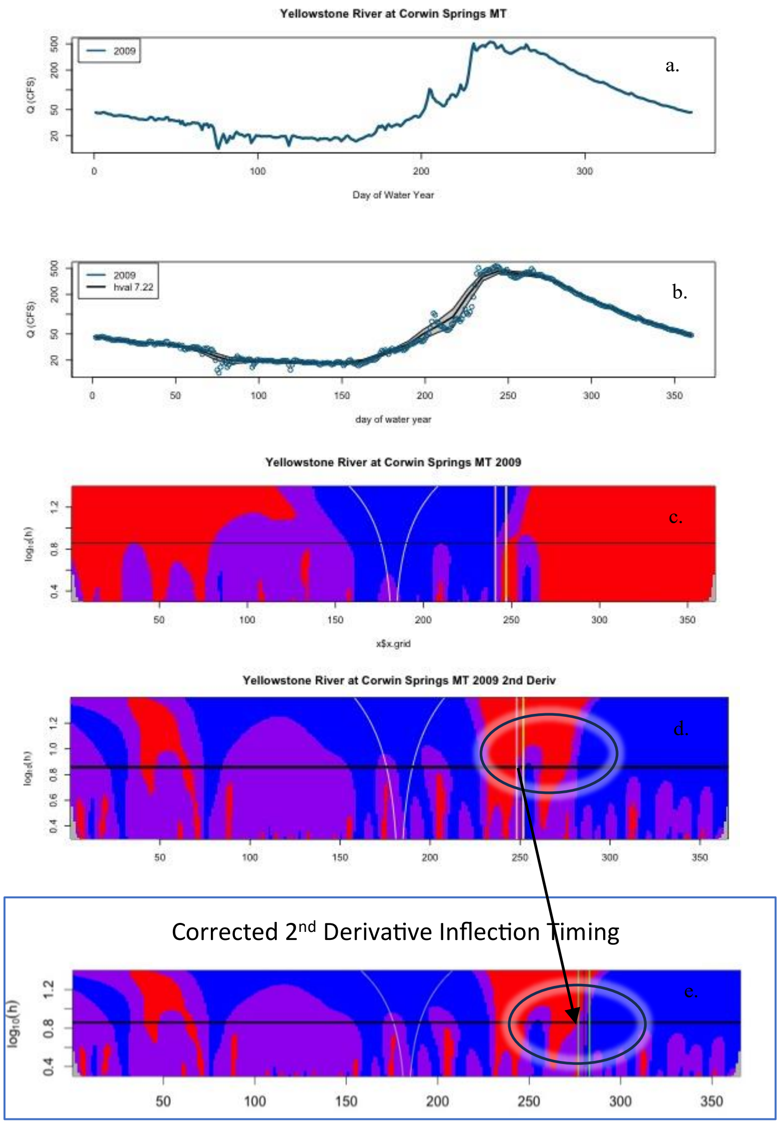

C4 SI Figure 1. An example of algorithmic miss-identification of the second derivative inflection and the corrected selection of bounds for the ST timing. (a) Plot of the hydrograph. (b) Plot of the smoothed hydrograph, with points showing the original hydrograph daily values. (c) 1st derivative SiZer map with the PT timing bounds based on the level of smoothing shown in panel b. (d) 2nd derivative SiZer map with the miss-identified second derivative timing bounds based on the level of smoothing shown in panel b. (e) 2nd derivative SiZer map showing the corrected bounds for timing of the second derivative.

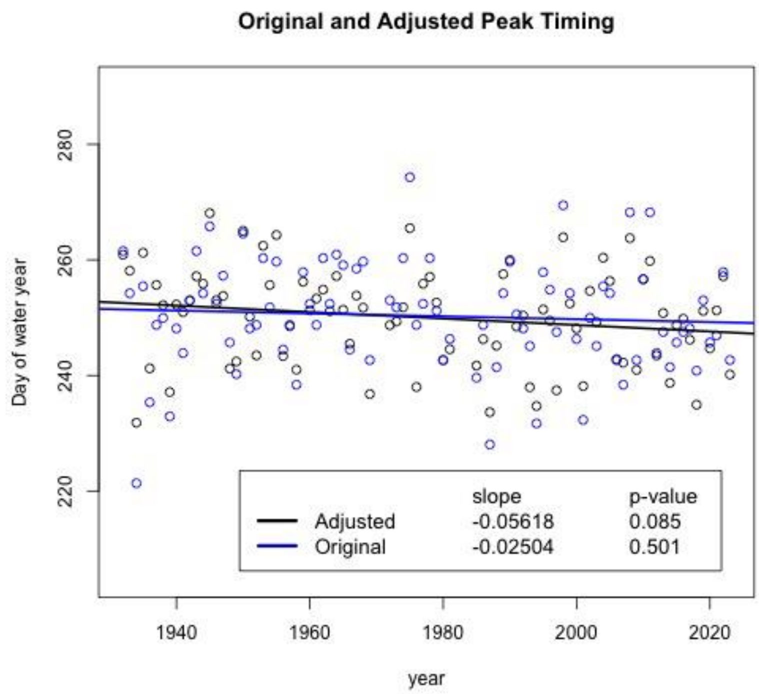

C4 SI Figure 2. An example of trend evaluation based on linear regression from the Gallatin River at Gallatin Gateway. Two linear regressions are shown including a linear regression for PT by year and adjusted PT by year.

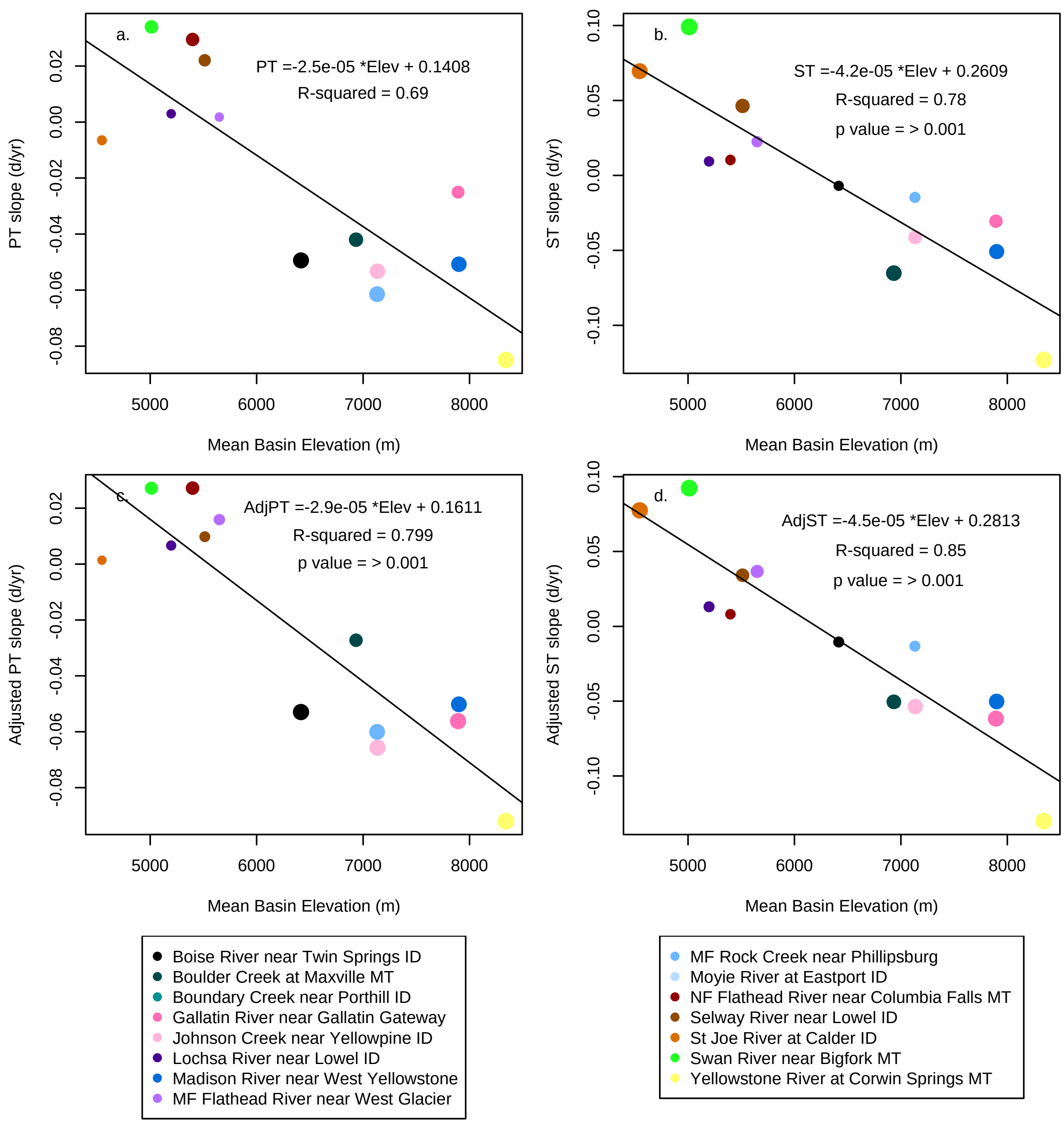

C4 SI Figure 3. Relationships between mean basin elevation and long-term trends in (a) PT, (b) ST, (c) adjusted PT, and (d) adjusted ST. The sizes of symbols are scaled by the confidence that associated data are indicating a long-term trend, based on one minus the p-value of the linear regression. Note two sites are not shown because mean basin elevation was unavailable Moyie River at Eastport, Boundary Creek near Porthill ID.

Supporting Information Tables

C4 SI Table 1. Summary of the results from evaluation of trends in total annual discharge volume for each gauge.

Site	Slope Estimate (m^3 $year^{-1}$)	p-value for Slope Estimate
Boise River nr Twin Springs ID	361732.250462818	0.711
Boulder Creek at Maxville MT	-40401.6982931652	0.469
Boundary Creek near Porthill ID	184524.262522118	0.299
Gallatin River nr Gallatin Gateway	1021436.14378123	0.074
Johnson Creek nr Yellowpine ID	254675.317984832	0.466
Lochsa River nr Lowel ID	-452053.912349939	0.847
Madison River nr West Yellowstone	-8486.63390381385	0.972
MF Flathead River nr West Glacier	-1527021.46739567	0.560
MF Rock Creek nr Phillipsburg	-17554.8499535645	0.891
Moyie River at Eastport ID	-620807.862421632	0.387
NF Flathead River near Columbia Falls MT	298312.252203684	0.895
Selway River near Lowel ID	1933187.19862624	0.527
St Joe River at Calder ID	-1241649.22217395	0.517
Swan River near Bigfork MT	368429.09433052	0.644
Yellowstone River at Corwin Springs MT	1040892.49899372	0.525

CHAPTER FIVE

SYNTHESIS: DRIVERS OF WATER QUALITY IN SNOWMELT DOMINATED SYSTEMS ARE AT THE NEXUS OF SOURCE, TRANSFORMATION, AND RELATIONSHIPS TO FLOW

Effective decisions toward mitigating water quality problems sit at the nexus of understanding the sources of contaminants, their potential to be transformed by watershed systems, and the hydrologic regimes that control their transport. Without this understanding, expanding populations and associated changes to land use and infrastructure will continue to degrade water quality across the globe. In addition, interactions with climate change have potential to exacerbate the direct drivers of water quality impairment.

While humans are increasingly responsible for water quality degradation, society has simultaneously recognized some sources of the problem and provided pressure to minimize environmental impact. Water pollution has been among Americans' top environmental concerns for the last 30 years (Keiser and Shapiro 2019). The US government has implemented considerable regulation of water quality since the 1970 Water Quality Improvement Act and the 1972 Clean Water Act, and we have seen subsequent improvements to water quality in some areas (Keiser *et al.* 2019). Rivers like the Cuyahoga in northern Ohio no longer catch on fire, largely due to strict controls on point sources of pollution. However, much of the effort to understand controls on water quality since the 1970s have been focused on localized solutions, with less emphasis on addressing fundamental or theoretical questions about mechanisms influencing water quality from more diffuse sources of pollution (Bentley *et al.* 2015; Keiser *et *al.* 2019; Keiser and Shapiro 2019). Furthermore, the influence of nonpoint sources of pollution and indirect human effects on water quality have continued to expand (Keiser and Shapiro 2019), contributing to the existential water crisis facing humanity if current trends in freshwater resource degradation remain unchecked (UNESCO 2020).

Decisions related to management, regulation, and governance of human influence often fall on people who are not scientifically trained in the mechanisms controlling the quality of water resources (Keiser *et al.* 2019; Keiser and Shapiro 2019). My personal motivation in hydrologic science stems from a desire to translate process-based scientific understanding into forms that will be useful for resource managers and other decision makers. The first half of my career as an environmental consultant was focused on "applied" understanding of controls on water quality in the context of large-scale mining and oil and gas production. That experience coupled with my research as a PhD student has taught me that the fiscal and human resource costs of quantifying the extent of water quality problems is often disproportionate to the costs of developing the mechanistic understanding necessary to provide a solution.

The high costs of determining the scope of water resource contamination problems likely originate from poor design decisions that do not recognize the complexity of the landscape-scale hydrologic processes that control contaminant transport (Blöschl et al., 2019, Chapter 2) and do not consider the biogeochemical transformation of contaminants (Chapter 3, Nimick *et al.* 2011). The overlap of multiple controls on contaminant fate and transport result in hydrological scientific challenges that do not necessarily have general, objective, and verifiable solutions. Furthermore, characterization of fundamental principles of water quality theory has been limited by a lack of repeatable experiments and reliance on inference from observational research

(Blöschl *et al.* 2019a). Observational studies like those included in this dissertation are often the best we can do with resources available, but more syntheses of these studies integrating process-based understanding across individual catchments is necessary for broader, transferable concepts. Ultimately, mechanistic understanding of solute sources, biogeochemical transformations, and their relationships with a hydrologic regime are necessary to facilitate effective management of fresh waters (Van Meter *et al.* 2016; Giri and Qiu 2016; Blöschl *et al.* 2019a; Downing *et al.* 2021).

The findings in this dissertation provide common examples of the variable but ubiquitous human alteration of flow and water chemistry within streams and rivers. Subsequent interpretations of these findings contribute improvements to process-based understanding of controls on water quality that are meaningful to management decisions. The work within the research Chapters 2-4 demonstrate links between water quality drivers and dramatic human alterations to the landscape and climate. Effects on water quality occurred through multiple pathways of influence that manifested through changes in solute delivery, alteration of biogeochemical processing, and influence on timing related to hydrologic flow regimes. Concepts synthesized across these chapters include: (1) the importance of differentiating issues with load or concentration and their relationship with flow; (2) understanding the seasonal and daily variation in contaminant concentrations and loads; and (3) recognizing the potential for stream ecosystems to alter contamination regimes.

1. The Nuance and Importance of Both Load and Concentration Perspectives

Assessment of controls on water quality in this dissertation were built through critical evaluation of relationships between solute concentrations, solute loads, and the flow of water in the stream or river. Additional inference related to solute sources and transformation was gained through patterns that spanned multiple scales of space and time and from the combined spatiotemporal patterns of multiple solutes.

Ultimately, the definition and regulation of water quality as a relative metric varies by country and government regulatory control (e.g. state vs. federal) on the concentration and loads of contaminants. In the US, water quality is generally based on a solute's potential to impair a beneficial use (US EPA 2015a). The regulation of Total Maximum Daily Loads (TMDL) in the US is the primary federal tool under the Clean Water Act to reduce introduction of nonpoint source contaminants (US EPA 2015a). TMDL's are based on allocating and regulating the additive loads from different sources of pollution in an effort to regulate the mass inputs that accumulate to unacceptable concentrations in receiving water bodies (Elshorbagy *et al.* 2005). However, in Canada, specifically solute contamination from the Elk Valley Coal Mines, regulations are based on permitted maximum concentrations of solutes emerging from mine operations (BC ENV, 2024). Therefore, international variation in even the basic definitions of water quality and regulatory tools present complexity in defining the scope of contamination issues in waters that cross borders.

In the Elk Valley, treatment related to nitrate and selenium has been focused on reducing the highest concentrations in the Elk River and surrounding tributaries and seemingly produced only a modest reduction in the total mass of nitrate and selenium that is moving downstream

(Storb *et al.* 2023). Regulating using only concentration targets prevents consideration of how the loading of solutes is distributed in space and time downstream. Regulation of contamination based on concentration alone may be problematic in the geographic setting of this water quality issue, where the Elk River feeds a large reservoir with portions regulated by different countries. The distribution of variation in the loading of contaminants in space and time will determine the accumulated concentrations downgradient in Lake Koocanusa and beyond. The Koocanusa physiographic setting is somewhat unique and may induce challenges among countries and first nations in regulatory perspectives - these waters highlight the importance of considering both load and concertation in establishing thresholds for action.

A system of regulation based on loads alone also has its limitations and could benefit from more nuanced understanding of the mechanisms that might influence temporal variation in concentrations (Chapter 3). The development of a TMDL for nutrients may not consider instream biogeochemical controls (Elshorbagy *et al.* 2005; Shoemaker *et al.*) and their potential to mask the true loads entering the stream via inducing diel oscillations and seasonal changes in concentration. Without consideration of diel or seasonal influences on biogeochemical processes, the typical limited sampling underlying derivation of most TMDL's may underestimate the true integrated loads within the stream (Chapter 3).

2. Understanding Controls on Solute Concentration Dynamics

Understanding the controls influencing temporal variation in concentrations of contaminants in streams is critical to effective management decisions toward improving water quality (Keiser *et al.* 2019; Keiser and Shapiro 2019). Considering the evidence of processes underlying seasonal and diel variation in this dissertation, improved sampling and analysis approaches may be necessary to quantify accurate integrated loads for addressing regulation standards. Furthermore, characterizations of these variations in contaminant concentrations are useful for inferring the magnitude of the relevant underlying processes. Research in Lake Koocanusa (Chapter 2) and the West Fork of the Gallatin (Chapter 3) directly highlight how dynamics of contaminant concentration influence potential decisions about water quality issues. And work on characterizing the timing of snowmelt hydrologic regimes highlights understanding of changes in flow regime that may be critical toward understanding dilution or flushing effects on contaminant concentration. Concentrations of solutes vary with flow when dilution or flushing patterns accompany the hydrologic regime, and the temporal signals of reactive solutes may be transformed by temporal variation in biogeochemical processing (Chapter 3). Together, these chapters emphasize a few of the primary hydrologic and biogeochemical controls on temporal variation in contaminant concentration that should be considered for more accurate predictive models, sampling schemes, or TMDL regulation.

The relationships of temporal variations in concentration with variation in discharge highlighted in the Lake Koocanusa study are particularly critical to understanding the mechanisms of stream flow and solute load generation specific to individual watersheds (Knapp *et al.* 2020). Past work has suggested that concentration-discharge relationships for dissolved weathering products in streams and rivers exhibit nearly chemostatic behavior (i.e. similar concentrations across a range in flow) across a geologically diverse range of catchments and flow regimes (Godsey *et al.* 2009). Data from the Elk River illustrates that human influence through extensive physical disturbance of bedrock may push watersheds away from typically chemostatic behavior. In the Elk River watershed, large scale increases in waste rock are likely the primary source of dissolved selenium species via mineral surface area newly exposed to the water necessary to enhance chemical weathering. This large-scale landscape alteration has generally increased baseflow selenium and nitrate concentrations to a degree that the outlet of the watershed has changed from a chemostatic to a snowmelt dilution pattern over the past 4 decades.

The higher resolution sampling necessary to fully characterize and accurately integrate temporal variation in contaminant concentrations is not always possible, but sufficient sampling to characterize the C-Q relationship may allow derivations of models that can fill gaps in the time series with reasonable confidence. The WRTDS modeling approach used in Chapter 2 (Hirsch and Cicco 2015) is an empirical model that uses information contained in C-Q relationships from lower resolution data to infer higher frequency variation in solute concentrations over time. The C-Q structure of this analytical tool allowed for important inference of the changing solute delivery in the Elk River watershed over time.

Diel variation in the influence of metabolic uptake on nutrient concentrations (Chapter 3) illustrate additional problems with conventional sampling related to deriving water quality regulations aimed at mitigating eutrophication. Conventional water quality sampling is based on hours when people work (9am to 5pm) and often during good weather. A sampling scheme limited to daylight hours, during the summer months, in a nutrient impaired stream will likely be subject to higher stream ecosystem uptake and thus not reflect the true loads entering the stream (Chapter 3). Derivation of TMDL's for metabolically important nutrients are most likely to be biased by sampling schemes that neglect daily or seasonal variation due to autotrophic uptake, which may be the case for the nitrate TMDL derived for the West Fork of the Gallatin (Schade and Kusnierz 2010). Seasonal and diel variation in biogeochemical or hydrological processes that effect corresponding variation in solute concentrations are a critical consideration for TMDL derivations that reflect the true threat to ecosystem integrity.

3. Stream Ecosystems as Mediators of Contamination

The metabolic chemical reactivity associated with freshwater ecosystems is known to have some capacity to mediate human influence on water quality (Alan Yeakley et al., 2016, Chapter 3). Stream corridors tend to have disproportionate influence on biologically reactive solutes in watershed export with respect to their area, due to the consistent transport of water from the landscape through a unique biogeochemical environment relative to the rest of the watershed (Wollheim *et al.* 2018). In many instances, streams have the biogeochemical capacity to buffer the effects of increased loading on solute concentrations. However, in the context of nutrients, the potential for the stream to mitigate increases in nutrient loading must be considered in the context of the response of the ecosystem to fertilization and any subsequent changes in uptake efficiencies (Earl *et al.* 2006).

Combining research on ecosystem eutrophication (Chapter 3) with research on the timing of ecologically relevant flow events (Chapter 4) demonstrate how predicting the trajectory of water quality in streams requires integrating the ecosystem transformation of nutrients with the hydrologic transport of nutrients or hydrologic disturbance to ecosystem biota. While stream ecosystems have the biogeochemical capacity to chemically transform solutes, human influence on hydrologic regimes can differentiate between when streams function as solute conduits vs. solute transformers (Chapter 2, O'Donnell and Hotchkiss 2019). Both flow and solute delivery can elongate or shorten the length of a stream needed to process a given fraction of solute

(Seybold and McGlynn 2018; O'Donnell and Hotchkiss 2019), but across all streams and rivers, flow is likely the primary driver in shaping whether a stream primarily functions to transform or transport nutrients (Poff *et al.* 1997). Flow impacts ecosystem function through solute mass delivery, changing concentrations via dilution, altering water residence time, and disturbance from scour events (Poff *et al.* 1997; Dodds *et al.* 2002a; Wollheim *et al.* 2018). Thus, changes in the flow regime with changes in climate have multiple pathways of influence on ecosystem function and water quality.

Research across this dissertation broadly illustrates that through a range of human influence, we may be inducing the loss or alteration of mediative effects of ecosystems on water quality through increased solute delivery and or changes to flow regimes that induce "over saturation" of contaminants. While stream function globally provides mediating effects to water chemistry, humans may be driving streams to a tipping point where loss of efficiency in abiotic and biotic processes results in diminishing mediative capacity in buffering water quality impairment (Wollheim *et al.* 2018; O'Donnell and Hotchkiss 2019). Recently the river network-scale saturation concept has been proposed (Wollheim *et al.* 2018), where saturation refers to conditions when the supply of a constituent (including nutrients and other solutes or sediment) overwhelms the demand for that constituent. The saturation effect therefore results in an increasing loss of the ability of a river network to control the amount exported from the watershed as loading to the stream within the watershed increases. Saturation state is thus perhaps the most important character of watersheds to understand when prioritizing water quality mitigation efforts.

4. Recommendations

Research in this dissertation collectively suggests that holistic conceptual models of controls on water quality and non-point-source pollution management should be based on a nexus of understanding contaminant sources, solute transformation, and hydrologic transport. Case studies from snowmelt driven hydrologic regimes of the northern Rocky Mountains particularly illustrate how each of component of this nexus is critical to both the science and regulation of water quality issues in the region that translate to issues common across the globe. Headwater systems also provide the starting point for chemistry, quantity, and timing for all downstream water users and ecosystems (Wollheim *et al.* 2018), making them critical locations for understanding controls on water quality as they are often the least human affected locations on the landscape (Jacobson *et al.* 2019). Information contained within relationships among, concentration, load, and discharge show promise for linking human effects to solute delivery, transformation, and transport by hydrologic regimes. Water Quality is one of the most critical existential problems that humanity will need to solve in the future, and successful mediation of problems requires approaches that integrate the three key elements of this nexus. My hope it the work within this dissertation and the nexus framework it supports can be used to strategize and prioritize the next round of studies to improve understanding of controls on water quality. Furthermore, my hope is that more holistic approaches to process-based understanding can be communicated to mangers and decision makers, so findings are implemented in ways that produce meaningful outcomes to water quality.

APPENDICES

APPENDIX A

SUPPORTING INFORMATION FOR CHAPTER TWO

Supporting Information for Chapter Two:

Growth of coal mining operations in the Elk River Valley (B.C. Canada) linked to increasing solute transport of Se, NO_3^-, and SO_4^{2-} into the transboundary Koocanusa Reservoir (USA-Canada)

Meryl B. Storb[1,3*], Ashley M. Bussell[1], Sara L. Caldwell Eldridge[1], Robert M. Hirsch[2], Travis S. Schmidt[1]

1. U.S. Geological Survey WY- MT Water Science Center, 3162 Bozeman Avenue, Helena MT 59601
2. U.S. Geological Survey Water Mission Area, 12201 Sunrise Valley Dr, Reston, VA 20192
3. Department of Land Resources and Environmental Sciences, Montana State University, Bozeman, Montana, USA

Journal: Environmental Science and Technology

Prepared June 2023

29 pp. in length, including text, 5 tables and 13 figures.

Methods

SI Geospatial Analysis for Mine Area

Total area of disturbance (waste rock deposits) was estimated using remote sensing and geospatial analysis techniques (SI Figure 1). Specifically, Sentinel 2 data [1] for August, 2022 were mosaicked and composited for the Elk River Watershed using Google Earth Engine. [2] A function to mask clouds from the image using bands 10 and 11 was applied and pixel values for all images included in the composite were reduced to the median value for each band. Random forest classification was then done on the composite image. [3] The classification model was trained with ten trees using the training classes and associated sample sizes shown in table SI 1a. Fifty percent of the training data were held out for validation for each tree. Total mean error from validation on holdout sites was 12.7%. The classified image was then imported to ArcPro[4] for postprocessing. The image was converted to a multipart polygon using the conversion tools. Next, the Region Group tool was used to eliminate polygons less than 5,000 square meters, as these small polygons likely represented misclassified pixels rather than actual landcover features. Additionally, because the objective of this exercise was to extract the perimeter of the waste rock area, small polygons located within the waste rock polygons associated with a class other than waste rock were eliminated on the assumption that while the surface reflectance in the imagery might indicate the presence of another landcover (e.g., water or vegetation) it is likely still underlain by waste rock. The final areas of waste rock are shown in table SI 1b.

Additional Site Information

The Kootenay River near Fenwick Station (BC08NG0009) is 13 km downstream of the Fort Steele discharge station (08NG065) and downstream of the confluence with the Saint Mary's River, but upstream of the confluence with the Bull River (Figure 1).[5] Sample collection at this site was discontinued in September 2019. The mean daily discharge for the Kootenay at Fort Steele (WSC site 08NG065) between 1963 and 2022 was 148 m^3sec^{-1}.[5] Because the discharge and water sampling locations are not concurrent, flow was corrected by the difference in contributing area between the two sites, meaning flow at the Fort Steele location was increased by 2.82% to estimate flows at the Fenwick location. Adjusted flows for the Fenwick site are available in Lange and Storb.[6]

There is a historical Water Survey of Canada (WSC) site the Elk River at Phillips Bridge (08NK005), 6.7 km upstream of the Highway 93 sampling location[5]. Flow at Phillips Bridge was measured from 1924-1996. The closest flow measurement location that is currently in operation is the WSC Elk River at Fernie site (08NK002). Thus, Move2 streamflow record extension techniques[7, 8] were implemented in R[55] using the smwrStats package[9] to extend the daily flow record at Phillips Bridge, based on the flow relationship between the two sites post 1970 (Correlation coefficient 0.9805). Once the record extension was complete, an area correction factor was applied to account for the difference in contributing area between the Phillips Bridge and the Highway 93 sampling location, flows from Phillips Bridge were increased by 0.49%. Adjusted flows for the Highway 93 site are available in Lange and Storb [6]

Geology

The Elk and Kootenay Watersheds are both contained within the Canadian Cordillera and bisected by faults that run north to south. In both watersheds faults have generated the valley bottoms where their respective rivers are present, however the bedrock geologies are different.[10] The Upper Kootenay Watershed is generally comprised of carbonate and silicate geology, the eastern side is primarily limestones and dolomites, and the western side is dominated by carbonate and siliciclastic formations. The Kootenay River overlays quaternary alluvium, and the riverbed mirrors the Rocky Mountain Trench fault.[10] The Elk River Watershed generally runs north to south, with the Elk River overlaying a quaternary alluvial aquifer and mirrors the Bourgeau thrust fault from its northern extent to the town of Fernie. The Elk Valley contains two of the three, structurally separate, major coalfields in British Columbia (B.C.).[11] Mining in the Elk River Watershed is focused on bituminous coal from the Mist Mountain Formation which is part of the Jurassic-Cretaceous Kootenay Group (deposited 150-130 M years ago; 450-550 m thick) and is underlain by limestone bedrock, which has high karst potential in some areas.[12, 13] Coal has been mined in the Elk River Watershed since 1897, with large-scale mining in the valley beginning in the 1970's with the transition to open pit drill and blast methods.[14] The Kootenay River Watershed is also home to mining operations, including a smelter and several gypsum and silica mines. Several metal explorations are also occurring[10] and the Sullivan Metal Mine (operated by Teck Resources for Pb, Zn and silver (Ag) production) near the town of Kimberly operated for almost a century, but closed in 2001. [15]

Analysis Methods

WRTDS Model Governing Equation. The Weighted Regression on Time Discharge and Seasons (WRTDS) model is based on using statistical smoothing by partitioning the variation present in constituent concentration values into three components and an error term. The four components are related to season within the year, the watershed hydrologic condition or discharge component, long-term trend, and the random unexplained portion of the variation.[16] The basic form of the underlying WRTDS model is below, where c is concentration; Q is discharge; t is time in years; and ε is unexplained variation:

$$\ln(c) = \beta0 + \beta1\, t + \beta2 \ln(Q) + \beta3 \sin(2\pi t) + \beta4 \cos(2\pi t) + \varepsilon \quad (1)$$

The equation is a weighted regression and is fit in the form of a weighted Tobit model (i.e., survival regression). The model accommodates the incorporation of non-detect data because each concentration value can be expressed as a single number for a data point with a detection or as an interval between 0 and the reporting limit for non-detect values.[17, 18] Likelihoods were determined from 250 bootstrap intervals assuming stationary flow normalization.

Kalman. Performance of WRTDS_Kalman[19] depends on the AR1 coefficient (ρ), and that relationship varies with constituents and sampling scenarios. The default for ρ within the WRTDS_Kalman function is 0.9.[19, 20] This was utilized for selenium and sulfate after exploration of larger and smaller ρ values (0.85 and 0.95) did not generate estimates that were substantially different (<5%), $\rho = 0.95$ was used for nitrate for WRTDS_Kalman[19] estimates for both rivers following results presented in Zhang and Hirsch.[19]

Exceedance Probability. One way of describing the trends in Se concentrations over the period of record is to use estimates of the expected number days in each year when Se concentrations exceeded the water quality criteria. These calculations are made by using the WRTDS model of Se for the Elk River. For each day of the 38-year long record[6] the WRTDS model provides an estimate of conditional mean and standard deviation of the natural log of concentration for that day (conditioned on year, time of year, and discharge). Using the observed residuals from the fitted WRTDS model as a representation of the probability distribution of the standardized residual for each day, we estimate, for each day in the period of record, the probability of exceedance of the criteria. The expected number of days that concentration exceeded the criteria is simply the sum of the probabilities for all days in the year.

The approach to calculating the expected number of days on which the Se concentrations exceed a specified criterion is based on the estimated WRTDS model and the discharge record.

Let x_i = the concentration on day i,

$y_i = \ln(x)_i$

$\bar{y}_i$ = the estimated conditional mean of y_i from the WRTDS model

s_i = the standard deviation of the distribution of y_i from the WRTDS model

where i is the index of all 14,004 days in sequence, starting with 1984-07-10 and ending with 2022-11-11.

We can express the value if y_i on any given day as:

$$y_i = \bar{y}_i + s_i \cdot e_i$$

The e_i values are standardized residuals, computed from the WRTDS model and the data set of 774 observed concentrations. They are computed as:

$$e_j = \frac{y_{j-}\bar{y}_j}{s_j} \text{ for } j = 1, 2, \ldots, 774$$

The subscript j here refers to the sequence number of sample values, (1 to 774).

Rather than using some theoretical distribution (such as gaussian) for these standardized residuals we use the population of observed standardized residuals from the data set.[6] In the case considered here, the Elk River Se data, we have 774 observations and hence 774 observed standardized residuals (these are a set of jack-knife cross-validation estimates computed in the modelEstimation() function in EGRET). [18] It is assumed here that each of these 774 residuals is equally likely to have occurred on any given day in the 14,004-day record.

For purposes of estimation of the probability of exceedance of the water quality criterion, denoted here as x^*. The natural log of the criterion is denoted as $y^* = \ln(x^*)$.

For each day in the period of record ($i = 1, 2, \dots 14004$) we compute 774 equally likely outcomes one for each sampled day ($j = 1, 2, \dots 774$)). Those 10,839,096 ($= 14004 \cdot 774$) outcomes are denoted $V_{i,j}$ and they are computed as:

$1\ if\ +$

$$V_{i,j} = \begin{cases} 1\ if\ \bar{y}_i + s_i \cdot e_j \geq y^* \\ 0\ \text{if}\ \bar{y}_i + s_i \cdot e_j < y^* \end{cases}$$

Then the estimated probability that concentration on day i exceeds the criterion x^* is defined as

$$p_i = \frac{\sum_{J=1}^{774} V_{I,J}}{774} \quad \text{for } i = 1, 2, \dots, 14004$$

We can then compute the expected number of exceedances for each water year in the record as $z_k = \sum_{i \in U_k} p_i$

Where, $i \in U_k$ denotes the set of all days, i, in year k.

The z_k represent the expected number of days of exceedances in year k and can take on any value from 0 to 365 (or 366 in a leap year).

Any use of trade, firm, or product names is for descriptive purposes only and does not imply endorsement by the U.S. Government

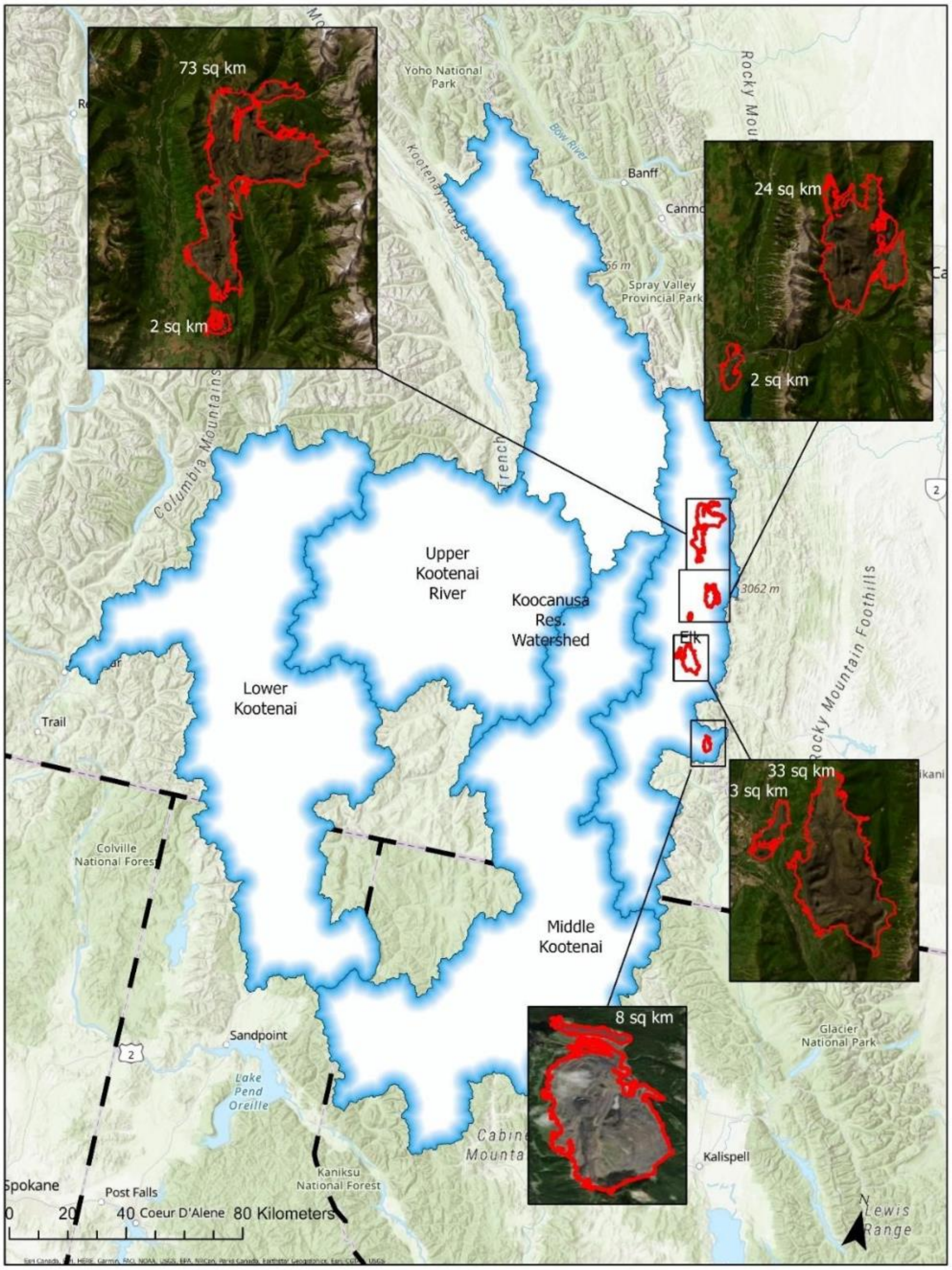

Appx.A SI Figure 1. Total area of mine disturbance (waste rock deposits) based on GIS analysis of aerial imagery.

Appx.A SI Table 1a. Training classes and associated sample sizes from the GIS analysis of mine waste rock area

Sample size (n)	Class
228	Waste rock
89	Forest
68	Water
81	Open rock
60	Deforested

Appx.A SI Table 1b. Final areas of waste rock from GIS analysis.

Mine	Area of disturbance, in square kilometers
Fording River Operations	75 km^2
Line Creek Operations	26 km^2
Elkview Operations	36 km^2
Coal Mountain Operations (in closure period)	8 km^2

Appx.A SI Table 2. Elk River Watershed cumulative waste rock volumes by mine, reported by Teck Resources in their 2022 Implementation Plan Adjustment Document (Table 2.1). [21] Existing volumes are values at the end of 2020 in millions of bank (in situ) cubic meters.

Operation	Existing Volume (BCM x 10^6)	Permitted Volume (BCM x 106) at the end of mining
Fording River	3,036	4,787
Greenhills	808	1,186
Line Creek	797	1,445
Elkview	1,787	3,304
Coal Mountain[1]	311	311
Total	**6,739**	**11,033**

1. No longer operating and c
2. Currently in a closure period

Appx.A SI Table 3. Se, NO3-, SO42- annual estimates of load (optimized for accuracy) for the Elk River (Elk) and Kootenay River (Koot). The proportion that the Elk River contributed by year, from the combined estimates of the two tributaries is shown in percent for each constituent and discharge.[16]

Year	Koot Flow (m^3/sec)	Elk Flow (m^3/sec)	Elk proportion of total combined (%)	Koot Se (t/Yr)	Elk Se (t/Yr)	Elk proportion of total combined (%)	Koot NO_{3-} (t/Yr)	Elk NO_{3-} (t/Yr)	Elk proportion of total combined (%)	Koot SO_{42-} (t/Yr)	Elk SO_{42} (t/Yr)	Elk proportion of total combined (%)
1979	128	58.8	31.50%				442.77	218	33%			
1980	173	67.3	28.00%				557.15	243	30%			
1981	214	90.3	29.70%				713.84	400	36%			
1982	189	72.5	27.70%				672.67	350	34%			
1983	173	67.8	28.20%				581.46	250	30%			
1984	154	60.5	28.20%				594.72	280	32%			
1985	142	61.6	30.30%		1.66		552.34	317	36%	103186	32077	24%
1986	188	75.8	28.70%		2.22		630.72	345	35%	123833	41149	25%
1987	154	61.1	28.40%		2.04		521.04	337	39%	115952	38303	25%
1988	139	52.1	27.30%		1.63		530.82	261	33%	104826	32286	24%
1989	166	63.1	27.50%		1.86		668.4	301	31%	114991	37871	25%
1990	204	89.8	30.60%		3.57		828.57	624	43%	126769	46310	27%
1991	238	100.4	29.70%		4.09		953.65	828	46%	141380	54032	28%
1992	143	53.6	27.30%		2.2		533.41	419	44%	104216	38947	27%
1993	159	67.9	29.90%		3.12		535.13	550	51%	112542	43943	28%
1994	158	61.6	28.10%		3.23		607.38	603	50%	119986	44531	27%
1995	171	76.5	30.90%		3.69		632.1	670	51%	122786	48108	28%
1996	228	101	30.70%		5.44		813.86	893	52%	153292	61970	29%
1997	181	80	30.70%		4.48		589.91	612	51%	132329	51921	28%
1998	175	75.9	30.30%		4.62		634.14	805	56%	136417	54786	29%
1999	220	78.7	26.30%		4.21			794			55958	
2000	185	70.8	27.70%		4.31			627			55155	
2001	108	39.6	26.80%		2.49			356			38955	
2002	169	84.3	33.30%		5.27			679			59197	
2003	133	64	32.50%	0.49	5.22	91.50%		672			58338	
2004	148	59.7	28.70%	0.36	4.22	92.10%		497			50190	
2005	168	77.6	31.60%	0.46	6.1	93.00%		811			62462	
2006	187	87.8	32.00%	0.49	7.83	94.20%		1214			73056	
2007	203	82.2	28.80%	0.56	7.78	93.30%		1115			69321	
2008	160	67.2	29.60%	0.4	6.88	94.50%		1153			63140	
2009	139	49.7	26.30%	0.4	5.54	93.30%	414.02	899	68%		50131	
2010	138	55.6	28.70%	0.38	6.05	94.10%	427.55	1104	72%		54625	
2011	204	80.8	28.40%	0.5	8.48	94.40%	596.62	1633	73%		66141	

Table Appx.A SI Table 3 CONTINUED

2012	238	100.1	29.60%	0.58	11.53	95.20%	712.9	2139	75%		79029	
2013	212	98.9	31.80%	0.49	12.6	96.20%	657.21	2645	80%	135270	88804	40%
2014	192	86.6	31.10%	0.44	12.4	96.60%	589.34	2815	83%	128185	85490	40%
2015	152	63.6	29.50%	0.35	9.99	96.60%	494.69	2038	80%	117210	74140	39%
2016	162	60.9	27.30%	0.42	9.12	95.60%	539.4	2031	79%	127970	76617	37%
2017	210	80.5	27.70%	0.51	9.96	95.20%	848.21	2115	71%	146569	79502	35%
2018	179	70.3	28.20%	0.45	10.21	95.80%	595.46	2169	78%	131452	84313	39%
2019	144	51.6	26.40%	0.37	7.88	95.50%	460.4	1448	76%	124535	64884	34%
2020		74.6			10.5			2198			80595	
2021		74			11.36			2501			82322	
2022		87.8			12.27			2549			89262	
Mean	174	72	29.20%	0.45	5.77	94.50%	615	1034	58%	124938	4.5E+07	30%
Mean Post 2009	179	74	28.60%	0.44	9.85	95.30%	576	2020	76%	130170	74353	38%

Appx.A SI Table 4. Selenium and Nitrate treatment, locations, timing, and volumetric capacity as presented in the 2022 Teck Implementation Plan Adjustment. 21 Pilot phase start dates sourced from mass removal data provided by Teck.6 Note, from pilot phase start to the operational date, treatment facilities did not operate continuously and additional treatment pilot projects occurred before 2015.

Water Treatment Facility	Facility Type	Pilot Phase Start	Operational Date	Hydraulic Capacity (m^3/day)
Line Creek Operation WLC Phase I	Active Water Treatment	October 25, 2015	December 31, 2018	6,000
Line Creek Operation WLC Phase II	Active Water Treatment	NA	January 1, 2020	1,500
Elkview Operation SRF Phase I	Saturated Rock Fill Treatment	January 1, 2018	September 1, 2021	20,000
Fording River Operation AWTF (FRO-South)	Active Water Treatment	December 22, 2021	September 1, 2022	20,000

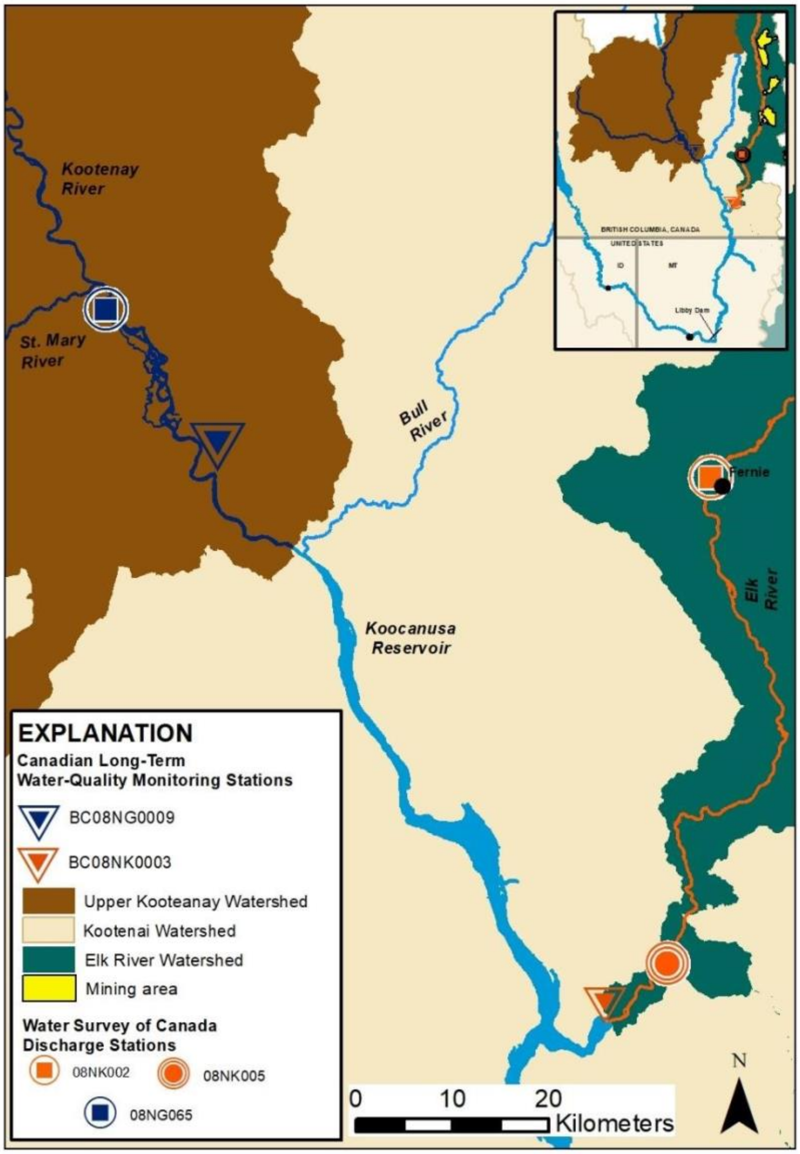

Appx.A SI Figure 2 Map illustrating Canadian Water Survey of Canada discharge monitoring stations (halo symbols) and water quality sampling locations (triangles) for both the Elk (orange) and Kootenay (blue) Rivers.

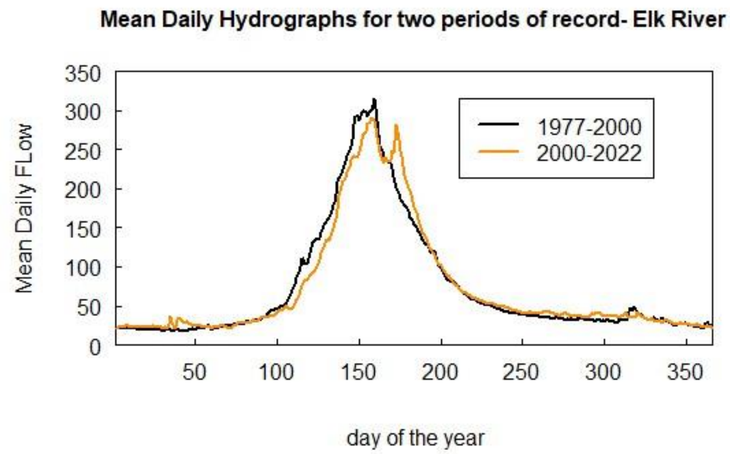

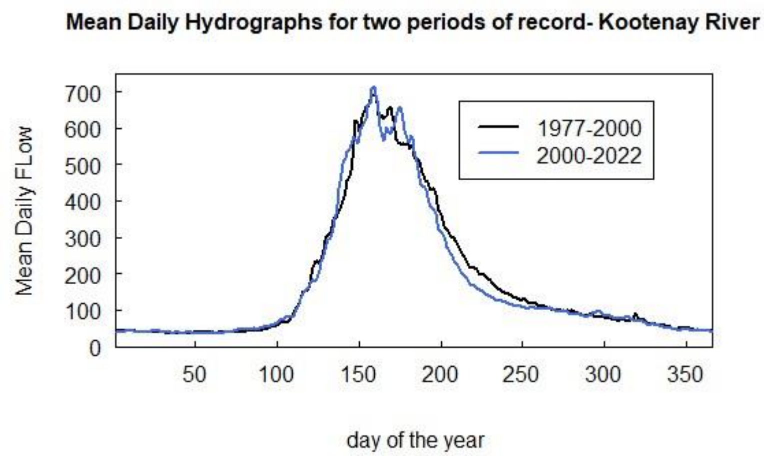

Appx.A SI Figure 3. Mean daily hodographs for the Elk River at Hwy 93 (top) and Kootenay River at Fenwick (bottom) [22], discharge in m^3/sec. Two time periods are shown one from 1977-2000 and from 2000-2022.

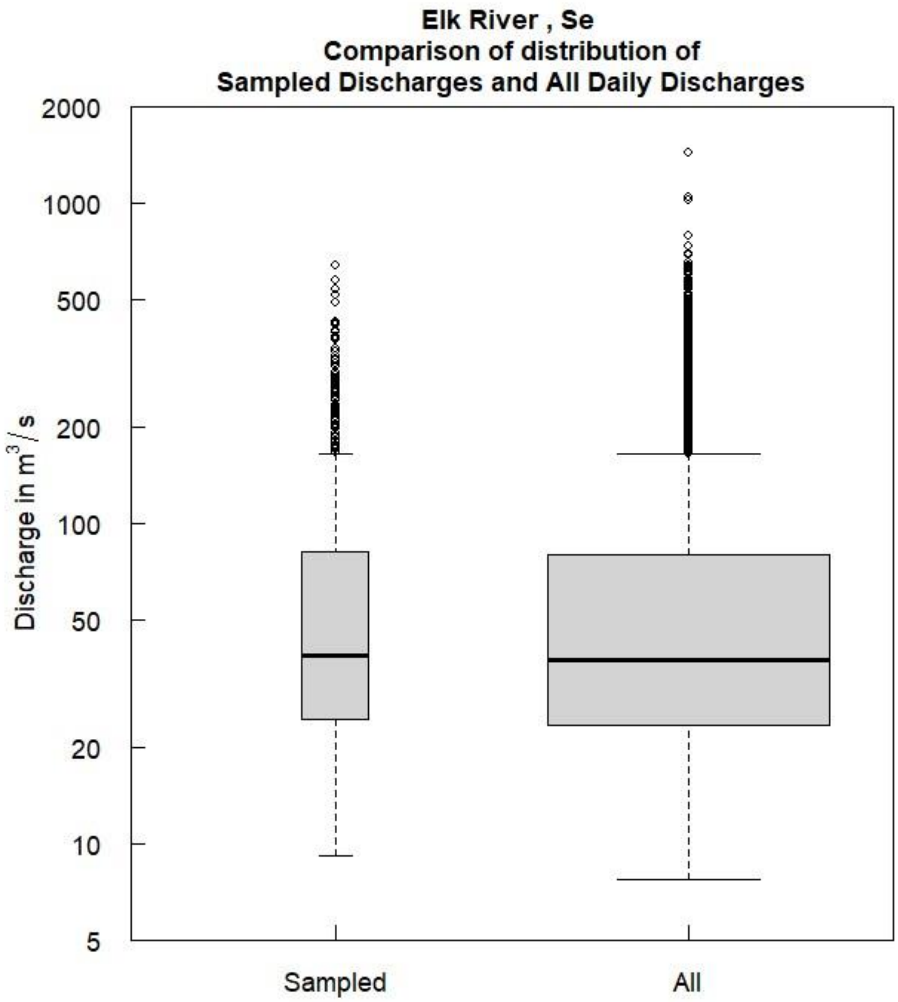

Appx.A SI Figure 4. Box plot illustrating the range of discharge on days with water quality sampling vs those without water 201 quality samples for Se in the Elk River at Highway 93.

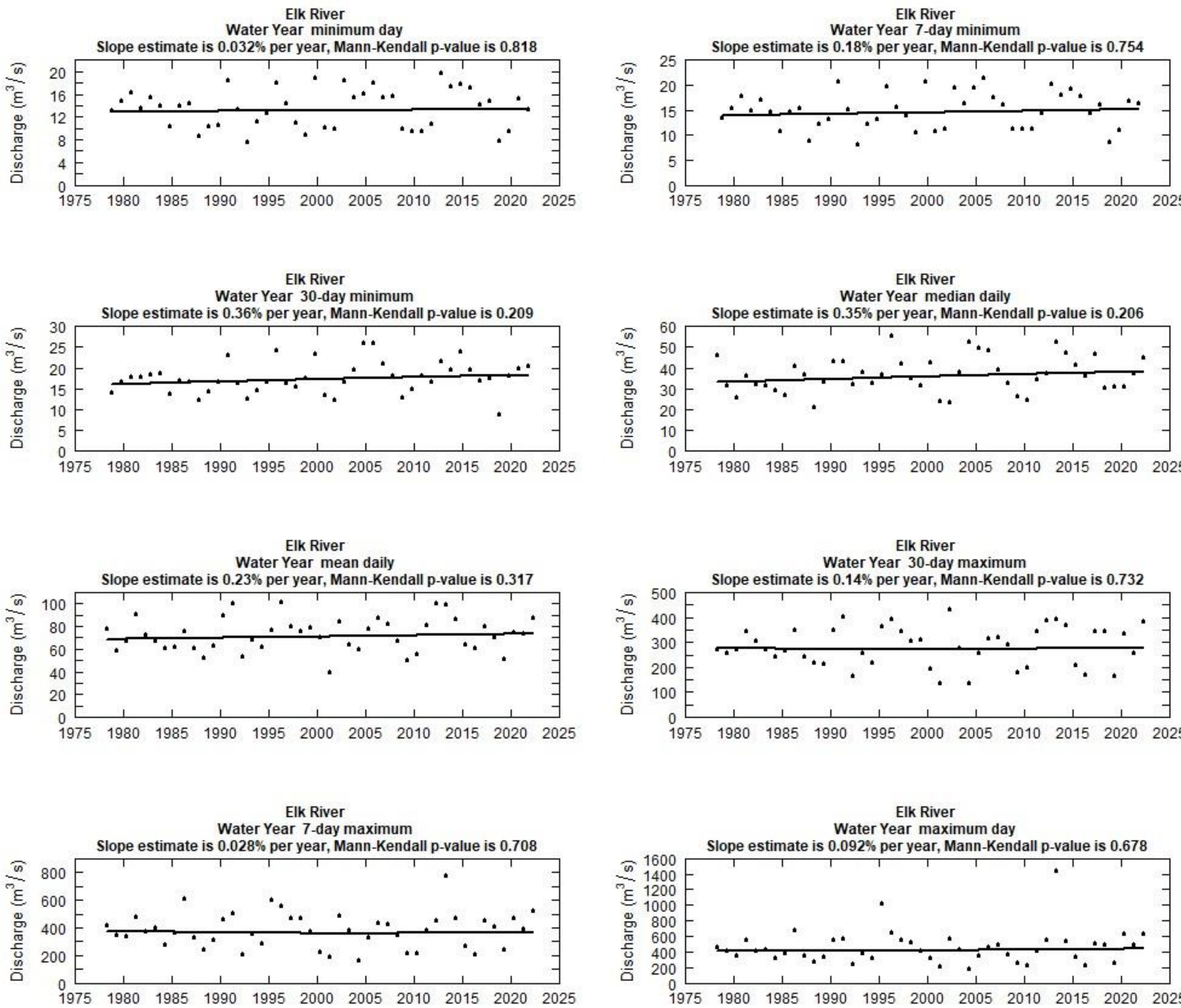

Appx.A SI Figure 5. Elk River at Highway 93, flow record from 1979-2021. [6] Plots showing 8 different statistical flow metrics, with the Mann-Kendall trend test and corresponding Theil-Sen slope estimate to evaluate flow stationarity. The Theil-Sen slope provides an estimate of the direction and magnitude of the Mann-Kendall trend. [23]

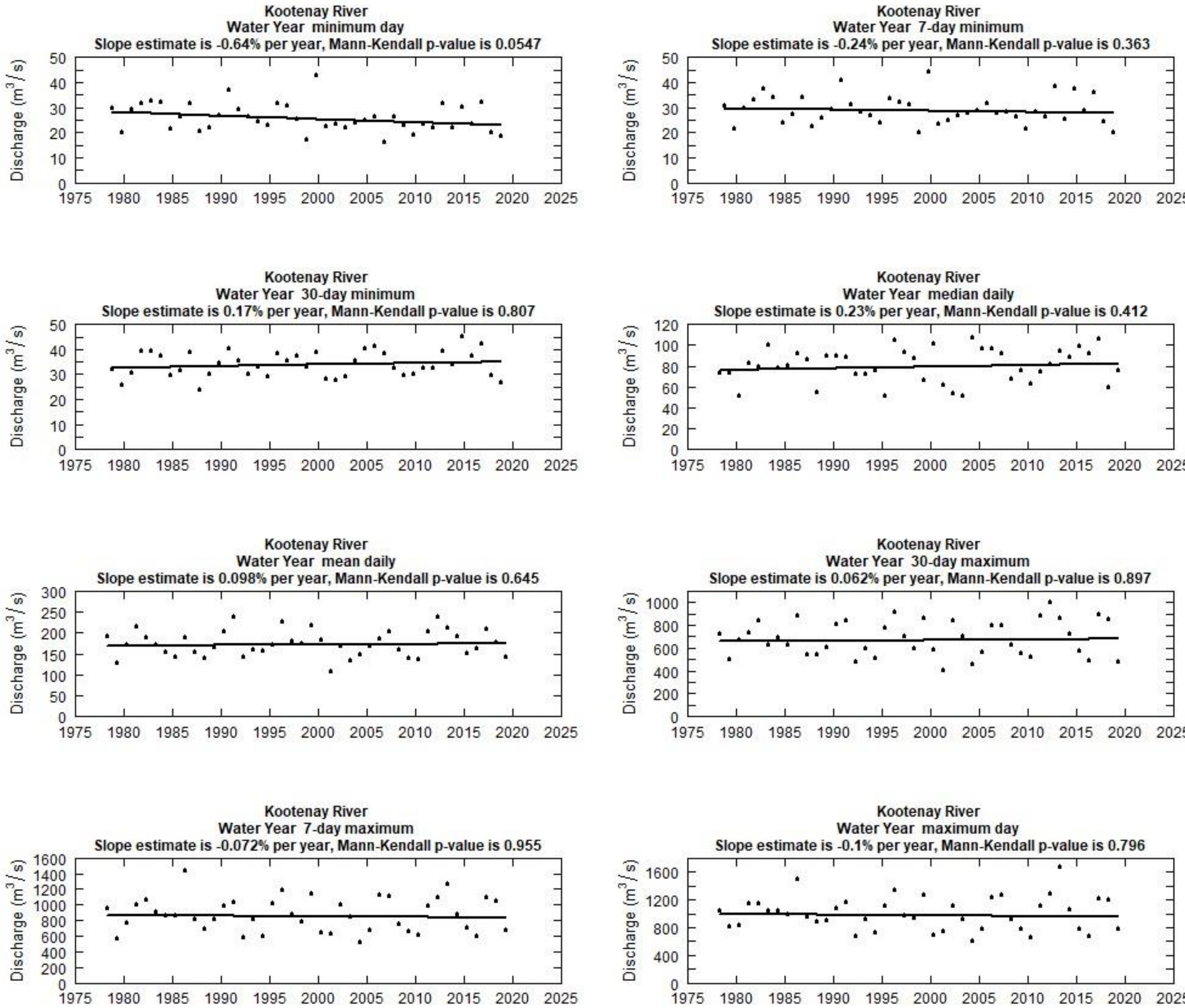

Appx.A SI Figure 6. Kootenay River at Fenwick, flow record from 1979-2019. [6] Plots showing 8 different statistical flow metrics, and the Mann-Kendall trend test and corresponding Theil-Sen slope estimate to evaluate flow stationarity. The Theil-Sen slope provides an estimate of the direction and magnitude of the Mann-Kendall trend. [23]

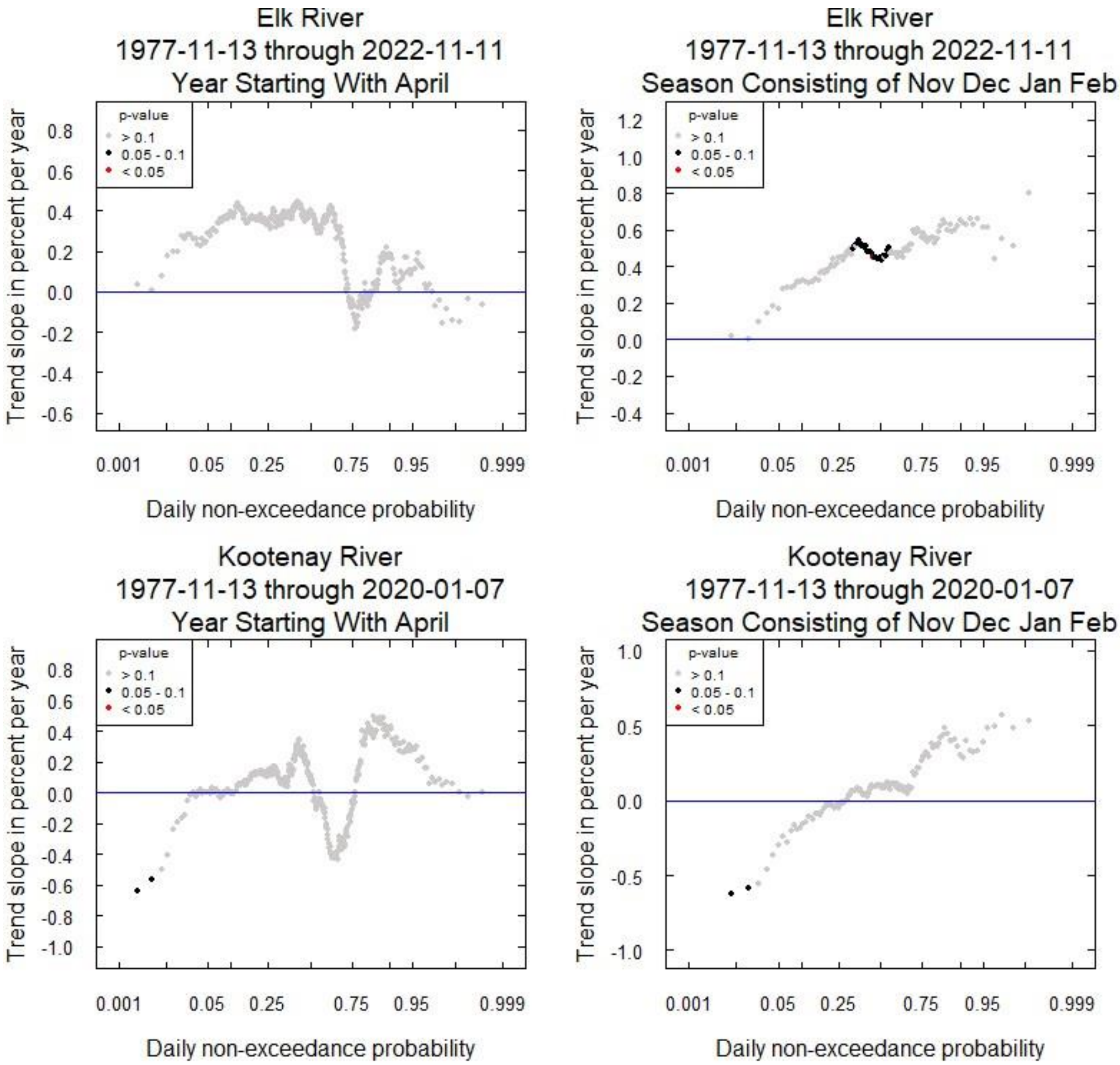

Appx.A SI Figure 7. Streamflow trends for the Elk River at Highway 93 (top two panels) and the Kootenay River at Fenwick (bottom two panels). Left panels are Quantile-Kendall plots for the water year. Right are Quantile-Kendall plots for the low flow period (February-October). Quantile-Kendall plots are visualizations of trends in slope for ranked discharge, where each point is a trend slope for a given order statistic, the lowest daily discharge is on the left and the highest is on the right. [24]

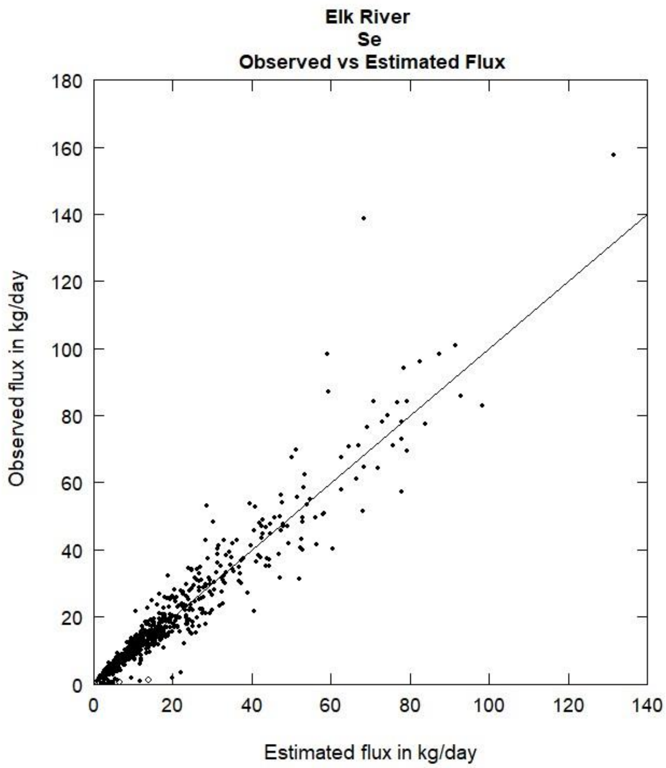

Appx.A SI Figure 8. Plot illustrating the difference between observed daily loads on the days when samples were collected vs modeled daily load on the same day for Se in the Elk River at Highway 93. Open circles are generated values that represent censored (below detection limit) values. Equivalent Rsquared value for this model (error in the estimates of log(Flux)) is 0.852. 20 of the 841 samples were below the detection limit. Models are available in Lange and Storb, 2023.[6]

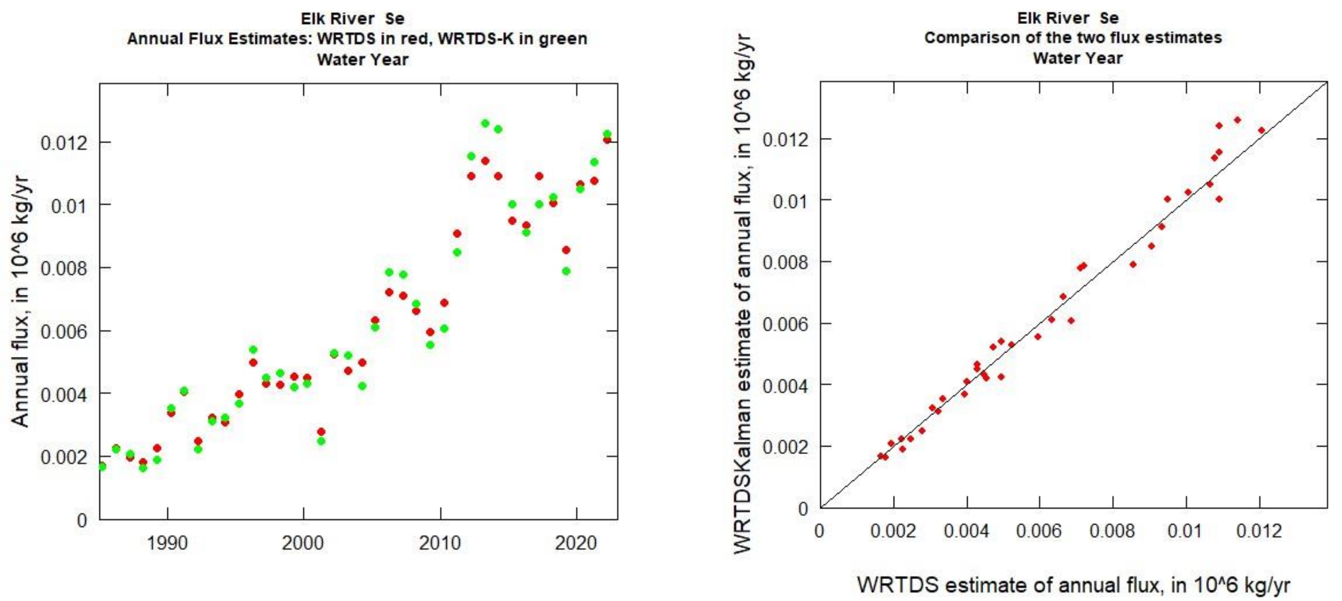

Appx.A SI Figure 9. Two plots illustrating the difference between WRTDS and WRTDS_kalman models for Se in the Elk River at Highway 93. Models are available in Lange and Storb, 2023.[6]

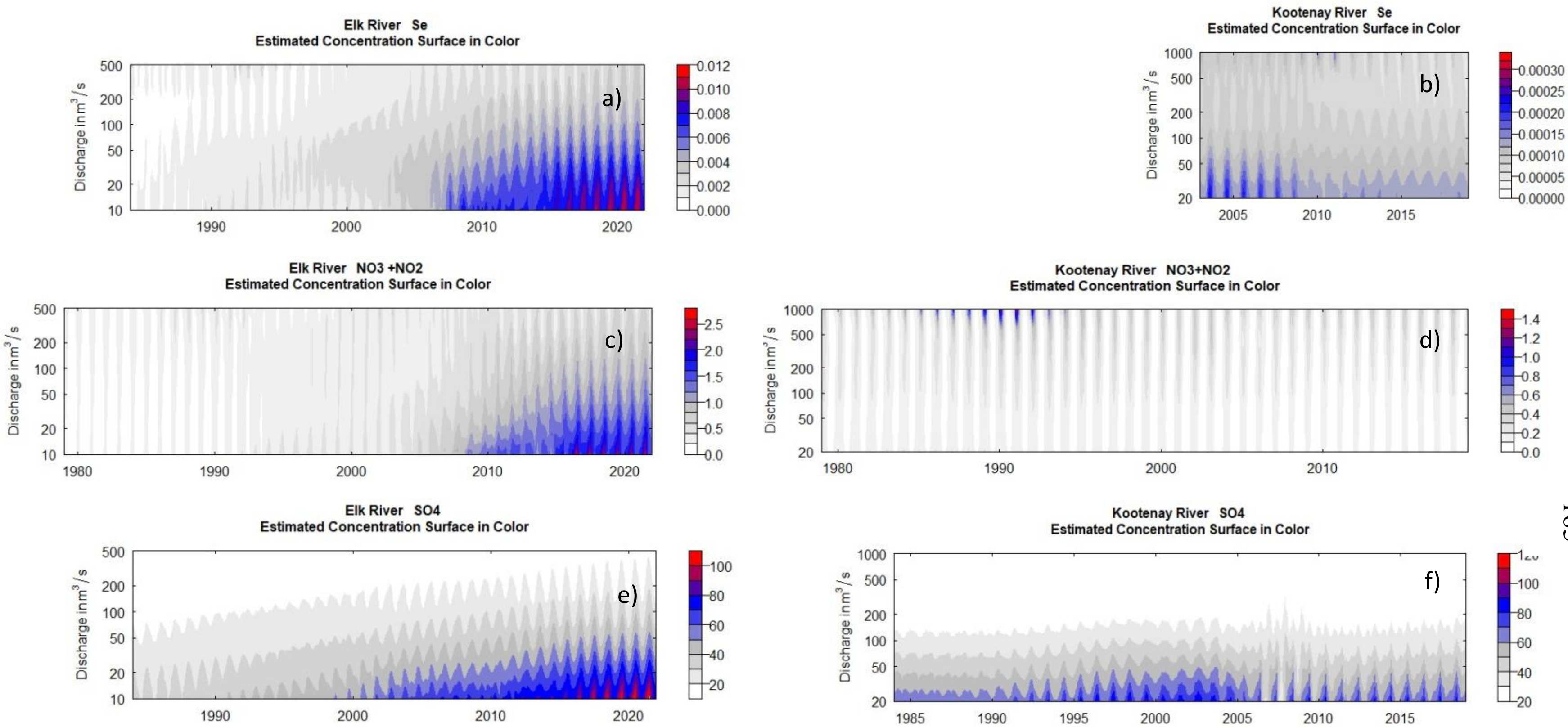

Appx.A SI Figure 10. Weighted Regression based on Time Discharge and Season (WRTDS) modeled 3-D surfaces for Se, NO_3^-, SO_4^{2-} for the Elk River at Highway 93 and the Kootenay River at Fenwick. Plots illustrate and quantify the relationship between concentration and discharge over time for each WRTDS model. Left plots are the three solutes for the Elk River at Highway 93 and Right plots are the three solutes for the Kootenay River at Fenwick. Top row of plots is Se, middle is NO_3^-, bottom row is SO_4^{2-}. The color ramp represents concentration of the respective constituent in mg/l. Models are available in Lange and Storb, 2023.[6]

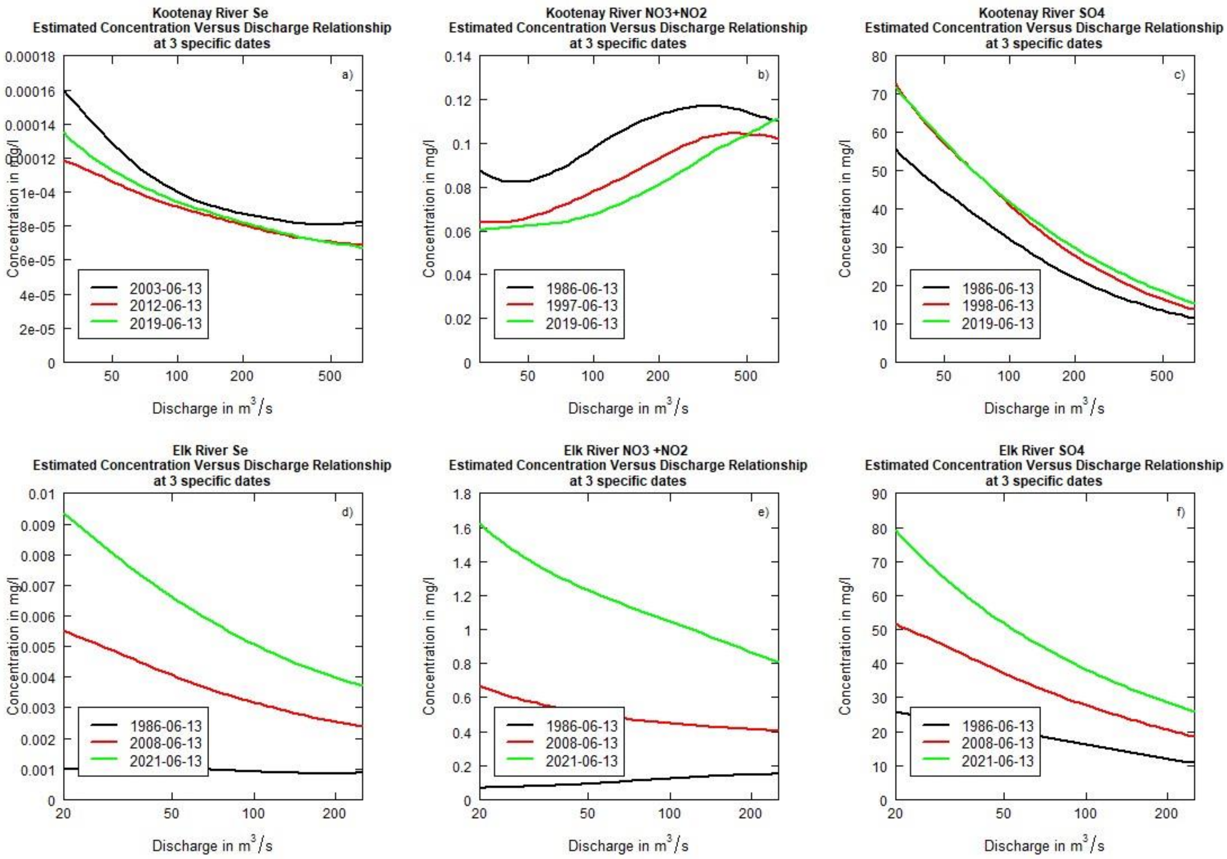

Appx.A SI Figure 11. Modeled concentration vs discharge relationships. Top row (a-c) is the Kootenay River at Fenwick, the bottom row is the Elk River at Highway 93 (d-e). Each column is a solute, from left to right (Se; a & d, NO_3^-: b & e, SO_4^{2-}; c & f). Each line is a different date. These plots are focused on high flow times of the year (June 13) over time. Low flow times (ex. January 1) exhibit similar patterns but are not shown. Models are available in Lange and Storb, 2023.[6]

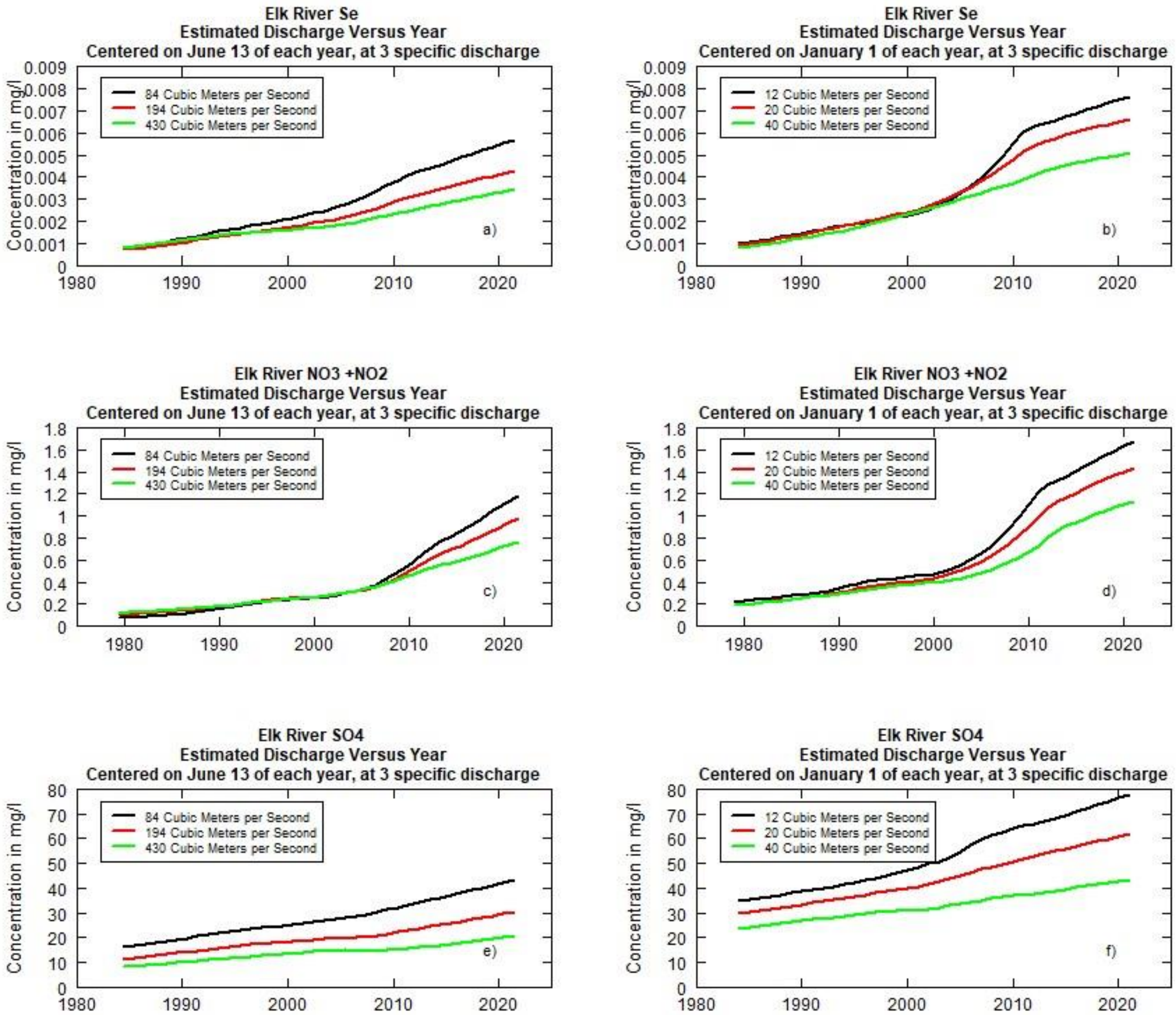

Appx.A SI Figure 12. Changes in concentration over time at different discharges and times of the year for the Elk River at Highway 93. The left column (a-c-e.) is high discharge time of year (June 13) and the right column (b-d-f.) is a low discharge time of year (Jan 1). Discharge lines roughly represent the 5th, 50th, and 95th percentiles for flow duration curves for 60 days around (30 days before and after) each date. Models are available in Lange and Storb, 2023.[6]

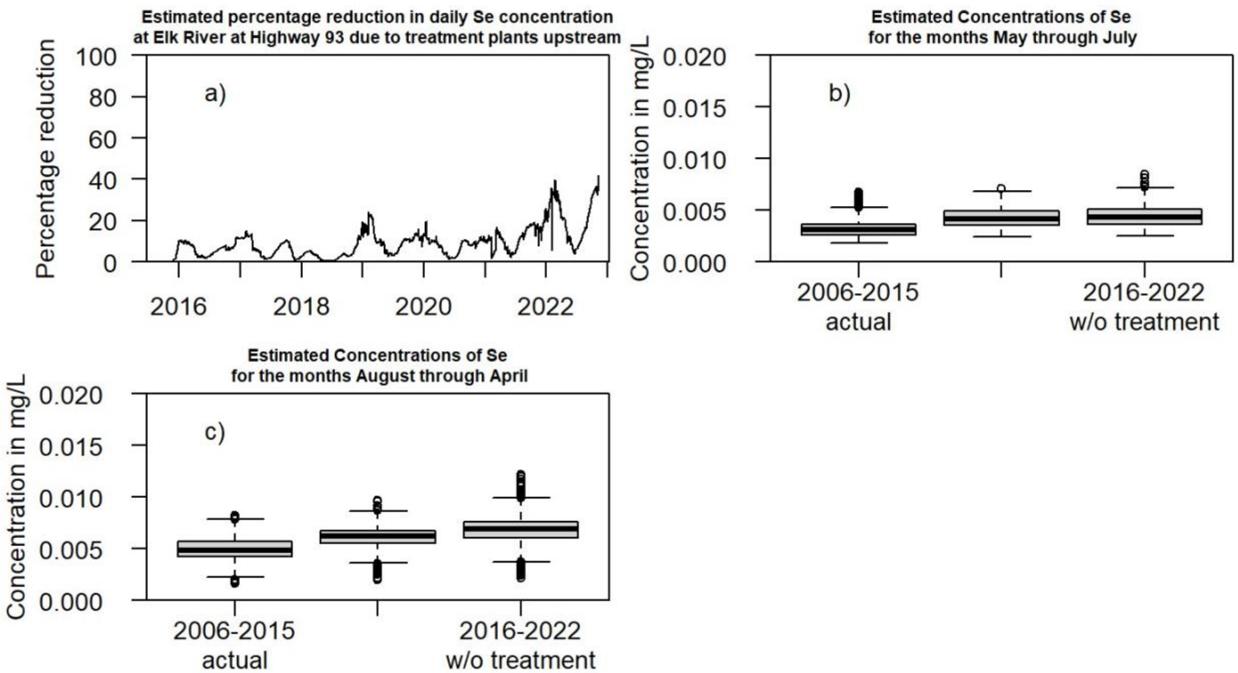

Appx.A SI Figure 13. Additional perspective on Elk River Mine water treatment. a.) Estimated percentage reduction in concentration due to treatment. Reductions range from 0% to 40%. b.) Boxplots of estimated daily concentrations of Se during the high discharge months of May, June, and July. First box is for water years 2006-2015, second is 2016 – 2022, and the third is also for 2016-2022 but simulated as if there had been no treatment upstream. [the medians of the three boxes shown are 0.0032, 0.0042, 0.0045]. c.) Boxplots of estimated daily concentrations of Se during the low discharge months of August through April. First box is for water years 2006-2015, second is 2016 – 2022, and the third is also for 2016-2022 but simulated as if there had been no treatment upstream [the medians of the three boxes shown are 0.0049, 0.0062, 0.0075].

Supporting Information References

(1) Copernicus Sentinel data processed by European Space Agency. (accessed January 18, 2023).

(2) Gorelick, N.; Hancher, M.; Dixon, M.; Ilyushchenko, S.; Thau, D.; Moore, R. Google Earth Engine: Planetary-scale geospatial analysis for everyone. *Remote Sensing of Environment* 2017, *202*, 18-27. DOI: 10.1016/j.rse.2017.06.031.

(3) Rodriguez-Galiano, V. F.; Ghimire, B.; Rogan, J.; Chica-Olmo, M.; Rigol-Sanchez, J. P. An assessment of the effectiveness of a random forest classifier for land-cover classification. *ISPRS Journal of Photogrammetry and Remote Sensing* 2012, *67*, 93-104. DOI: 10.1016/j.isprsjprs.2011.11.002.

(4) *ArcGIS Desktop*; Redlands, CA, 2013. (accessed June 22, 2023).

(5) British Columbia Ministry of Forests Lands Natural Resource Operations and Rural Development. *BC Water Tool - Watershed*. 2023. https://kwt.bcwatertool.ca/watershed (accessed February 9, 2023).

(6) Lange, D. A.; Storb, M. B. *Input files and WRTDS model output for the two major tributaries of Lake Koocanusa*; 2023. (accessed June 2023). DOI: 10.5066/P9JP8VGL.

(7) Granato, G. E. *Computer programs for obtaining and analyzing daily mean streamflow data from the U.S. Geological Survey National Water Information System web site*; 2009. DOI: 10.3133/ofr20081362.

(8) Medalie, L. *Effects of urban best management practices on streamflow and phosphorus and suspended-sediment transport on Englesby Brook in Burlington, Vermont, 2000-2010*; Reston, VA, 2012. DOI: 10.3133/sir20125103.

(9) Lorenz, D. L. *smwrBase—An R package for managing hydrologic data, version 1.1.1*; Reston, VA, 2015. (accessed May 8, 2023). DOI: 10.3133/ofr20151202.

(10) Katay, F. *Exploration and mining in the Kootenay-Boundary Region, British Columbia. In: Exploration and Mining in British Columbia, 2014*; Information Circular 2015-2; British Columbia Ministry of Energy and Mines, British Columbia Geological Survey, 2015. https://cmscontent.nrs.gov.bc.ca/geoscience/publicationcatalogue/InformationCircular/BCGS_IC 2016-01-03.pdf (accessed February 9, 2023).

(11) Goodarzi, F.; Grieve, D. A.; Sanei, H.; Gentzis, T.; Goodarzi, N. N. Geochemistry of coals from the Elk Valley coalfield, British Columbia, Canada. *International Journal of Coal Geology* **2009**, *77* (3), 246-259. DOI: 10.1016/j.coal.2008.08.010.

(12) Wellen, C.; Shatilla, N. J.; Carey, S. K. The influence of mining on hydrology and solute transport in the Elk Valley, British Columbia, Canada. *Environmental Research Letters* 2018, *13* (7), 074012. DOI: 10.1088/1748-9326/aaca9d.

(13) British Columbia Forest Analysis and Inventory Branch. *Reconnaissance karst potential mapping*; 2023. https://catalogue.data.gov.bc.ca/dataset/reconnaissance-karst-potential-mapping (accessed May 10, 2023).

(14) Lussier, C.; Veiga, V.; Baldwin, S. The geochemistry of selenium associated with coal waste in the Elk River Valley, Canada. *Environmental Geology* 2003, *44* (8), 905-913. DOI: 10.1007/s00254-003-0833-y.

(15) Teck Resources Limited. *Sullivan Mine*. 2023. https://www.teck.com/operations/canada/legacy/sullivan-mine/ (accessed June 6, 2023).

(16) Hirsch, R. M.; Moyer, D. L.; Archfield, S. A. Weighted Regressions on Time, Discharge, and Season (WRTDS), with an application to Chesapeake Bay River inputs. *Journal of the American Water Resources Association* 2010, *46* (5), 857-880. DOI: 10.1111/j.17521688.2010.00482.x.

(17) Hirsch, R. M.; Archfield, S. A.; De Cicco, L. A. A bootstrap method for estimating uncertainty of water quality trends. *Environmental Modelling & Software* 2015, *73*, 148-166. DOI: 10.1016/j.envsoft.2015.07.017.

(18) Hirsch, R. M.; De Cicco, L. A. *User guide to Exploration and Graphics for RivEr Trends (EGRET) and dataRetrieval: R packages for hydrologic data: U.S. Geological Survey Techniques and Methods 4-A10*; Reston, VA, 2015. (accessed February 9, 2023). DOI: 10.3133/tm4A10.

(19) Zhang, Q.; Hirsch, R. M. River water-quality concentration and flux estimation can be improved by accounting for serial correlation through an autoregressive model. *Water Resources Research* 2019, *55* (11), 9705-9723. DOI: 10.1029/2019WR025338.

(20) Lee, C. J.; Hirsch, R. M.; Crawford, C. G. *An evaluation of methods for computing annual water-quality loads: U.S. Geological Survey Scientific Investigations Report 2019-5084*; Reston, VA, 2019. (accessed February 9, 2023). DOI: 10.3133/sir20195084.

(21) Teck Resources Limited. *Elk Valley water quality plan: 2022 implementation plan adjustment*; 2022.https://www.teck.com/media/EVWQP_2022_ImplementationPlanAdjustment_Main_Report.pdf (accessed January 9, 2023).

(22) British Columbia Ministry of Forests Lands Natural Resource Operations and Rural Development. *B.C. Water Tool - Streamflow & Water Levels*. 2023. https://kwt.bcwatertool.ca/streamflow (accessed June 6, 2023).

(23) Helsel, D. R.; Hirsch, R. M.; Ryberg, K. R.; Archfield, S. A.; Gilroy, E. J. *Statistical methods in water resources*; Reston, VA, 2020. (accessed February 13, 2023). DOI: 10.3133/tm4A3.

(24) U.S. Geological Survey. *Daily Streamflow and Trend Analysis*. 2023. https://doiusgs.github.io/EGRET/articles/streamflow_trend.html#the-quantile-kendall-plot (accessed February 9, 2023).

APPENDIX B

AUTHORSHIP LETTERS RELATED TO CHAPTER TWO

United States Department of the Interior

U. S. GEOLOGICAL SURVEY
Water Mission Area
Wyoming-Montana Water Science Center
3162 Bozeman Ave
Helena, MT 59601

MEMORANDUM

Date:3/27/24

To: Meryl Storb's Graduate Committee inclusive: Dr. Robert Payn, Dr. Wyatt Cross, Dr. Stephanie Ewing, Dr. Geoffrey Poole, Dr. Kristin Gardner

From: Dr. Travis S. Schmidt, Research Ecologist
Project lead Lake Koocanusa/Clark Fork

Subject: Meryl Storb's authorship attribution for the manuscript and data release on Lake Koocanusa

Dear Committee,

I am writing to provide an overview of Meryl Storb's significant contributions to the manuscript referenced above.

Meryl serves as a part-time staff scientist at the WY-MT Water Science Center. As a Pathways Student, she was tasked with managing the Flaxville groundwater project while also assisting with the Lake Koocanusa project. Within the latter, Meryl undertook a comprehensive study focusing on selenium, nitrate, and sulfate discharge from metallurgical mines in British Columbia into the Koocanusa area, intersected by the US/CA international boundary. Initially, her project encompassed various facets, including loading, trend, and flux studies. However, she eventually narrowed her focus to the loading and trend analysis specifically on the Elk River.

Meryl demonstrated exceptional attention to detail and expertise in hydrology and water quality principles during the data acquisition phase from British Columbia. Collaborating with Canadian agencies, she identified and rectified discrepancies in the data, ensuring transparency and adherence to USGS principles of open science. Subsequently, she applied standard USGS loading and trends code to analyze the data, uncovering shifts in the hydrologic regime and exploring the impact of active and passive treatment operations on water quality along the Elk River.

When she encountered limitations in existing USGS code for her analysis, Meryl collaborated with Dr. Robert Hirsch, a renowned USGS scientist, to develop novel code resources tailored to her research needs. This collaborative effort culminated in significant advancements in code, analysis techniques, and interpretations.

The manuscript resulting from Meryl's work was recognized as an Office of Budget and Management Influential Scientific Product by the USGS, necessitating rigorous internal and external reviews. It underwent review by notable USGS scientists and external reviewers selected by the journal Environmental Science and Technology, as well as Environment and Climate Change Canada scientists. Meryl effectively navigated the multifaceted review process, ensuring compliance with USGS

United States Department of the Interior

U. S. GEOLOGICAL SURVEY
Water Mission Area
Wyoming-Montana Water Science Center
3162 Bozeman Ave
Helena, MT 59601

Fundamental Science Practice goals. This is to say the manuscript and data release were subjected to the highest level of reviews for both any government document but also that of a journal article. She led data acquisition, analysis, writing, revisions, and final manuscript preparations.

Beyond her scholarly achievements, Meryl's work garnered substantial attention from the press and policymakers. She conducted interviews with national press outlets and provided expert testimony to the Montana Legislature, showcasing her ability to communicate complex scientific findings to diverse audiences.

In summary, Meryl's contributions to this manuscript were that of any lead author and extend far beyond that. She demonstrated exceptional leadership, technical expertise, and resilience throughout the project, making significant contributions to the advancement of scientific knowledge and its impact on policy and society.

Sincerely,

Travis Schmidt, PhD
Research Ecologist
US Geological Survey
WY-MT Water Science Center
Helena, MT 56901

Storb, M. B., Bussell, A. M., Caldwell Eldridge, S. L., Hirsch, R. M., Schmidt, T. S. 2023. Growth of Coal Mining Operations in the Elk River Valley (Canada) Linked to Increasing Solute Transport of Se, NO_3^-, and SO_4^{2-} into the Transboundary Koocanusa Reservoir (USA-Canada). Environ Sci Technol 2023, 57 (45), 17465-17480. DOI: 10.1021/acs.est.3c050902023.

Lange, D.A., and Storb, M.B., 2023, Input Files and WRTDS Model Output for the two major tributaries of Lake Koocanusa: U.S. Geological Survey data release, https://doi.org/10.5066/P9JP8VGL.

United States Department of the Interior

U. S. GEOLOGICAL SURVEY
409 National Center
Reston, VA 20192

MEMORANDUM

April 5, 2024

To: Meryl Storb's Graduate Committee inclusive: Dr. Robert Payn, Dr. Wyatt Cross, Dr. Stephanie Ewing, Dr. Geoffrey Poole, Dr. Kristin Gardner

From: Dr. Robert M. Hirsch, Research Hydrologist Emeritus, USGS Water Mission Area, Reston, VA

Subject: Meryl Storb's authorship attribution for the manuscript: *Storb, M. B., Bussell, A. M., Caldwell Eldridge, S. L., Hirsch, R. M., Schmidt, T. S. 2023. Growth of Coal Mining Operations in the Elk River Valley (Canada) Linked to Increasing Solute Transport of Se, NO_3^-, and SO_4^{2-} into the Transboundary Koocanusa Reservoir (USA-Canada). Environ Sci Technol 2023, 57 (45), 17465-17480. DOI: 10.1021/acs.est.3c050902023.*

Dear Committee,

I am writing to provide an overview of Meryl Storb's role in the research that resulted in the above referenced paper published in Environmental Science and Technology (ES&T) in 2023 and to describe my role as well. Let me start by saying that it is truly a great accomplishment for a young scientist such as Meryl to have had her worked published in ES&T, which I believe to be a journal of the highest quality and impact in the world of environmental science.

Meryl's role in the research and writing of the paper was, without question, the central role in the effort. She decided on the scope of the work and determined the directions that the paper would take. She was the person who obtained the data and, most importantly, worked with all of the public and private participants in Canada who were responsible for the data to make sure it was quality assured and that we understood the strengths and limitations of the data. She conceived of structuring the study as a paired watershed analysis, to demonstrate the direct linkage between the surface mining activity and the water quality of the Elk River in contrast to the unmined portion of the Kootenai River watershed.

During this work, Meryl quickly realized that the large deposits of waste rock that filled the valleys between the mined areas had become a significant part of the Elk River watershed flow system. Furthermore, she recognized that the geochemistry and solute transport through these man-made shallow aquifers was the primary source of the elevated selenium and nitrate that found its way to the Elk River and ultimately to the Koocanusa Reservoir. She employed the concepts of concentration versus discharge relationships to characterize the systems in terms of mobilization, dilution, and chemostasis. Evaluating how these generic solute transport relationships evolved over time was entirely a result of her interpretation of the patterns observed in the data.

My involvement in the project came about because she was a student in a USGS training class on statistical methods, in which I was one of the instructors. She recognized that the Weighted Regressions on Time, Discharge, and Season (WRTDS) method of statistical modeling was well suited to the issue of pollutants in the surface waters of the Koocanusa Reservoir watershed. After taking the class she became very proficient at using the EGRET software that implements the WRTDS method (EGRET stands for

Exploration and Graphics for RivEr Trends, an R package of which I am the co-author). She contacted me after the training course to ask for my help in finding the best ways to apply the method to her specific study. I was intrigued with the significance of the water quality issues and the extremely strong trends as well as the seasonality of the data. I quickly saw this as a project of scientific and public policy significance with an excellent scientific leader (Meryl) so I agreed to join in on the project as a volunteer collaborator. I am always excited to be involved in new types of applications of my WRTDS method and EGRET software to water quality problems that are distinctly different from most of the prior work that has been done with the method, focused on primarily agricultural or urban non-point source pollution. This project has helped broaden the scope of applications of my methods.

Meryl, as project leader developed the overall framework of the paired basin analysis and conceptualized the three competing hypotheses for the causes of the distinct change in slope of the trends in nitrate and selenium. She developed the analyses and approaches to evaluating the plausibility of each of these hypotheses. We interacted closely, through a series of meetings, in which she would pose questions relevant to these hypotheses and I would identify new ways to employ the WRTDS model to attempt to shed light on these ideas. One of these questions related to evaluating the impact that the removal of selenium at the various treatment plants had on concentrations and loads of selenium in the Elk River. Meryl and I worked together to find an appropriate way to blend the statistical representation of water quality in the river with the mass balance calculations to develop a with-and-without-treatment characterization of the water quality.

A major conclusion of the paper is that although the treatment plants, which process surface water, can have a beneficial impact on river concentrations of selenium, a meaningful reduction in annual selenium load can only be achieved through treatment of the groundwater that is moving through the waste rock deposits. This conclusion, which was developed and articulated by Meryl, is a major contribution of this paper. It will help set the research and engineering-design work that will lead to meaningful mitigation of the water quality problems associated with the coal mining operations.

In addition to the scientific challenges of this study, this is a high visibility project and that many critical eyes are on this work. Meryl was totally responsible for the edits and improvements to the paper that came about as a result of reviewers' comments: internal USGS reviewers, Canadian government reviewers, and ES&T reviewers. She would turn to me for a few details of these revisions, but the bulk of that effort was carried out by Meryl. This paper received a great deal of attention when published and throughout it all Meryl was the spokesperson for the work. She "owned" every part of it and could speak authoritatively on every aspect of it.

From my perspective, Meryl was an ideal person to collaborate with. She set the stage for all of the work, she posed the questions, and she assembled and quality assured the data. My role was to provide some statistical support that would help quantify and interpretations that she brought forward and demonstrate the degree of uncertainty of the analyses. She handled her role with great knowledge, imagination, and scientific leadership ability. I had not known her before this collaboration and at the end of it I was surprised to learn that she did not yet have a Ph.D. She certainly operated with the kind of knowledge and creativity that one would expect from a Ph.D. scientist.

Sincerely,

Robert M. Hirsch

Robert M. Hirsch, Ph.D.
Research Hydrologist Emeritus

REFERENCES CITED

Adam JC, Hamlet AF, and Lettenmaier DP. 2009. Implications of global climate change for snowmelt hydrology in the twenty-first century. *Hydrol Process* **23**: 962–72.

Alan Yeakley J, Ervin D, Chang H, *et al.* 2016. Ecosystem services of streams and rivers. River Science. John Wiley & Sons, Ltd.

Alexander RB, Boyer EW, Smith RA, *et al.* 2007. The role of headwater streams in downstream water quality1. *JAWRA J Am Water Resour Assoc* **43**: 41–59.

Allan JD and Castillo MM. 2007. Stream Ecology: Structure and function of running waters. Springer Science & Business Media.

Appling A and Heffernan J. 2014. Nutrient limitation and physiology mediate the fine-scale (de)coupling of biogeochemical cycles. *American Naturalist* **184**: 384–406.

Arrigoni AS, Greenwood MC, and Moore JN. 2010. Relative impact of anthropogenic modifications versus climate change on the natural flow regimes of rivers in the Northern Rocky Mountains, United States. *Water Resour Res* **46**: W12542.

Arroita M, Elosegi A, and Hall Jr. RO. 2019. Twenty years of daily metabolism show riverine recovery following sewage abatement. *Limnol Oceanogr* **64**: S77–92.

Bentley PJ, Gulbrandsen M, and Kyvik S. 2015. The relationship between basic and applied research in universities. *High Educ* **70**: 689–709.

Bernhardt ES, Heffernan JB, Grimm NB, *et al.* 2017. The metabolic regimes of flowing waters: Metabolic regimes. *Limnol Oceanogr* **63**: S99–118.

Blöschl G, Bierkens MFP, Chambel A, *et al.* 2019a. Twenty-three unsolved problems in hydrology (UPH) – a community perspective. *Hydrol Sci J* **64**: 1141–58.

Blöschl G, Hall J, Viglione A, *et al.* 2019b. Changing climate both increases and decreases European river floods. *Nature* **573**: 108–11.

Brown JH, Gillooly JF, Allen AP, *et al.* 2004. Toward a metabolic theory of ecology. *Ecology* **85**: 1771–89.

Bundi U and Brittain JE (Eds). 2010. Alpine waters. Heidelberg: Springer.

Burns DA, Pellerin BA, Miller MP, *et al.* 2019. Monitoring the riverine pulse: Applying high-frequency nitrate data to advance integrative understanding of biogeochemical and hydrological processes. *WIREs Water* **6**: e1348.

Campos N, Lawrence R, McGlynn B, and Gardner K. 2011. Using Quickbird and Landsat imagery to analyze temporal changes in mountain resort development: Big Sky, Montana 1990–2005. *J Appl Remote Sens* **5**: 053541-053541–14.

Carpenter SR, Stanley EH, and Zanden MJV. 2011. State of the world's freshwater ecosystems: physical, chemical, and biological changes. *Annu Rev Environ Resour* **36**: 75–99.

Chamberlin C. 2020. The Role of Ecology in Creating diel nitrate concentration patterns in streams and rivers (Ph.D.). United States -- North Carolina: Duke University.

Chamberlin CA, Bernhardt ES, Rosi EJ, and Heffernan JB. 2019. Stoichiometry and daily rhythms: experimental evidence shows nutrient limitation decouples N uptake from photosynthesis. *Ecology* **100**: e02822.

Chaudhuri P and Marron JS. 1999. SiZer for exploration of structures in curves. *J Am Stat Assoc* **94**: 807.

Clarke FW. 1924. The composition of the river and lake waters of the united states. U.S. Government Printing Office.

Clow DW. 2010. Changes in the timing of snowmelt and streamflow in Colorado: A response to recent warming. *J Clim* **23**: 2293–306.

Covino T, McGlynn B, and McNamara R. 2012. Land use/land cover and scale influences on in-stream nitrogen uptake kinetics. *J Geophys Res Biogeosciences* **117**: G02006.

Cross WF, Benstead JP, Frost PC, and Thomas SA. 2005. Ecological stoichiometry in freshwater benthic systems: recent progress and perspectives. *Freshw Biol* 1895–912.

Cross WF, Wallace JB, Rosemond AD, and Eggert SL. 2006. Whole-system nutrient enrichment increases secondary production in a detritus-based ecosystem. *Ecology* **87**: 1556–65.

Dettinger MD and Cayan DR. 1995. Large-scale atmospheric forcing of recent trends toward early snowmelt runoff in California. *J Clim* **8**: 606–23.

Dodds WK. 2007. Trophic state, eutrophication and nutrient criteria in streams. *Trends Ecol Evol* **22**: 669–76.

Dodds WK, López AJ, Bowden WB, *et al.* 2002. N uptake as a function of concentration in streams. *J North Am Benthol Soc* **21**: 206–20.

Dodds WK and Smith VH. 2016. Nitrogen, phosphorus, and eutrophication in streams. *Inland Waters* **6**: 155–64.

Dodds WKK and Welch EB. 2000. Establishing nutrient criteria in streams. *J North Am Benthol Soc* **19**: 186–96.

Downing JA, Polasky S, Olmstead SM, and Newbold SC. 2021. Protecting local water quality has global benefits. *Nat Commun* **12**: 2709.

Doyle MW, Stanley EH, Strayer DL, *et al.* 2005. Effective discharge analysis of ecological processes in streams. *Water Resour Res* **41**.

Dudgeon D, Arthington AH, Gessner MO, *et al.* 2006. Freshwater biodiversity: importance, threats, status and conservation challenges. *Biol Rev* **81**: 163–82.

Durum WH. 1953. Relationship of the mineral constituents in solution to stream flow, Saline River near Russell, Kansas. *Trans Am Geophys Union* **34**: 435–42.

Earl SR, Valett HM, and Webster JR. 2006. Nitrogen saturation in stream ecosystems. *Ecology* **87**: 3140–51.

Edwards AMC. 1973. The variation of dissolved constituents with discharge in some Norfolk rivers. *J Hydrol* **18**: 219–42.

BC ENV. 2024. Elk Valley Water Quality Hub. https://elkvalleywaterquality.gov.bc.ca/. Viewed 22 May 2024.

Elshorbagy A, Teegavarapu RSV, and Ormsbee L. 2005. Total maximum daily load (TMDL) approach to surface water quality management: concepts, issues, and applications. *Can J Civ Eng* **32**: 442–8.

Esri. 2024. Esri. Topographic basemap. Scale Not Given. World Topographic Map.

Gallatin River Task Force. 2024. https://gallatinrivertaskforce.org/. Viewed 17 Jan 2024.

Gardner KK and McGlynn BL. 2009. Seasonality in spatial variability and influence of land use/land cover and watershed characteristics on stream water nitrate concentrations in a developing watershed in the Rocky Mountain west: Human impacts on spatial N patterns. *Water Resour Res* **45**: n/a-n/a.

Gardner KK, McGlynn BL, and Marshall LA. 2011. Quantifying watershed sensitivity to spatially variable N loading and the relative importance of watershed N retention mechanisms: Watershed sensitivity to N loading. *Water Resour Res* **47**: n/a-n/a.

Giri S and Qiu Z. 2016. Understanding the relationship of land uses and water quality in Twenty First Century: A review. *J Environ Manage* **173**: 41–8.

Gleeson T, Wang-Erlandsson L, Porkka M, *et al.* 2020. Illuminating water cycle modifications and Earth system resilience in the Anthropocene. *Water Resour Res* **56**: e2019WR024957.

Gleick PH. 1987. The development and testing of a water balance model for climate impact assessment: Modeling the Sacramento Basin. *Water Resour Res* **23**: 1049–61.

Godsey SE, Kirchner JW, and Clow DW. 2009. Concentration–discharge relationships reflect chemostatic characteristics of US catchments. *Hydrol Process* **23**: 1844–64.

Gordon BL, Brooks PD, Krogh SA, *et al.* 2022. Why does snowmelt-driven streamflow response to warming vary? A data-driven review and predictive framework. *Environ Res Lett* **17**: 053004.

Grimm NB. 1987. Nitrogen Dynamics During Succession in a Desert Stream. *Ecology* **68**: 1157–70.

Hall FR. 1970. Dissolved solids-discharge relationships: 1. Mixing Models. *Water Resour Res* **6**: 845–50.

Hall FR. 1971. Dissolved solids-discharge relationships: 2. Applications to field data. *Water Resour Res* **7**: 591–601.

Hall RJrO and Tank JL. 2003. Ecosystem metabolism controls nitrogen uptake in streams in Grand Teton National Park, Wyoming. *Limnol Oceanogr* **48**: 1120–8.

Hall RO, Tank JL, Baker MA, *et al.* 2016. Metabolism, gas exchange, and carbon spiraling in rivers. *Ecosystems* **19**: 73–86.

Hansen AJ, Rasker R, Maxwell B, *et al.* 2002. Ecological causes and consequences of demographic change in the new West. *BioScience* **52**: 151–62.

Heffernan JB and Cohen MJ. 2010. Direct and indirect coupling of primary production and diel nitrate dynamics in a subtropical spring-fed river. *Limnol Oceanogr* **55**: 677–88.

Hem JD. 1948. Fluctuations in concentration of dissolved solids of some southwestern streams. *Eos Trans Am Geophys Union* **29**: 80–4.

Hem JD. 1985. Study and interpretation of the chemical characteristics of natural water. U.S. Geological Survey.

Hensley RT and Cohen MJ. 2016. On the emergence of diel solute signals in flowing waters. *Water Resour Res* **52**: 759–72.

Hensley RT, Cohen MJ, and Korhnak LV. 2014. Inferring nitrogen removal in large rivers from high-resolution longitudinal profiling. *Limnol Oceanogr* **59**: 1152–70.

Hill WR, Fanta SE, and Roberts BJ. 2009. Quantifying phosphorus and light effects in stream algae. *Limnol Oceanogr* **54**: 368–80.

Hirsch RM and Cicco LAD. 2015. User guide to Exploration and Graphics for RivEr Trends (EGRET) and dataRetrieval: R packages for hydrologic data. U.S. Geological Survey.

Hucks Sawyer A, Bayani Cardenas M, Bomar A, and Mackey M. 2009. Impact of dam operations on hyporheic exchange in the riparian zone of a regulated river. *Hydrol Process* **23**: 2129–37.

Hynes HBN. 2001. The ecology of running waters. Blackburn Press.

Jacobson AP, Riggio J, M. Tait A, and E. M. Baillie J. 2019. Global areas of low human impact ('Low Impact Areas') and fragmentation of the natural world. *Sci Rep* **9**: 14179.

Katz BG, Eberts SM, and Kauffman LJ. 2011. Using Cl/Br ratios and other indicators to assess potential impacts on groundwater quality from septic systems: A review and examples from principal aquifers in the United States. *J Hydrol* **397**: 151–66.

Kaushal SS, Delaney-Newcomb K, Findlay SEG, *et al.* 2014. Longitudinal patterns in carbon and nitrogen fluxes and stream metabolism along an urban watershed continuum. *Biogeochemistry* **121**: 23–44.

Kaushal SS, Gold AJ, and Mayer PM. 2017. Land use, climate, and water resources—Global stages of interaction. *Water* **9**: 815.

Keiser DA, Kling CL, and Shapiro JS. 2019. The low but uncertain measured benefits of US water quality policy. *Proc Natl Acad Sci* **116**: 5262–9.

Keiser DA and Shapiro JS. 2019. US Water pollution regulation over the past half century: burning waters to crystal springs? *J Econ Perspect* **33**: 51–75.

Knapp JLA, Freyberg J von, Studer B, *et al.* 2020. Concentration–discharge relationships vary among hydrological events, reflecting differences in event characteristics. *Hydrol Earth Syst Sci* **24**: 2561–76.

Knowles N and Cayan DR. 2004. Elevational dependence of projected hydrologic changes in the San Francisco estuary and watershed. *Clim Change* **62**: 319–36.

Kormos PR, Luce CH, Wenger SJ, and Berghuijs WR. 2016. Trends and sensitivities of low streamflow extremes to discharge timing and magnitude in Pacific Northwest mountain streams. *Water Resour Res* **52**: 4990–5007.

Lane BA, Dahlke HE, Pasternack GB, and Sandoval-Solis S. 2017. Revealing the diversity of natural hydrologic regimes in California with relevance for environmental flows applications. *JAWRA J Am Water Resour Assoc* **53**: 411–30.

Ledford SH and Toran L. 2020. Downstream evolution of wastewater treatment plant nutrient signals using high-temporal monitoring. *Hydrol Process* **34**: 852–64.

Lettenmaier DP and Gan TY. 1990. Hydrologic sensitivities of the Sacramento-San Joaquin River Basin, California, to global warming. *Water Resour Res* **26**: 69–86.

Luce CH. 2018. Effects of Climate Change on Snowpack, Glaciers, and Water Resources in the Northern Rockies. In: Halofsky JE, Peterson DL (Eds). Climate Change and Rocky Mountain Ecosystems. Cham: Springer International Publishing.

Lutz BD, Mulholland PJ, and Bernhardt ES. 2012. Long-term data reveal patterns and controls on stream water chemistry in a forested stream: Walker Branch, Tennessee. *Ecol Monogr* **82**: 367–87.

Manning DWP, Rosemond AD, Gulis V, *et al.* 2018. Nutrients and temperature additively increase stream microbial respiration. *Glob Change Biol* **24**: e233–47.

Maurer EP, Stewart IT, Bonfils C, *et al.* 2007. Detection, attribution, and sensitivity of trends toward earlier streamflow in the Sierra Nevada. *J Geophys Res Atmospheres* **112**.

Mayer B, Shanley JB, Bailey SW, and Mitchell MJ. 2010. Identifying sources of stream water sulfate after a summer drought in the Sleepers River watershed (Vermont, USA) using hydrological, chemical, and isotopic techniques. *Appl Geochem* **25**: 747–54.

MBMG. 2024. Montana Bureau of mine and Geology- Ground Water Investigations Program. https://mbmg.mtech.edu/WaterEnvironment/GWIP/ProjectUpdate.asp?projectid=BWIPBS&#gsc.tab=0. Viewed 6 Feb 2024.

McCabe GJ and Clark MP. 2005. Trends and variability in snowmelt runoff in the western United States. *J Hydrometeorol* **6**: 476–82.

Milly PCD, Betancourt J, Falkenmark M, *et al.* 2008. Stationarity is dead: Whither water management? *Science* **319**: 573–4.

Montross GG, McGlynn BL, Montross SN, and Gardner KK. 2013. Nitrogen production from geochemical weathering of rocks in southwest Montana, USA: Nitrogen from geochemical weathering. *J Geophys Res Biogeosciences* **118**: 1068–78.

Moore JN, Harper JT, and Greenwood MC. 2007. Significance of trends toward earlier snowmelt runoff, Columbia and Missouri Basin headwaters, western United States. *Geophys Res Lett* **34**: L16402.

Mote PW, Hamlet AF, Clark MP, and Lettenmaier DP. 2005. Declining mountain snowpack in western north America*. *Bull Am Meteorol Soc* **86**: 39–49.

Mulholland PJ, Fellows CS, Tank JL, *et al.* 2001. Inter-biome comparison of factors controlling stream metabolism. *Freshw Biol* **46**: 1503–17.

Mulholland PJ, Thomas SA, Valett HM, *et al.* 2006. Effects of light on NO_3^- uptake in small forested streams: diurnal and day-to-day variations. *J North Am Benthol Soc* **25**: 583–95.

Mulholland PJ and Webster JR. 2010. Nutrient dynamics in streams and the role of *J-NABS*. *J North Am Benthol Soc* **29**: 100–17.

Musselman KN, Clark MP, Liu C, *et al.* 2017. Slower snowmelt in a warmer world. *Nat Clim Change* **7**: 214.

Nimick DA, Gammons CH, and Parker SR. 2011. Diel biogeochemical processes and their effect on the aqueous chemistry of streams: A review. *Chem Geol* **283**: 317.

O'Donnell B and Hotchkiss ER. 2019. Coupling concentration- and process-discharge relationships integrates water chemistry and metabolism in streams. *Water Resour Res* **55**: 10179–90.

Patterson NK, Lane BA, Sandoval-Solis S, *et al.* 2020. A hydrologic feature detection algorithm to quantify seasonal components of flow regimes. *J Hydrol* **585**: 124787.

Payn RA, Gooseff MN, McGlynn BL, *et al.* 2009. Channel water balance and exchange with subsurface flow along a mountain headwater stream in Montana, United States. *Water Resour Res* **45**.

Pederson GT, Betancourt JL, and McCabe GJ. 2013. Regional patterns and proximal causes of the recent snowpack decline in the Rocky Mountains, U.S. *Geophys Res Lett* **40**: 1811–6.

Pederson GT, Gray ST, Ault T, *et al.* 2011. Climatic controls on the snowmelt hydrology of the northern Rocky Mountains. *J Clim* **24**: 1666–87.

Peterson BJ, Wollheim WM, Mulholland PJ, *et al.* 2001. Control of nitrogen export from watersheds by headwater streams. *Science* **292**: 86–90.

Poff NL, Allan JD, Bain MB, *et al.* 1997. The natural flow regime. *BioScience* **47**: 769–84.

Poff NL and Zimmerman JKH. 2010. Ecological responses to altered flow regimes: a literature review to inform the science and management of environmental flows. *Freshw Biol* **55**: 194–205.

Power ME, Sun A, Parker G, *et al.* 1995. Hydraulic Food-Chain Models: An approach to the study of food-web dynamics in large rivers. *BioScience* **45**: 159–67.

Rattray G and Sievering H. 2001. Dry deposition of ammonia, nitric acid, ammonium, and nitrate to alpine tundra at Niwot Ridge, Colorado. *Atmos Environ* **35**: 1105–9.

Richards S, Withers PJA, Paterson E, *et al.* 2017. Potential tracers for tracking septic tank effluent discharges in watercourses. *Environ Pollut* **228**: 245–55.

Roberts BJ and Mulholland PJ. 2007. In-stream biotic control on nutrient biogeochemistry in a forested stream, West Fork of Walker Branch: Biotic control on stream nutrient uptake. *J Geophys Res Biogeosciences* **112**: n/a-n/a.

Rood SB, Pan J, Gill KM, *et al.* 2008. Declining summer flows of Rocky Mountain rivers: Changing seasonal hydrology and probable impacts on floodplain forests. *J Hydrol* **349**: 397–410.

Rose LA, Karwan DL, and Godsey SE. 2018. Concentration–discharge relationships describe solute and sediment mobilization, reaction, and transport at event and longer timescales. *Hydrol Process* **32**: 2829–44.

Rose J and Waren K. 2022. Hydrogeology and groundwater availability at Big Sky, Montana. *Mont Bur Mines Geol Open-File Rep 747* 98.

Rosemond AD, Benstead JP, Bumpers PM, *et al.* 2015. Experimental nutrient additions accelerate terrestrial carbon loss from stream ecosystems. *Science* **347**: 1142–5.

Runkel RL and Bencala KE. 1995. Transport of reacting solutes in rivers and streams. Environmental Hydrology. Dordrecht: Springer Netherlands.

Schade P and Kusnierz L. 2010. The West Fork Gallatin River watershed total maximum daily loads (TMDLs) and framework watershed water quality improvement plan. *Mont Dep Environ Qual*.

Serreze MC, Clark MP, Armstrong RL, *et al.* 1999. Characteristics of the western United States snowpack from snowpack telemetry (SNOTEL) data. *Water Resour Res* **35**: 2145–60.

Shoemaker L, Dai T, and Koenig J. TMDL Model Evaluation and Research Needs. 403.

Slavik K, Peterson BJ, Deegan LA, *et al.* 2004. Long-term responses of the Kuparuk River ecosystem to phosphorus fertilization. *Ecology* **85**: 939–54.

Sonderegger D. 2011. Package 'SiZer.'

Sonderegger DL, Wang H, Clements WH, and Noon BR. 2009. Using SiZer to detect thresholds in ecological data. *Front Ecol Environ* **7**: 190–5.

Stahle DW, Cook ER, Burnette DJ, *et al.* 2020. Dynamics, Variability, and change in seasonal precipitation reconstructions for North America. *J Clim* **33**: 3173–95.

Stewart IT. 2009. Changes in snowpack and snowmelt runoff for key mountain regions. *Hydrol Process* **23**: 78–94.

Stewart IT, Cayan DR, and Dettinger MD. 2004. Changes in snowmelt runoff timing in western North America under abusiness as usual'climate change scenario. *Clim Change* **62**: 217–32.

Stewart IT, Cayan DR, and Dettinger MD. 2005. Changes toward earlier streamflow timing across western North America. *J Clim* **18**: 1136–55.

Storb MB, Bussell AM, Caldwell Eldridge SL, *et al.* 2023. Growth of coal mining operations in the Elk River Valley (Canada) linked to increasing solute transport of Se, NO_3^-, and SO_4^{2-} into the transboundary Koocanusa Reservoir (USA–Canada). *Environ Sci Technol* **57**: 17465–80.

StreamStats. https://streamstats.usgs.gov/ss/. Viewed 24 May 2024.

Suberkropp K, Gulis V, Rosemond AD, and Benstead JP. 2010. Ecosystem and physiological scales of microbial responses to nutrients in a detritus-based stream: Results of a 5-year continuous enrichment. *Limnol Oceanogr* **55**: 149–60.

Surkan. 1969. Synthetic hydrographs: Effects of network geometry. *Water Resour Res*.

UNESCO. 2009. UN World water development report 2009.

UNESCO. 2020. The United Nations world water development report 2020: Water and climate change, Paris, UNESCO.

US EPA O. 2013. History of the Clean Water Act. https://www.epa.gov/laws-regulations/history-clean-water-act. Viewed 23 May 2018.

US EPA O. 2015a. Overview of Total Maximum Daily Loads (TMDLs). https://www.epa.gov/tmdl/overview-total-maximum-daily-loads-tmdls. Viewed 2 Apr 2024.

US EPA O. 2015b. TMDL Support Documents. https://www.epa.gov/tmdl/tmdl-support-documents. Viewed 23 Feb 2024.

US EPA O. 2018. Nutrient criteria technical guidance manuals. https://www.epa.gov/nutrient-policy-data/nutrient-criteria-technical-guidance-manuals. Viewed 23 Jan 2020.

Valett HM, Lima RF de, Peipoch M, and Engstrom RC. 2023. Bloom succession and nitrogen dynamics during snowmelt in a mid-order montane river. *Biogeochemistry* **166**: 227–46.

Valett HM, Peipoch M, and Poole GC. 2022. Nutrient processing domains: Spatial and temporal patterns of material retention in running waters. *Freshw Sci* **41**: 195–214.

Van Meter K, Thompson SE, and Basu NB. 2016. Chapter 11 - Human impacts on stream hydrology and water quality. In: Jones JB, Stanley EH (Eds). Stream Ecosystems in a Changing Environment. Boston: Academic Press.

Vitousek PM, Aber JD, Howarth RW, *et al.* 1997. Human alteration of the global nitrogen cycle: Sources and consequences. *Ecol Appl* **7**: 737–50.

Walling DE and Foster IDL. 1975. Variations in the natural chemical concentration of river water during flood flows, and the lag effect: Some further comments. *J Hydrol* **26**: 237–44.

Waren K, Rose J, and Breitmeyer R. 2021. Groundwater model of the meadow village aquifer at Big Sky, Montana. Montana Bureau of Mines and Geology Groundwater Investigation Report.

Westall F and Brack A. 2018. The Importance of water for life. *Space Sci Rev* **214**: 50.

Wetzel RG. 1995. Death, detritus, and energy flow in aquatic ecosystems. *Freshw Biol* **33**: 83–9.

Whitlock C, Cross W, Maxwell B, *et al.* 2017. 2017 Montana Climate Assessment.

Wollheim WM, Bernal S, Burns DA, *et al.* 2018. River network saturation concept: factors influencing the balance of biogeochemical supply and demand of river networks. *Biogeochemistry* **141**: 503–21.

Xie Z, Zhang P, Wu Z, *et al.* 2022. Legacy and emerging organic contaminants in the polar regions. *Sci Total Environ* **835**: 155376.

Xu D, Ivanov VY, Li X, and Troy TJ. 2021. Peak runoff timing is linked to global warming trajectories. *Earths Future* **9**: e2021EF002083.

Yarnell SM, Stein ED, Webb JA, *et al.* 2020. A functional flows approach to selecting ecologically relevant flow metrics for environmental flow applications. *River Res Appl* **36**: 318–24.

Yarnell SM, Viers JH, and Mount JF. 2010. Ecology and Management of the Spring Snowmelt Recession. *BioScience* **60**: 114–27.

Yvon-Durocher G, Jones JI, Trimmer M, *et al.* 2010. Warming alters the metabolic balance of ecosystems. *Philos Trans R Soc B Biol Sci* **365**: 2117–26.

Zhao S, Zettler ER, Bos RP, *et al.* 2022. Large quantities of small microplastics permeate the surface ocean to abyssal depths in the South Atlantic Gyre. *Glob Change Biol* **28**: 2991–3006.